STATIC AND DYNAMIC BEHAVIOR OF STIFFENED COMPOSITE HYPAR SHELLS WITH CUTOUT

Thesis submitted by

PUJA BASU CHAUDHURI

Doctor of Philosophy

(Engineering)

DEPARTMENT OF MECHANICAL ENGINEERING

FACULTY COUNCIL OF ENGINEERING & TECHNOLOGY

JADAVPUR UNIVERSITY

KOLKATA, INDIA

2022

JADAVPUR UNIVERSITY

KOLKATA-700032, INDIA

INDEX NO: 234/16/E

1. Title of The Thesis:

Static and Dynamic Behavior of Stiffened Composite Hypar Shells with Cutout

2. Name, Designation & Institution of the Supervisor(s):

i. **Dr. Anirban Mitra**

Associate Professor, Department of Mechanical Engineering

Jadavpur University, Kolkata 700032

ii. **Dr.Sarmila Sahoo**

Associate Professor, Department of Civil Engineering

Heritage Institute of Technology, Kolkata 700107

3. List of Publications (Referred Journals):

1. P. B. Chowdhury, A. Mitra and S. Sahoo, 2016, Relative performance of antisymmetric angle-ply laminated stiffened hypar shell roofs with cutout in terms of static behaviour.*Curved and Layered Structures*, 3(1), pp.22-46. [SCOPUS, WOS]
2. P. B. Chaudhuri, A. Mitra and S. Sahoo, 2017, Bending analysis of laminated stiffened hypar shell roofs with cutout. *Materials Today: Proceedings*, 4(2) pp.575-583. [SCOPUS]
3. P. B. Chaudhuri, A. Mitra and S. Sahoo, 2017, Deflection, forces and moments of composite stiffened hypar shells with cut-out, *Materials Today: Proceedings*,4(9), pp.9718-9722.[SCOPUS]

4.P.B.Chaudhuri, A. Mitra and S.Sahoo, 2018, Free Vibration analysis of antisymmetric angle ply laminated composite stiffened hypar shell with cut-out, *Materials Today: Proceedings*, 5(1), pp.5563-5572.[SCOPUS]

5. P B. Chaudhuri, A.Mitra and S. Sahoo, 2019, Mode- frequency analysis of anti-symmetric angle-ply laminated composite stiffened hypar shell with cut-out, *Mechanics and Mechanical Engineering,* 23(1), pp.162-171.[SCOPUS]

6.P B. Chaudhuri, A.Mitra and S. Sahoo, 2019, Higher mode vibration of composite stiffened hypar shell with cutout for varying boundary conditions and ply orientation,*i-manager's Journal on Structural Engineering,* 8(2), pp.37-51.

7. P B. Chaudhuri, A.Mitra and S. Sahoo, 2022, Design of experiments analysis of fundamental frequency of laminated composite hypar shells with cut-out, *Materials Today: Proceedings*, 66 (4), pp.2332-2337.[SCOPUS]

8. P B. Chaudhuri, A.Mitra and S. Sahoo, 2022, Maximization of Fundamental Frequency of Composite Stiffened Hypar Shell with Cutout by Taguchi Method, *Mechanics of Advanced Composite Structures,* Accepted for publication (in press).[SCOPUS]

4. List of presentations in National/International Conferences:

1.P. B. Chaudhuri, A. Mitra and S. Sahoo, 2018, Frequency Analysis of laminated composite stiffened hypar shell with cut-out on higher modes, *Proceedings of 1st International conference on Mechanical Engineering (INCOM 2018),* Kolkata,4-6th January 2018, pp26-29.

2.P. B. Chaudhuri, A. Mitra and S. Sahoo, Free vibration performance of cut-out borne stiffened composite hypar shells using Taguchi Methodology, *Proceedings of International Conference on Advanced Technologies in Chemical, Construction and Mechanical Sciences (iCATCHCOME 2022)* 24-25th March 2022, Coimbatore, Tamilnadu (Paper id-CCM 5016).

3. P. B. Chaudhuri, A. Mitra and S. Sahoo, Taguchi analysis of fundamental frequency for simply supported laminated composite stiffened hypar shells with cut-out, *Proceedings of 4th International Conference on Material Science and Manufacturing Technology (ICMSMT 2022)*8-9th April 2022, Coimbatore, Tamilnadu (Paper id -MS3047).

STATEMENT OF ORIGINALITY

I, PUJA BASU CHAUDHURI registered on 06.04.2016 do hereby declare that the thesis entitled **"Static and dynamic behavior of stiffened composite hypar shells with cutout"** contains literature survey and original research work done by the undersigned candidate as part of Doctoral studies.

All information in this thesis have been obtained and presented in accordance with existing academic rules and ethical conduct. I declare that, as required by these rules and conduct, I have fully cited and referred all materials and results that are not original to this work.

I also declare that I have checked this thesis as per the "Policy on Anti Plagiarism, Jadavpur University,2019", and the level of similarity as checked by iThenticate software is 8%.

Signature of Candidate: Puja Basu Chaudhuri

(PUJA BASU CHAUDHURI)

Date:

Certified by Supervisors: Associate Professor Dept. of Mechanical Engineering Jadavpur University, Kolkata-32

(Signatures with Date, seal)

Dr. Sarmila Sahoo
Associate Professor, Dept. of Civil Engg.
Heritage Institute of Technology, Kolkata

CERTIFICATE OF SUPERVISOR(S)

This is to certify that the thesis entitled **"Static and Dynamic Behavior of stiffened composite hypar shells with cutout"** submitted by PUJA BASU CHAUDHURI, who got his name registered on 06.04.2016 for the award of Ph.D. (Engineering) degree of Jadavpur University, is absolutely based upon her own work under oursupervision and that neither her thesis nor any part of the thesis has been submitted for any degree/diploma or any other academic award anywhere before.

Certified by Supervisors:

(Signatures with Date, seal)

Associate Professor
Dept. of Mechanical Engineering
Jadavpur University, Kolkata-32

Dr. Sarmila Sahoo
Associate Professor, Dept. of Civil Engg.
Heritage Institute of Technology, Kolkata

ABSTRACT

Laminated composite shells constitute a large percentage of structures including aerospace, marine and automotive structural components. Structural engineers have already picked up laminated composite hypar shells (hyperbolic paraboloid bounded by straight edges) as roofing units. Hypar shells are used in civil engineering industry to cover large column free areas such as in stadiums, airports and shopping malls. Being a doubly curved and doubly ruled surface, it satisfies aesthetic as well as ease of casting requirements of the industry. Moreover, hypar shell allows entry of daylight and natural air which is preferred in food processing and medicine units. Cutout is sometimes necessary in roof structure to allow entry of light, to provide accessibility of other parts of the structure, for venting and at times to alter the resonant frequency. Shell structure that are normally thin walled, when provided with cutout, exhibits improved performances with stiffeners. To use these doubly curved, doubly ruled surfaces efficiently, the behavior of these forms under bending are required to be understood comprehensively. The use of laminated composites to fabricate shells is preferred to civil engineers from second half of the last century. The reasons are high strength/stiffness to weight ratio, low cost of fabrication and better durability. Moreover, the stiffness of laminated composites can be altered by varying the fiber orientations and lamina thicknesses which gives designer flexibility. As a result, laminated shells are found more cost effective compared to the isotropic ones as application of laminated composites to fabricate shells reduces their mass induced seismic forces and foundation costs.Shells with cutout, stiffened along the margin are an efficient way to enhance the stiffness of the structure without adding much mass. These stiffeners slightly increase the overall weight of the structure but have positive effect on structural strength and stability. So to apprehend the laminated composite stiffened hypar shells with cutout and to use this shell form efficiently, its characteristics under bending and vibration need to be explored comprehensively.

The vibration frequencies of laminated panels depend on laminations, edge conditions, shell dimensions (thickness, length) and cutout (size and position). Therefore, for cutout borne stiffened hypar shells with various material system and geometric shape, obtaining an appropriate combination of lamination angle, thickness, cutout position and end conditions for

maximization of the fundamental frequency becomes an interesting problem. This is more so because fundamental frequency needs to be higher to skip any resonance effect occurring from ground vibrations and other natural disturbances. However, there has not been much of an activity in this respect perhaps due to the complexities involving so many shell parameters and complicated algorithm flow as well. The present study thus also emphasizes on the maximization of fundamental frequency of cutout borne hypar shells based on Design of Experiments technique.

Realizing the importance of cutout bornestiffened composite hypar shell, the scope of present study is outlined and laminated composite graphite epoxy skewed hypar shells with cutout and stiffeners are taken up for bending and vibration studies. A finite element formulation has been established by combining eight noded isoparametric shell element and a three-noded beam element for the stiffeners. The formulation is validated through some benchmark problemsfrom literature. The entire numerical study is divided into three parts- first part deals with static behavior of laminated stiffened hypar shell with cutout, second part deals with free vibration criteria and mode frequency analysis of laminated stiffened hypar shell with cutout, and third part deals with Design of Experiment analysis and optimization of fundamental frequency of laminated composite stiffened hypar shells with cut-out using Taguchi Methodology. The effects of different parametric variations are studied on the shell actions including deflection, force and moments and also on fundamental frequencies and mode shapes. The boundary conditions along the four edges are varied for the stiffened shell with cut-outs. The position of cut-out is also varied for the study of fundamental frequencies and modes of laminated stiffened hypar shell. The thesis ends with an overall conclusion of present work and future scope of research is also mentioned.

It is believed that the outcome of the present study will be of both academic interest and practical/industrial importance to structural engineers and designers dealing with such laminated composite shell structures.

ACKNOWLEDGEMENT

The journey towards completion of PhD thesis has been an enchanting learning experience. The journey would not be accomplished without guidance of certain people. I would like to thank them for standing beside me whenever I required support throughout the course of the journey.

Firstly, I would like to express my deepest gratitude to my supervisor, Dr. Sarmila Sahoo for her complete assistance, constant encouragement and unlimited inputs. Without her guidance, I could not have finished my thesis work successfully. Next, I would like to convey my heartfelt gratitude to supervisor, Dr. Anirban Mitra for his insightful suggestions. His knowledge and attitude towards excellence always encourage me.

It would not be possible to complete my doctoral work without blessings, sacrifice and encouragement of my parents from the very first day of my student life.

I would like to thank my husband and my son for their dedication and patience to assure my devotion towards research work.

I am also grateful to all my colleagues, family, friends and professors directly and indirectly who contributed during the course of my entire journey.

Signature of Candidate: Puja Basu Chaudhuri

(PUJA BASU CHAUDHURI)

Table of Contents

LIST OF FIGURES

LIST OF TABLES

NOMENCLATURES

a, b	length and width of shell in plan
$a^{/}, b^{/}$	length and width of cutout in plan
b_{sx}, b_{sy}	width of x and y stiffener respectively
B_{sx}, B_{sy}	strain displacement matrix of stiffener element
c	rise of hypar shell
$\{d\}$	global displacement vector
d_{st}	depth of stiffener
d_{sx}, d_{sy}	depth of x and y stiffener respectively
$\{d_e\}$	element displacement
D	flexural rigidity
e	eccentricity of stiffeners with respect to mid surface of shell
e_{sx}, e_{sy}	eccentricities of x and y stiffeners with respect to mid surface of shell
E_{11}, E_{22}	elastic moduli
G_{12}, G_{13}, G_{23}	shear moduli of a lamina with respect to 1, 2 and 3 axes of fibre
h	shell thickness
M_x, M_y	moment resultants
M_{sxx}, M_{syy}	moment resultants of stiffener
M_{xy}	torsion resultant
$\overline{M}_x$, $\overline{M}_y$	non-dimensional moment resultant[=(M_x or M_y)/P]
$\overline{M}_{xy}$	non-dimensional torsion resultant[= M_{xy}/P]
np	number of plies in a laminate
N_1-N_8	shape functions
N_x, N_y	in-plane force resultants
N_{sxx}, N_{syy}	axial force resultants of stiffeners
N_{xy}	in-plane shear resultant
$\overline{N}_x$, $\overline{N}_y$	non-dimensional in-plane force resultants[=(N_x or N_y)a/P]
$\overline{N}_{xy}$	non-dimensional in-plane shear resultant[= N_{xy}a /P]

Q_x, Q_y	transverse shear resultants
Q_{sxxz}, Q_{syyz}	transverse shear resultants of stiffener
P	transverse concentrated load
R_{xy}	radii of cross curvature of hypar shell
T_{sxx}, T_{syy}	torsion resultants of stiffeners
u, v, w	translational degrees of freedom at each node of shell element
w_{st}	width of stiffener
u_{sx}, w_{sx}	translational degrees of freedom at each node of x-stiffener element
v_{sy}, w_{sy}	translational degrees of freedom at each node of y-stiffener element
x, y, z	local co-ordinate axes
X, Y, Z	global co-ordinate axes
$\bar{x}$, $\bar{y}$	non-dimensional x co-ordinate [= x / a] and y co-ordinate [= y / b]
z_k	distance of bottom of the kth ply from mid-surface of a laminate
α, β	rotational degrees of freedom at each node of shell element
α_{sx}, β_{sx}	rotational degrees of freedom at each node of x-stiffener element
α_{sy}, β_{sy}	rotational degrees of freedom at each node of y-stiffener element
δ_{sxi} , δ_{syi}	nodal displacement of stiffener element
ε_x, ε_y	in-plane strain component
γ_{xy} ,γ_{xz}, γ_{yz}	shearing strain components
ν_{12}, ν_{21}	Poisson's ratios
ξ, η, τ	isoparametric co-ordinates
ρ	density of material
σ_x, σ_y	in-plane stress components
τ_{xy}, τ_{xz}, τ_{yz}	shearing stress components
ω	natural frequency
$\bar{\omega}$	non-dimensional natural frequency $\left[= \omega a^2 \left(\rho / E_{11} h^2\right)^{1/2}\right]$

Chapter 1

INTRODUCTION

1.1 GENERAL

A shell is a curved structural surface which resist any externally superimposed load by combined in-plane thrusts and bending of the surface. This coupling of in-plane force and bending moments provide high strength and stiffness. Thus, a shell gains its strength through its form more than its mass. The doubly curved surface is a specialized structural element which is efficient in terms of strength and aesthetics. Hence the idea of constructing stiffened structures such as steel chimneys, pipes and conduits, bridge, aircrafts, ship and off-shore structures has gained momentum. The idea that structures can be made of thin plate and shells can be strengthened by integrating them with row of ribs which is an innovative idea and economically acceptable without compromising strength or stability.

Usually, composites are defined as combination of two or more materials to achieve specific properties. From Engineering point of view composite may be defined as combination of materials which differ in composition or form on macroscopic level and remain chemically inactive with respect to each other to form a useful material. Commonly composites are two types: a) Particulate composites b) Fibre reinforced composites. Particulate composites are those in which particles of various shapes and size are dispersed within matrix in random manner. As the particles are of different shapes and size and particles are in randomly dispersed within matrix, they are treated as quasi-homogenous and quasi-isotropic. Both particle and matrix may be metallic or non-metallic. Fibre reinforced composites consists of fibres of significant strength and stiffness embedded in a matrix with distinct boundaries between them. Both fibres and matrix contain their own physical and chemical identities, their combination performs better which cannot be done singly. Fibrous composites consist of large number of strong, stiff, continuous or chopped fibres

embedded in matrix having large length to diameter ratio (100 or more) to ensure a reinforcing action. They are either in-organic (glass, carbon, boron) or organic (aramid, Kevlar) materials. The matrix also can be metallic (Aluminum) or non-metallic (polyester, epoxy, phenolic, resin and ceramics).

A widely used geometry for continuous fibre composites is termed as Laminate. Laminates are made of plies, in which all fibres are often have the same direction. The fibres are usually stronger and stiffer than matrix so a ply is also stiffer and stronger in fibre direction. Lamina is formed when an array of fibres is given a resin bath and hardened. The matrix transfers the loads to fibres. A number of laminae or plies are bonded together in different orientation to form a laminate. Laminae are homogeneous and anisotropic in larger view scale and laminate is orthotropic. These are used in beams, plates, shells stiffened plates, stiffened shells etc. The lower cost of assembly, easy to repair, high specific stiffness and strength, excellent damage protection and higher fatigue response criteria increased the use of laminated components in important engineering fields.

1.2 METHOD OF ANALYSIS

The exact analysis of stiffened plate or shells based on theory of elasticity is rarely carried out for its difficult computational methods in evaluating deflection and stresses. Analysis of stiffened shells has been approached from three different angles. In the first approach, the elastic properties of stiffeners are distributed uniformly along the orthogonal directions and stiffened plate or shell is replaced by an equivalent orthotropic plate or shell of constant thickness. The orthotropic plate or shell theory demands equal and closely spaced stiffeners. Also, the stiffeners can be changed into an 'equivalent plate or shell'. In this method the evaluation of stresses in the plate and stiffeners separately becomes difficult. So, it may restrict the application of this technique into engineering field.

In the second approach, the stiffened plate or shell can be treated as grillage, which is a plane structure of intersecting beams and carry lateral load through the beam bending action. There are basically two drawbacks in this method. Firstly, the centroidal plane of beam in different direction are assumed to be coincident which affect the accuracy of stresses calculated. Secondly, the beam properties are derived based on effective width of plate or shell remain inconclusive. Therefore, this method has also got restriction in usage.

The third method of modeling is most idealistic and accurate. In this approach the plate or shell sheet and the array of beams are treated as separate existence initially. The stiffness of stiffeners is derived by adding the individual stiffness to maintain the compatibility of the deformation at the interfaces. this method makes the analysis sufficiently involved and complex, but it gives a better significance in structural applications. However, the invention of high-speed digital computers and parallel development of numerical techniques in structure make the analysis simpler and accurate. There are various numerical methods in which plate or shell and stiffeners are considered as separate entities. These include: i) Finite Difference Method, ii) Energy Methods, such as Rayleigh's method, Rayleigh-Ritz method, Galerkin method etc., iii) Dynamic relaxation method, iv) Finite element method.

Out of all these methods, Finite element method is considered as versatile due to its ability to incorporate geometry, loading and boundary conditions. Accordingly, researchers from all over the world adopted the analysis of composite stiffened plates and shells using finite element approach. The present approach also concentrates on the static and dynamic behavior of laminated composite stiffened hypar shell with cut-out using finite element method.

1.3 IMPORTANCE OF PRESENT STUDY

Laminated composite shells now constitute a large percentage of structures including aerospace, marine and automotive structural components. Structural engineers have already picked up laminated composite hypar shells (hyperbolic paraboloid bounded by straight edges) as roofing units. Hypar shells are used in civil engineering industry to cover large column free areas such as in stadiums, airports and shopping malls. Being a doubly curved and doubly ruled surface, it satisfies aesthetic as well as ease of casting requirements of the industry. Moreover, hypar shell allows entry of daylight and natural air which is preferred in food processing and medicine units. Cutout is sometimes necessary in roof structure to allow entry of light, to provide accessibility of other parts of the structure, for venting and at times to alter the resonant frequency. Shell structure that are normally thin walled, when provided with cutout, exhibits improved performances with stiffeners. To use these doubly curved, doubly ruled surfaces efficiently, the behavior of these forms under bending are required to be understood comprehensively. The use of laminated composites to fabricate shells is preferred to civil engineers from second half of the last century. The reasons are high strength/stiffness to weight ratio, low cost of fabrication and better durability. Moreover, the stiffness of laminated composites can be altered by varying the fiber orientations

and lamina thicknesses which gives designer flexibility. As a result, laminated shells are found more cost effective compared to the isotropic ones as application of laminated composites to fabricate shells reduces their mass induced seismic forces and foundation costs. Shells with cutout, stiffened along the margin are an efficient way to enhance the stiffness of the structure without adding much mass. These stiffeners slightly increase the overall weight of the structure but have positive effect on structural strength and stability. So to apprehend the laminated composite stiffened hypar shells with cutout and to use this shell form efficiently, its characteristics under bending and vibration need to be explored comprehensively.

The vibration frequencies of laminated panels depend on laminations, edge conditions, shell dimensions (thickness, length) and cutout (size and position). Therefore, for cutout borne stiffened hypar shells with various material system and geometric shape, obtaining an appropriate combination of lamination angle, thickness, cutout position and end conditions for maximization of the fundamental frequency becomes an interesting problem. This is more so because fundamental frequency needs to be higher to skip any resonance effect occurring from ground vibrations and other natural disturbances. However, there has not been much of an activity in this respect perhaps due to the complexities involving so many shell parameters and complicated algorithm flow as well. The present study thus also emphasizes on the maximization of fundamental frequency of cutout borne hypar shells based on Design of Experiments technique.

1.4 PRESENT THESIS

Bending and vibration characteristics of laminated composite stiffened hypar (hyperbolic paraboloid shell bounded by straight edges) with cut-out are analyzed. A finite element code is developed for the purpose by combining an eight noded curved shell element with a three noded curved beam element for stiffener. Finite element formulation is based on first order shear deformation theory and includes the effect of cross curvature. The isoparametric shell element used in the present model consists of eight nodes with five degrees of freedom per node while beam element has four degrees of freedom per node. The code is validated by solving benchmark problems available in the literature and comparing the results. The generalized Eigen value solution is chosen for the un-damped free vibration analysis.

Performances of antisymmetric angle-ply laminated composite stiffened hypar shells in terms of displacements and stress resultants are studied under static loading. A number of

additional problems of antisymmetric angle-ply laminated composite stiffened hypar shells are solved for various fibre orientations, number of layers and boundary conditions. Results are interpreted from practical application standpoints and findings important for a designer to decide on the shell combination among a number of possible options are highlighted.

The first five modes of natural frequency are considered here. The numerical studies are conducted to determine the effects of width to thickness ratio (b/h), degree of orthotropy (E_{11}/E_{22}) and fibre orientation angle (θ) on the non-dimensional natural frequency. The results furnished here may be readily used by practicing engineers dealing with stiffened composite hypars with cut-outs.

A numerical study of free vibration response of composite stiffened hypar shells with cutout using finite element procedure and optimization of different parametric combinations based on Taguchi approach is also considered. Numerical investigations are carried out following L27 Taguchi design with four design factors, viz., fiber orientation, width/thickness factor of shell, degree of orthotropy and position of the cutout for different edge constraints. The optimum parametric combination for maximum fundamental frequency of cutout borne stiffened hypar shell is obtained from the analysis.

The present thesis is organized into 8 chapters. Chapter 1 introduces the present study including the organization of the thesis. Chapter 2 is devoted to the brief review of existing literature in the related area. Chapter 3 describes the scope of the present study. Chapter 4 details the mathematical formulation needed for the present analysis. Chapter 5 incorporates the study of bending behavior of stiffened hypar shell with cutout. Chapter 6 illustrates the vibration behavior of the shell with cutout. Chapter 7 describes the optimization of fundamental frequency of stiffened shell with cutout. Finally, chapter 8 includes the overall conclusions from the present study and future scope of research.

Chapter 2

REVIEW OF LITERATURE

2.1 GENERAL

The application of shell structures and related research have a long history and the volume of literature accumulated in this area is large. In this chapter, a brief review of recent literature is presented to give a brief description on development of shell research in particular context to cutout borne shells carried out in last two decades.

2.2 STATE OF ART REVIEW

While the theory of shell structures was being simplified and improved from time to time by many researchers, investigators started developing exotic materials with high strength and stiffness properties. This resulted in the use of laminated composite materials to fabricate shell forms. As a result, bending and vibration analysis of laminated composite shells emerged as a new field. Ruotolo [2001] studied on the comparison of thin shell theories used for dynamic analysis of isotropic and laminated composite stiffened cylinders. Prusty and Satsangi [2001a, b] investigated transient dynamic response of stiffened composite plates and shells using an eight noded isoparametric shell element and three noded curved isoparametric stiffener element. Different aspects of laminated composite stiffened shell behavior were studied by Nayak and Bandyopadhyay [2002a, b], Rikards et al. [2001]. Sai Ram and Babu [2001a] explained bending behavior of fibre reinforced plastic laminated shells without cut-out using finite element method based on higher order shear deformation theory. The higher order shear deformation theory was derived assuming transverse displacement constant throughout the thickness of shell considering eight-noded degenerated shell element having nine degrees of freedom. They also extended their study to bending behavior of fibre reinforced plastic laminated shells with cut-out using same formulation. Lee et al. [2002] studied free vibration of joined cylindrical-spherical shell structures

at various boundary conditions. The Flügge shell theory and Rayleigh's energy method were applied in order to analyze free vibration characteristics of the joined shell structures and individual shell components. Nayak and Bandyopadhyay [2002b] studied the free vibration of stiffened shallow shells using finite element method. The stiffened shell element was obtained by appropriate combination of eight/nine noded doubly curved isoparametric thin shallow shell element with three noded curved isoparametric beam element. Numerical results were presented to study the effects of various parameters of shells and stiffeners.

Free-vibration behavior of partially liquid-filled and sub-merged and horizontal cylindrical shell were studied by Ergin and Temarel [2002]. Qatu [2002a, b] reviewed in details on shell dynamics for both isotropic and composite materials for cylindrical and spherical shell. A three-dimensional analysis was presented by Kang and Leissa [2005] for determining the free vibration frequencies and mode shapes of thick conical shells of revolution. Sahoo and Chakravorty [2005] investigated the vibration characteristics of composite hypar shallow shells with various edge supports using finite element method. Numerical experiments were carried out for different parametric variations including boundary conditions and stacking sequences to obtain fundamental frequencies and mode shapes. Nayak and Bandyopadhyay [2005] studied the free vibration behavior of laminated composite anticlastic doubly curved stiffened shell using finite element method. An efficient tool for free vibration analysis of rotating truncated conical shells were presented by Civalek [2006]. A discrete singular convolution method was described for the analysis. Frequency parameters for various boundary conditions were described. Free vibration analysis of skewed open circular cylindrical shells was studied by Kandasamy and Singh [2006]. First order shear deformation theory was presented including rotary inertia so that thin to moderately thick shells can be analyzed. Rayleigh-Ritz method was used to calculate frequency and mode shapes. The higher order shear deformation theory was presented to solve static and free vibration analysis of composite shells by Ferreira et al. [2006]. Reddy shell theory allowed at the top and bottom surface of shells.

Sahoo and Chakraborty [2006a] developed a finite element code to analyze stiffened composite hypar shell having eight noded shell element and three noded beam element. Benchmark problems are solved to validate the approach and free vibration response has been studied for fundamental frequency and mode shapes by varying the number and depth of stiffeners, laminations and boundary conditions. Hota and Chakravorty [2007] developed a finite element

code for analyzing free vibration characteristics of a stiffened conoidal shell by combining an eight noded curved shell element with a three noded curved beam element. The effect of various parameters on fundamental frequencies were studied and discussed in details. The non-linear free vibration characteristics of composite cylindrical shell panels with cut-out was investigated by Nanda and Bandyopadhyay [2007]. Parametric variations were carried out at varying aspect ratio, lamination schemes and material properties of shell at simply supported boundary conditions. Free vibration analysis of skewed cylindrical shell panel was analyzed by Halder [2008] using finite element method. First order shear deformation theory was used incorporating transverse displacement and bending rotation as independent field variables. Numerical results were obtained at various parametric variation of shallow shells and compared with the published results. To investigate large amplitude free flexural vibration of doubly curved shallow shell in presence of cut-out, Nanda and Bandyopadhyay [2008] employed finite element model. Nonlinear strains of von Karman type are incorporated into the first-order shear deformation theory in this approach. Static and dynamic analysis of smart cylindrical shell was studied by Kumar et al. [2008]. A finite element formulation has been used to show static and dynamic response of laminated composite shells containing piezoelectric sensors and actuators subjected to electrical, mechanical and thermal loadings. The influence of stacking sequence and positions of sensors/actuators on the response of laminated cylindrical shell was evaluated. Study on free vibration analysis of circular cylindrical shells using wave propagation method was studied by Xuebin [2008]. The validity and accuracy of the wave approach was studied in detail including aspects of frequencies, vibration shapes and wavenumbers. An exact solution for free vibration analysis was explained. at various boundary conditions.

A four noded quadrilateral shell element with smoothed membrane-bending based on Mindlin-Reissner theory has been proposed by Nguyen-Thanh et al. [2008]. This type of element is a combination of plate bending and membrane element which is based on mixed interpolation where bending and membrane stiffness matrices are calculated on the boundaries of smoothing cells while the shear terms are approximated by independent interpolation functions in natural coordinates. The proposed element is robust, computationally inexpensive and free of locking. The bending behavior of delaminated composite shallow cylindrical shells subjected to uniformly distributed load with corner point supported, simply supported and clamped boundary conditions was studied by Acharyya et al. [2008]. Lamination, curvature and extent of delamination area were

varied to compare the performances of delaminated cylindrical shells against those with no damage. Bending characteristics of laminated composite conoidal shell on damage due to manufacturing defects and over-loading were studied by Kumari and Chakravorty [2010]. A finite element method using isoparametric shell element was presented incorporating multipoint constraint algorithm to take care of compatibility of deformation and equilibrium of forces and moments at the delamination crack front.

Qatu et al. [2010] reviewed most of the research done during 2000–2009 on the dynamic behavior (including vibration) of composite shells. This review was conducted with emphasis on the type of testing or analysis performed (free vibration, impact, transient, shock, etc.) at the various shell geometries subjected to dynamic research. A nine noded isoparametric plate bending element has been used for bending analysis of isotropic skewed cylindrical shell panels were studied by Halder et al. [2010]. First order shear deformation theory has been incorporated. The results have been checked at different type of loads, shell thickness, length to curvature ratio, skewed angle and various boundary conditions. A survey on bending analysis of symmetrically cross-ply laminated plates was done by Mokhtar et al. [2010].

A review on recent literature on static analysis of composite shells was presented by Qatu et al. [2012]. This paper reviews most of the research done during 2000-2010 on the static and buckling behavior (including post buckling) of composite shells. This review was conducted with emphasis on the type of testing or analysis performed (static, buckling, post-buckling, and others.) at the various shell geometries. Shadmehri et al. [2014] studied the effect of displacement field on bending, buckling and vibration of cross-ply cylindrical shells using first-order shear deformation theory. The effect of various boundary conditions (clamped, simply supported and free edge), radius-thickness ratio and radius-length ratio on the displacement of mid-surface were investigated.

Das and Chakravorty [2011] studied the bending behavior of stiffened composite conoidal shell roofs through finite element application. An eight noded shell element with three noded beam element has been considered to analyze the stiffened composite conoidal shell roofs subjected to concentrated load at center. Reddy et al. [2012] investigated bending of laminated composite plate subjected to uniformly distributed load. The effect of transverse shear deformation on deflection and stresses were studied for various parameters. Kumar et al. [2012] analyzed laminated composite skew shells using higher order shear deformation theory. Static analysis of skew

composite shell was done using a C_0 finite element model based on higher order shear deformation theory. Results were presented considering different geometry, boundary conditions, ply orientation, loadings and skew angles. Bending analysis of paraboloid of revolution shell was studied by Tamboli and Kulkarni [2014] using finite element method. Vlasov bending theory was used to solve the problem theoretically. Ashwinkumar et al. [2015] presented a parametric study of thin cylindrical shells.

Non-linear bending response of laminated composite spherical shell panels subjected to hygro-thermo mechanical loading was studied by Lal et al. [2011]. System properties such as material properties, thermal expansion co-efficient, hygro contraction co-efficient, load intensity and lamina plate thickness were common random variables. The higher order shear deformation theory and von-Karman non-linear kinematics were used for basic formulation. The influence of system properties on laminated spherical shell panels were studied in detail. Bending and free vibration analysis of isotropic and multilayered plates and shells by using a new accurate higher order shear deformation theory were investigated by Mantari et al. [2012]. The governing equations and boundary conditions were derived by employing principle of virtual work. These equations were solved by Navier type, closed form solutions. Bending and dynamic results were presented for cylindrical and spherical shells and plates for simply supported boundary conditions. The results were compared with exact three dimensional elasticity theory and several well-known HSDT theories of previous investigations. Free vibration characteristics of laminated composite hypar shell roofs with cut-out using finite element method was studied by Sahoo [2011]. Kumar et al. [2013a] studied finite element analysis of laminated composite and sandwich shells using higher order zigzag theory. Free vibration response of laminated composite and sandwich shell was studied by Kumar et al. [2013b] using an efficient 2D finite element model based on higher order zigzag theory (HOZT). Kumar et al. [2015] again developed accurate dynamic response criteria of laminated composite and sandwich shells using higher order zigzag theory. They explained forced vibration response of laminated composite and sandwich shells using 2D finite element based on higher order zigzag theory.

Chen et al. [2013] studied free vibration of circular cylindrical shell with non-uniform elastic boundary constraints. The exact solution for the problem was obtained using improved Fourier series method. Sahoo [2013] presented dynamic characteristics of stiffened composite conoidal shell roofs with cut-outs in terms of natural frequency and mode shapes. The effect of

various parametric variations on fundamental frequencies and mode shapes were considered in details for laminated composite conoids. A unified and exact solution method was developed for the free vibration analysis of composite laminated shallow shells with general elastic boundary conditions by Ye et al. [2013, 2014a, b]. A general Fourier solution for the vibration analysis of composite laminated structural elements with general elastic constraints were developed by Jin et al. [2014]. Regardless of boundary conditions, each displacement and rotation component of the structures was invariantly expressed as the superposition of a Fourier cosine series and two supplementary functions were introduced to remove any potential discontinuous of the original displacements and their derivatives. On the basis of energy functional of structure elements, the exact series solutions were obtained using the Rayleigh–Ritz formulation.

Naghsh and Azhari [2015] presented non-linear free vibration analysis of point supported laminated composite skew plates. The element -free Galerkin method was employed to analyze the composite skew plates. Assuming a periodic solution and applying the weighted residual method, non-linear governing equation was used and the problem was solved by direct iteration technique. Thermal bending analysis of doubly curved composite laminated shell panels with general boundary condition and lamination was investigated by Maghami et al. [2015]. A semi analytical method based on multi-term extended Kantorovich method was developed to analyze thermal bending of laminated shell panels with general boundary conditions and laminations. The principle of minimum potential energy was used to derive the governing equations within a framework of general and highly accurate first order shell theory. Simply supported spherical and cylindrical shell panels were studied and results were compared with those obtained by analytical method. Vibration analysis of circular cylindrical double shell structures under general coupling and end boundary conditions was studied by Zhang et al. [2016]. Free and forced vibration analysis under arbitrary boundary condition was presented. This was achieved by employing improved Fourier series based on Hamilton's principle. The natural frequencies and mode shapes of the structures as well as frequency responses under forced vibration were obtained with the Rayleigh-Ritz procedure. The convergence of the method was validated by comparing the results with those obtained by finite element method. To show the accuracy of the current method various numerical results including natural frequencies and mode shapes were studied.

A considerable volume of literature is found regarding the effect of an opening in thin cylindrical shells under different loading. Among these, quite a few of the references are directly

related to the cutouts along the length of the shells in the form of entrance doors. Sahoo [2014a] solved the free vibration problems of laminated composite stiffened saddle shells with cutouts employing eight-noded curved quadratic isoparametric element for shell with a three noded beam element for stiffener formulation. Stochastic free vibration analysis of composite shallow doubly curved shell with Kriging model approach was presented by Dey et al. [2014]. A finite element formulation was carried out considering rotary inertia and transverse shear deformation based on Mindlin's theory. Sahoo [2014b] analyzed laminated composite stiffened shallow spherical panels with cut-out to consider different size and position of cut-outs at different edge constraints. The results were further analyzed for optimum size and position of cut-out at different practical constraints. Sahoo [2015a, b] investigated free vibration of laminated composite stiffened elliptical paraboloid shell and cylindrical shell panel with cut-out respectively. A deep doubly curved shell element was developed for the free vibration analysis of general shells of revolution was explained by Naghsh et al. [2015]. Lagrange polynomials were used to interpolate the displacement variables. Free vibration analysis of a circular cylindrical shell using Rayleigh-Ritz method was presented by Lee and Kwak [2015]. To determine mass and stiffness matrices a computer simulation under different shell theories and boundary condition was implemented.

An experimental investigation was presented by Biswal et al. [2015] on free vibration behavior of woven fibre glass/ epoxy laminated composite shells subjected to hygrothermal environments. First order shear deformation theory was considered for free vibration analysis of shells subjected to elevated temperatures and moisture concentrations. Parametric study was carried out for varying curvature ratios, number of layers and laminates. Numerical and experimental results showed reduction of natural frequencies with increase of temperature and moisture concentration. Free vibration analysis of conical shells reinforced with agglomerated carbon nanotubes was explained by Kamarian et al. [2016]. The equation of motion was derived by first order shear deformation theory. To obtain natural frequencies of the structure the generalized differential method was implemented. A parametric study was developed to investigate the influence of some characteristic parameters on vibrational behavior of conical shell. Sahoo [2016] evaluated the performance of free vibration of laminated composite stiffened hyperbolic paraboloid shell panel with cut-out. Finite element analysis of laminated composite skew hypar shell under oblique impact was studied by Neogi et al. [2017]. Time dependent equations were solved using Newmark's Time integration algorithm. Monge et al. [2018] studied

static analysis of laminated composite doubly curved shells using kinematic model with polynomial and non-polynomial functions. Halder et al. [2019] studied bending analysis of composite skew cylindrical shell panel. An experimental study of unstiffened graphite-epoxy cylindrical shells with cut-outs subjected to bending load was presented by Labans et al. [2019]. Nwoji et al. [2021] studied static bending of isotropic circular cylindrical shells based on higher order shear deformation theory.

2.3 CRITICAL DISCUSSION

A thorough scrutiny of available literature on the bending behavior of laminated composite hypar shells with a cutout reveals that no study has been reported so far on this aspect. Sanders Jr. [1970] and Ghosh and Bandyopadhyay [1994] have considered the bending of isotropic shells with a cutout. The static behavior of a cylindrical composite panel in presence of cutouts has been reported using a geometrically non-linear theory [Dennis and Palazotto, 1990] while the free vibration of cylindrical panel with square cutout has been studied based on finite element method [Sivasubramanian et al., 1997]. The axisymmetric free vibration of isotropic shallow spherical shell with circular cutout has also been analyzed [Hwang and Foster Jr., 1992]. Madenci and Barut [1994] studied buckling of composite panels in presence of cutouts. Non-linear post-buckling analysis of composite cylindrical panels with central circular cutouts but having no stiffeners was studied by Noor et al. [1996] to consider the effect of edge shortening as well as uniform temperature change. Later Sai Ram and Babu [2001a, b] investigated the bending behavior of axisymmetric composite spherical shell both punctured and un-punctured using the finite element method based on a higher order theory. Qatu et al [2012] reviewed the recent research studies on the static and buckling / post-buckling behavior of composite shells. Qatu et al. [2010] reviewed the work done on the vibration aspects of composite shells between 2000-2009 and observed that most of the researchers dealt with closed cylindrical shells. Other shell geometries are also receiving considerable attention. Recently, Kumar et al. [2013a, b, c, 2014] considered finite element formulation for shell analysis using higher order zigzag theory. Vibration analysis of spherical shells and panels both shallow and deep has also been reported for different boundary conditions [Ye et al., 2013, 2014a, b]. A complete and general view on mathematical modeling of laminated composite shells using higher order formulations has been provided in recent literature [Tornabene et al., 2014a, b, 2013]. However, the bending behavior of antisymmetric angle-ply

laminated composite stiffened hypar shell with cutout for various boundary conditions is scanty in the literature.

Some of the earlier information regarding the behavior of doubly curved composite shells [Narita and Leissa, 1984; Reddy and Chandrashekhara, 1985] considered the practical boundary condition like corner point support and presented the frequency and mode shapes of spherical, circular cylindrical and hyperbolic paraboloidal (bounded by parabolas) shells. Liew et al. [1993] analyzed plates and shells for bending, buckling and vibration behavior using a super element. Point supported boundary conditions were also considered [Schwarte, 1994; Chakravorty et al., 1995]. Qatu and Leissa [1991a, b] studied the free vibration behavior of doubly curved laminated composite shallow shells. Qatu and Leissa [1991c], and Sivasubramonian et al. [1997] studied the free vibration characteristics of doubly curved panels considering combinations of different boundary conditions. Liew and his colleagues [1994a-e, 1995a-d, 1996] carried out extensive research work on the vibrations of different types of shell surfaces. The developments in the vibration of shallow shells reviewed in an excellent paper by Liew et al. [1997]. The fundamental frequencies of hypar shells with different boundary conditions were also reported [Chakravorty et al., 1998; Sahoo and Chakravorty, 2005]. Pradyumna and Bandyopadhyay [2008] reported the vibration characteristics of composite hypar shells based on HSDT but they did not consider higher modes, hence further improvement in these results have to be sought.

In this field of shell research, large number of research articles [Richards et al., 2001; Nayak and Bandyopadhyay, 2002a, b; 2005, 2006, Sahoo and Chakravorty, 2005, 2006; Kumar et al., 2012, 2013, 2015; GulshanTaj and Chakraborty, 2013; Tornabene et al., 2015; Dey et al., 2015; Zhang et al., 2016] is available. Free vibration aspects of stiffened shell panels with cut-out for six shell forms, viz., cylindrical, elliptic paraboloid, hyperbolic paraboloid, hypar, conoid and spherical shells have been studied using finite element method [Sahoo, 2012, 2013, 2014a, b, 2015a, b; 2016]. But analysis of stiffened shell with cut-out for modes of vibration other than fundamental mode are scanty in the literature. Though Topal [2006], Srinivasa et al. [2014] presented the mode frequency analysis of laminated spherical shell but they did not consider hypar shells. Despite the engineering importance of cut-outs involved in composite panels, the number of research articles and reports in the subject topic are found to be limited. Some recent studies have addressed advanced aspects such as stochastic natural frequencies [Dey et al., 2016].

However, it is observed that there is no literature available on free vibration analysis of composite stiffened hypar shells with cut-out for other natural modes.

Design of stacking sequence for optimization of vibration frequency of laminated structures is a common approach [Narita and Nitta, 1998; Hufenbach et al., 2002; Narita and Robinson, 2006]. Discrete material optimization [Stegmann and Lund, 2005] using finite element approach has also been attempted for optimization of fiber angle and material. Genetic algorithm is employed for optimization of composite structures with respect to vibration and buckling [Narita et al, 1996; Narita and Zaho, 1998; Roy and Chakraborty, 2009]. Modified feasible direction technique was utilized [Topal, 2009; 2012] to maximize the fundamental frequency for varying thickness ratios and aspect ratios of shells. Other modern advanced heuristic algorithms [Aymerich and Serra, 2008; Sebaey et al., 2013; Erdal and Sonmez, 2005; Almeida, 2016; Rao and Arvind, 2005; Gholami et al, 2021; Barroso et al, 2017; Kaveh et al., 2018; Vo-Duy et al., 2017] were also utilized for stacking sequence design of composites. However, features of most heuristic algorithms are random in the search process. Accordingly, local optimum or pre-convergence may occur if initial parameters are unsuitable. Reliable optimization results depend only on designers' experience. Also, computational cost of heuristic algorithms is relatively high. Thus, researchers are on the search of alternative ways of optimization. Shahgholian-Ghahfarokhi and Rahimi [2020] recently used Taguchi approach [Taguchi, 1990] to consider a sensitivity study of vibration of composite sandwich cylindrical shells having grid cores. Dynamic behavior of plates and shells made of different types of materials has been analysed [Duc, 2014]. Galerkin method coupled with higher order shear deformation theory has been used for analyzing stability and vibration behavior of such structure under different types of loadings.

SCOPE OF PRESENT STUDY

3.1 GENERAL

Literature review presented in the last chapter explained developments on shell research in recent past two decades. It has been found that skewed hypar shell configuration has received significant attention from researchers due to its relevance to practical applications. But the behavior of cutout borne shell in terms static and dynamics response has received relatively less attention. Maximization of fundamental frequencies of hypar shell based on parametric variations is yet to receive proper attention from researchers. To avoid the resonance due to ground vibration and natural disturbances, fundamental frequency needs to be maximized depending on various shell parameter. Accordingly, finite element method is used to determine bending characteristics and vibration frequencies of cutout borne stiffened laminated composite hypar shells. Design of experiments approach is utilized to obtain the optimum fundamental frequency of the shell.

3.2 PRESENT SCOPE

A mathematical formulation in terms of finite element method is presented in Chapter 4. An eight noded curved isoparametric shell bending element is combined with three noded curved isoparametric beam element to develop finite element code for analyzing bending and free vibration characteristics of stiffened skewed hypar shells with cutout. The review of literature presented in the previous chapter reveals that static analysis of laminated composite cylindrical, spherical, elliptical and paraboloid shells have received quite large attention. But the investigations on static and dynamic behavior of laminated composite stiffened hypar shell with cut-out at different parametric variations have not received much attention.

Static behavior of laminated composite stiffened hypar shell with cut-out at various ply orientations, different boundary conditions and cut-out positions has been discussed in Chapter 5. Benchmark problems have been solved and results are compared with the present approach. Numerical problems have been solved to obtain force, moment and deflection values subjected to static loading at different ply orientation and different boundary conditions for stiffened composite hypar shell with cut-out. The results are discussed in details and significant conclusions are identified. Dynamic analysis of laminated composite stiffened hypar shell with cut -out has been studied in Chapter 6. This study deals with vibration analysis of a hypar shell stiffened along the margin of cut outs with different boundary conditions and antisymmetric angle ply lamination. The formulation is based on first order shear deformation theory. The numerical studies are conducted to determine the effects of degree of orthotropy (E_{11}/ E_{22}), fibre orientation (θ) and width to thickness ratio (b/h) on the non-dimensional fundamental frequency. The results are given in graphical form and tabular charts as necessary. Mode frequency analysis of antisymmetric angle ply laminated stiffened hypar shell with cut-out at various boundary conditions and ply orientation has also been studied in Chapter 6. First five modes of natural frequencies are presented.

Extensive scrutiny of literature reveals paucity of reports on optimization of the fiber orientation, dimension, thickness, material orthotropy and position of the cutout for different edge constraints leading to maximum fundamental frequency of laminated shells. This issue is taken care of in Chapter 7. This study of stiffened hypar shells considers the application of the Taguchi method along with an efficient finite element formulation to determine the suitable combination of multi-parametric design optimization to yield maximum frequency of cutout borne shell. Taguchi orthogonal design is applied with four design factors namely, fiber orientation, width-to-thickness, level of orthotropy of the composite and position of the cutout as independent variables. Taguchi analysis is performed to obtain the suitable combination of factors that results maximum fundamental frequency.

The different conclusions that are arrived at Chapters 5 to 7 are included in the respective chapters only. Chapter 8 presents abroad conclusion of overall study and indicates some future scope of research.

Chapter 4

MATHEMATICAL FORMULATION

4.1 GENERAL

This chapter deals with mathematical formulation and solution methods for bending and vibration characteristics of laminated composite unstiffened and stiffened hypar shells. In the finite element analysis, the structure has to be discretized into a number of elements connected at the nodal points. In present analysis, the surface of stiffened shells is discretized into number of elements. Each element is further combined of shell element and beam element. The stiffeners placed along *X*- direction are known as *x* stiffener and those placed along *Y*- direction are known as *y* stiffener. The overall element matrices of the stiffened shell element are obtained by combinations of element matrices of shell element and beam elements at shell nodal points. The mathematical formulation of shell and beam element are presented in section 4.2. The implementation of boundary conditions and the solution procedure is detailed in section 4.3. Modeling of the cutout is discussed in section 4.4. The suitable information about the computer program and input parameters is included in section 4.5.

4.2 FINITE ELEMENT FORMULATION

A laminated composite hypar shell with cutout is shown in Fig.4.1. Differentiating the surface equation of shell in the form z = f(x, y) yields the radius of cross curvature R_{xy} and for shallow shells considered in the present study the same is expressed as $\frac{1}{R_{xy}} = \frac{d^2 z}{dxdy}$. An eight noded-curved quadratic isoparametric element (Fig. 4.2) is used for the analysis of hypar shell.

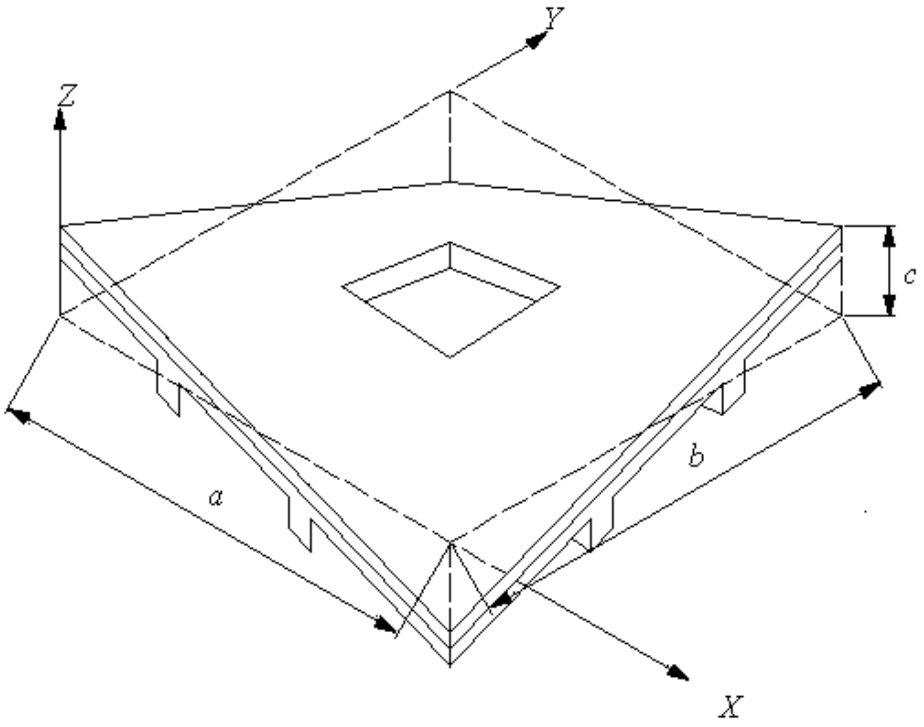

Surface equation: $z = \frac{4c}{ab}(x - a/2)(y - b/2)$

Fig. 4.1 Surface of a skewed hypar shell with cutout

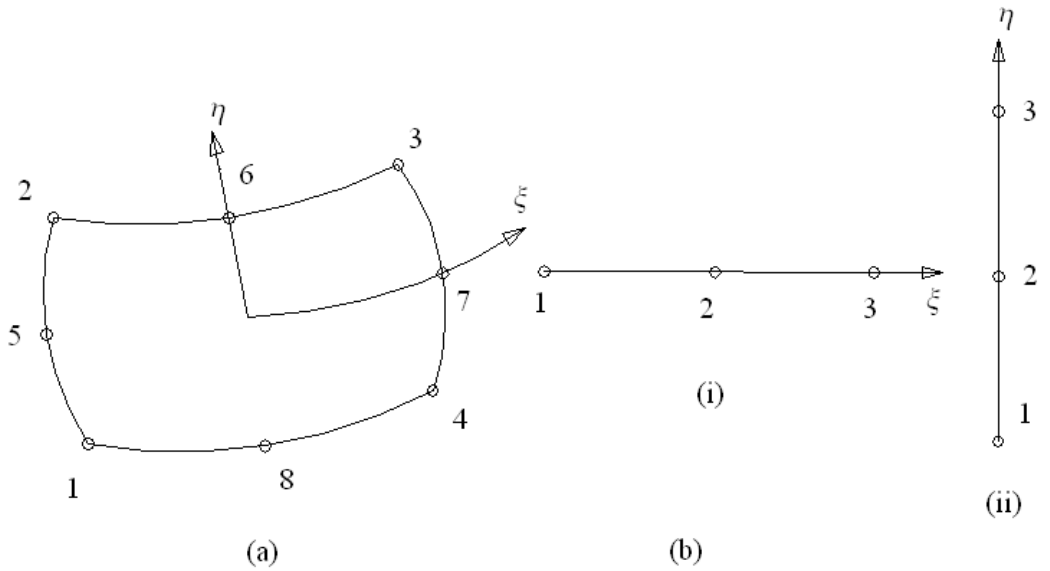

Fig.4.2 (a) Eight noded shell element with isoparametric co-ordinates (b) Three noded stiffener elements (i) x-stiffener (ii) y-stiffener

The five degrees of freedom taken into consideration at each node are u, v, w, α, β. The relations between the displacement at any point with respect to the co-ordinates ξ and η and the nodal degrees of freedom are expressed as:

$$u=\sum_{i=1}^{8}N_i u_i \qquad v=\sum_{i=1}^{8}N_i v_i \qquad w=\sum_{i=1}^{8}N_i w_i \qquad \alpha=\sum_{i=1}^{8}N_i \alpha_i \qquad \beta=\sum_{i=1}^{8}N_i \beta_i \tag{4.1}$$

In the isoparametric formulation the element geometry is also defined by the same shape functions,

i.e., $x=\sum_{i=1}^{n}N_i x_i \qquad y=\sum_{i=1}^{n}N_i y_i$. (4.2)

Here the shape functions are derived from a cubic interpolation polynomial and are given as:

$N_i=(1+\xi\xi_i)(1+\eta\eta_i)(\xi\xi_i+\eta\eta_i-1)/4$ for i=1, 2, 3, 4

$N_i=(1+\xi\xi_i)(1-\eta^2)/2$ for i=5,7

$N_i=(1+\eta\eta_i)(1-\xi^2)/2$ for i=6,8 (4.3)

The cubical shape functions [*N*] adopted in the present study is same as those reported elsewhere [Sahoo and Chakravorty, 2006].

The constitutive equations for the shell are given by (a list of notations is provided separately):

$\{F\}=[D]\{\varepsilon\}$ (4.4)

where $\{F\}=\{N_x \quad N_y \quad N_{xy} \quad M_x \quad M_y \quad M_{xy} \quad Q_x \quad Q_y\}$ (as shown in Fig. 4.3)

and $\{\varepsilon\}=\{\varepsilon_x^0 \quad \varepsilon_y^0 \quad \gamma_{xy}^0 \quad k_x \quad k_y \quad k_{xy} \quad \gamma_{xz}^0 \quad \gamma_{yz}^0\}^T$

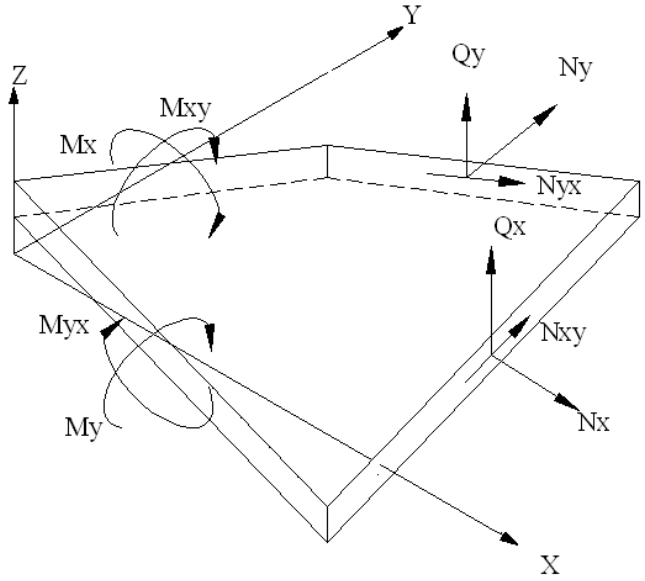

Fig. 4.3 Generalized force and moment resultants

The laminate constitutive matrix [*D*] and the finite element formulation for stiffeners used in the present study are adopted from Sahoo and Chakravorty [2006].

The strain vector is related to the nodal values of element degree of freedoms by the strain displacement matrix [*B*]. The strain displacement matrix [*B*] is also adopted from Sahoo and Chakravorty [2006].

The strain-displacement relation is given by

$$\{\varepsilon\} = [B]\{d_e\}, \tag{4.5}$$

where $\{d_e\} = \{u_1 \quad v_1 \quad w_1 \quad \alpha_1 \quad \beta_1 \quad . \quad . \quad . \quad . \quad . \quad u_8 \quad v_8 \quad w_8 \quad \alpha_8 \quad \beta_8\}^T$,

$$[B] = \sum_{i=1}^{8} \begin{bmatrix} N_{i,x} & 0 & 0 & 0 & 0 \\ 0 & N_{i,y} & 0 & 0 & 0 \\ N_{i,y} & N_{i,x} & -2N_i / R_{xy} & 0 & 0 \\ 0 & 0 & 0 & N_{i,x} & 0 \\ 0 & 0 & 0 & 0 & N_{i,y} \\ 0 & 0 & 0 & N_{i,y} & N_{i,x} \\ 0 & 0 & N_{i,x} & N_i & 0 \\ 0 & 0 & N_{i,y} & 0 & N_i \end{bmatrix}$$

Improved first order approximation theory for thin shell is used to establish the strain-displacement relations and the same are given as:

$$\{\varepsilon_x \quad \varepsilon_y \quad \gamma_{xy} \quad \gamma_{xz} \quad \gamma_{yz}\}^T = \{\varepsilon_x^0 \quad \varepsilon_y^0 \quad \gamma_{xy}^0 \quad \gamma_{xz}^0 \quad \gamma_{yz}^0\}^T + z\{k_x \quad k_y \quad k_{xy} \quad k_{xz} \quad k_{yz}\}^T \tag{4.6}$$

Where, $\begin{Bmatrix} \varepsilon_x^0 \\ \varepsilon_y^0 \\ \gamma_{xy}^0 \\ \gamma_{xz}^0 \\ \gamma_{yz}^0 \end{Bmatrix} = \begin{Bmatrix} \partial u / \partial x \\ \partial v / \partial y \\ \partial u / \partial y + \partial v / \partial x - 2w / R_{xy} \\ \alpha + \partial w / \partial x \\ \beta + \partial w / \partial y \end{Bmatrix} and \begin{Bmatrix} k_x \\ k_y \\ k_{xy} \\ k_{xz} \\ k_{yz} \end{Bmatrix} = \begin{Bmatrix} \partial \alpha / \partial x \\ \partial \beta / \partial y \\ \partial \alpha / \partial y + \partial \beta / \partial x \\ 0 \\ 0 \end{Bmatrix}$

In the above expression, the first vector denotes the mid-surface strain for a hypar shell and the second vector denotes the curvature.

The element stiffness matrix is

$$[K_{she}] = \iint [B]^T [D][B] dxdy \tag{4.7}$$

The two-dimensional integral is then converted to isoparametric coordinates and is evaluated by 2x2 Gauss-quadrature. This is because the shape functions are derived from a cubic interpolation polynomial and a polynomial of degree 2n-1 is integrated exactly by n point Gauss quadrature.

4.2.1 Finite Element Formulation for Stiffener of the Shell

The stiffeners are modeled using three noded curved isoparametric beam elements which are considered to run only along the boundaries of the shell elements. The shape functions of these beam elements for x and y directional stiffeners (shown in Fig. 4.2) are as follows:

For x-stiffeners:

$$N_{\xi i} = \xi\xi_i\left(1+\xi\xi_i\right) \qquad \text{for i=1,3,}$$

$$N_{\xi i} = \left(1-\xi^2\right) \qquad \text{for i=2.} \tag{4.8}$$

For y-stiffeners:

$$N_{\eta i} = \eta\eta_i\left(1+\eta\eta_i\right) \qquad \text{for i=1,3,}$$

$$N_{\eta i} = \left(1-\eta^2\right) \qquad \text{for i=2.} \tag{4.9}$$

In the stiffener element, each node has four degrees of freedom i.e. u_{sx}, w_{sx}, α_{sx} and β_{sx} for x-stiffener and u_{sy}, w_{sy}, α_{sy} and β_{sy} for y-stiffener. The displacement field at any point can be expressed in terms of nodal displacements as follows:

for x-stiffener: $\left\{\delta_{sx}\right\} = \left[N_{\xi i}\right]\left\{\delta_{sxi}\right\}$

for y-stiffener: $\left\{\delta_{sy}\right\} = \left[N_{\xi i}\right]\left\{\delta_{syi}\right\}$ (4.10)

where, $\left\{\delta_{sxi}\right\} = \left[u_{sx1} \quad w_{sx1} \quad \alpha_{sx1} \quad \beta_{sx1} \quad . \quad . \quad . \quad u_{sx3} \quad w_{sx3} \quad \alpha_{sx3} \quad \beta_{sx3}\right]^T$,

$\left\{\delta_{syi}\right\} = \left[v_{sy1} \quad w_{sy1} \quad \alpha_{sy1} \quad \beta_{sy1} \quad . \quad . \quad . \quad v_{sy3} \quad w_{sy3} \quad \alpha_{sy3} \quad \beta_{sy3}\right]^T$.

The generalized force-displacement relation of stiffeners can be expressed as:

for x-stiffener: $\left\{F_{sx}\right\} = \left[D_{sx}\right]\left\{\varepsilon_{sx}\right\} = \left[D_{sx}\right]\left[B_{sx}\right]\left\{\delta_{sxi}\right\}$

for y-stiffener: $\left\{F_{sy}\right\} = \left[D_{sy}\right]\left\{\varepsilon_{sy}\right\} = \left[D_{sy}\right]\left[B_{sy}\right]\left\{\delta_{syi}\right\}$ (4.11)

where, $\left\{F_{sx}\right\} = \left[N_{sxx} \quad M_{sxx} \quad T_{sxx} \quad Q_{sxxz}\right]^T$

$\left\{\varepsilon_{sx}\right\} = \left[u_{sx.x} \quad \alpha_{sx.x} \quad \beta_{sx.x} \quad \left(\alpha_{sx} + w_{sx.x}\right)\right]^T$

and $\left\{F_{sy}\right\} = \left[N_{syy} \quad M_{syy} \quad T_{syy} \quad Q_{syyz}\right]^T$

$$\{\varepsilon_{sy}\} = \left[v_{sy.y} \quad \beta_{sy.y} \quad \alpha_{sy.y} \quad (\beta_{sy} + w_{sy.y}) \right]^T$$

Elasticity matrices are as follows:

$$[D_{sx}] = \begin{bmatrix} A_{11}b_{sx} & B'_{11}b_{sx} & B'_{12}b_{sx} & 0 \\ B'_{11}b_{sx} & D'_{11}b_{sx} & D'_{12}b_{sx} & 0 \\ B'_{12}b_{sx} & D'_{12}b_{sx} & \frac{1}{6}(Q_{44}+Q_{66})d_{sx}b_{sx}^3 & 0 \\ 0 & 0 & 0 & b_{sx}S_{11} \end{bmatrix}$$

and $$[D_{sy}] = \begin{bmatrix} A_{22}b_{sy} & B'_{22}b_{sy} & B'_{12}b_{sy} & 0 \\ B'_{22}b_{sy} & \frac{1}{6}(Q_{44}+Q_{66})b_{sy} & D'_{12}b_{sy} & 0 \\ B'_{12}b_{sy} & D'_{12}b_{sy} & D'_{11}d_{sy}b_{sy}^3 & 0 \\ 0 & 0 & 0 & b_{sy}S_{22} \end{bmatrix}.$$

where, $D'_{ij} = D_{ij} + 2eB_{ij} + e^2A_{ij}$

$$B'_{ij} = B_{ij} + eA_{ij} \tag{4.12}$$

A_{ij}, B_{ij}, D_{ij} and S_{ij} are the stiffness coefficients. Here the shear correction factor is taken as 5/6.

The sectional parameters are calculated with respect to the mid-surface of the shell by which the effects of eccentricity of the x-stiffener, e_{sx} and y-stiffener, e_{sy} are automatically included.

The element stiffness matrix:

for x-stiffener: $$[K_{xe}] = \int [B_{sx}]^T [D_{sx}][B_{sx}]dx$$

for y-stiffener: $$[K_{ye}] = \int [B_{sy}]^T [D_{sy}][B_{sy}]dy \tag{4.13}$$

The integrals are then converted to isoparametric coordinates and are evaluated by 2 point Gaussian quadrature.

Finally, appropriate matching of the nodes of the stiffener and shell elements through the connectivity matrix yields the element stiffness matrix of the stiffened shell and the same is given as:

$$[K_e] = [K_{she}] + [K_{xe}] + \lfloor K_{ye} \rfloor. \tag{4.14}$$

The element stiffness matrices are assembled to get the global matrices.

4.2.2 Element Mass Matrices

The element mass matrix for shell is obtained from the integral

$$[M_e] = \iint [N]^T [P][N] dxdy, \tag{4.15}$$

where,

$$[N] = \sum_{i=1}^{8} \begin{bmatrix} N_i & 0 & 0 & 0 & 0 \\ 0 & N_i & 0 & 0 & 0 \\ 0 & 0 & N_i & 0 & 0 \\ 0 & 0 & 0 & N_i & 0 \\ 0 & 0 & 0 & 0 & N_i \end{bmatrix}, \qquad [P] = \sum_{i=1}^{8} \begin{bmatrix} P & 0 & 0 & 0 & 0 \\ 0 & P & 0 & 0 & 0 \\ 0 & 0 & P & 0 & 0 \\ 0 & 0 & 0 & I & 0 \\ 0 & 0 & 0 & 0 & I \end{bmatrix},$$

in which

$$P = \sum_{k=1}^{np} \int_{z_{k-1}}^{z_k} \rho dz \text{ and } I = \sum_{k=1}^{np} \int_{z_{k-1}}^{z_k} z\rho dz \tag{4.16}$$

Element mass matrix for stiffener element

$$[M_{sx}] = \iint [N]^T [P][N] dx \qquad \textit{for X stiffener}$$

and $$[M_{sy}] = \iint [N]^T [P][N] dy \qquad \textit{for Y stiffener} \tag{4.17}$$

Here, $[N]$ is a 3x3 diagonal matrix.

$$[P] = \sum_{i=1}^{3} \begin{bmatrix} \rho.b_{sx}d_{sx} & 0 & 0 & 0 \\ 0 & \rho.b_{sx}d_{sx} & 0 & 0 \\ 0 & 0 & \rho.b_{sx}d_{sx}^2/12 & 0 \\ 0 & 0 & 0 & \rho(b_{sx}.d_{sx}^3 + b_{sx}^3.d_{sx})/12 \end{bmatrix} \textit{for X-stiffener}$$

$$[P] = \sum_{i=1}^{3} \begin{bmatrix} \rho.b_{sy}d_{sy} & 0 & 0 & 0 \\ 0 & \rho.b_{sy}d_{sy} & 0 & 0 \\ 0 & 0 & \rho.b_{sy}d_{sy}^2/12 & 0 \\ 0 & 0 & 0 & \rho(b_{sy}.d_{sy}^3 + b_{sy}^3.d_{sy})/12 \end{bmatrix} \textit{for Y stiffener}$$

The mass matrix of the stiffened shell element is the sum of the matrices of the shell and the stiffeners matched at the appropriate nodes.

$$[M_e] = [M_{she}] + [M_{xe}] + [M_{ye}]. \tag{4.18}$$

The element mass matrices are assembled to get the global matrices.

4.3 IMPOSITION OF BOUNDARY CONDITIONS AND SOLUTION PROCEDURE

Imposing boundary conditions mean the presence or absence of generalized displacements u, v, w,α, β in different nodes of the discretized structures. The zero displacement boundary conditions are incorporated by removing the corresponding terms from the global matrices and vector. A 2x2 Gauss quadrature is used to integrate to stiffness, mass and load matrices of the shell element because shape functions are derived from cubic interpolation polynomial. In a similar way 2-point Gauss quadrature is used to integrate stiffness and mass matrices of beam element.

The static and free vibration analysis are only special cases of general dynamic problem and the solution techniques are elaborated in the following sub-sections.

4.3.1 Formulation of General Dynamic Problem

Hamilton's principle, when applied to undamped dynamic analysis of an elastic body, provides the equation as given by

$$[M]\{\ddot{d}\} + [K]\{d\} = \{P\} \tag{4.19}$$

where $[M]$ and $[K]$ are the global mass and stiffness matrices, and $\{P\}$ and $\{d\}$ are the global load and displacement vectors.

4.3.2 Formulating Static Problem

If the inertia force term of equation (4.19) is dropped and the displacement and load vectors are assumed to be time independent the following equation of static equilibrium is obtained,

$$[K]\{d\} = \{P\} \tag{4.20}$$

After imposing the boundary conditions, the Gauss elimination technique is used to solve the above equation that yields the global nodal displacement vector $\{d\}$. Hence the element displacement vectors $\{d_e\}$ are known. Using $\{d_e\}$ in equation (4.5) the strains can be evaluated at the Gauss

points, which when used in equation (4.4) the generalized force and moment resultants are obtained at the Gauss points. Extrapolation of these values yields the nodal values.

4.3.3 Formulating Free Vibration Problem

If the load vector of equation (4.19) is dropped, the equation of free vibration is obtained as

$$[M]\{\ddot{d}\} + [K]\{d\} = 0 \quad (4.21)$$

In this equation (4.21) the displacement $\{d\}$ is a function of space and time. To solve free vibration problem separation of space and time coordinates is done by following substitution

$$\{d(x,y,z,t)\} = ae^{i\omega t}\{\varphi(x,y)\}$$

or $$\{d\} = ae^{i\omega t}\{\varphi\} \quad (4.22)$$

therefore, $$\{\ddot{d}\} = -a\omega^2 e^{i\omega t}\{\varphi\} \quad (4.23)$$

Substituting equations (4.22) and (4.23) into equation (4.21) obtain

$$ae^{i\omega t}(-\omega^2[M]\{\varphi\} + [K]\{\varphi\}) = 0 \quad (4.24)$$

As $ae^{i\omega t} \neq 0$ in equation (4.22) is an assumed solution, therefore,

$$\omega^2[M]\{\varphi\} = [K]\{\varphi\} \quad (4.25)$$

where ω and $\{\varphi\}$ represent natural frequencies the corresponding eigenvectors of the generalized eigen value problem. The problem is solved by the subspace iteration algorithm.

4.4 MODELING OF CUTOUT

In regards to modeling of the cutout, the code developed can take the position and size of cutout as input. The program is capable of generating non uniform finite element mesh all over the shell surface. So the element size is gradually decreased near the cutout margins. One such typical mesh arrangement is shown in Fig.4.4. Such finite element mesh is redefined in steps and a particular grid is chosen to obtain the fundamental frequency when the result does not improve by more than one percent on further refining. Convergence of results is ensured in all the problems taken up here.

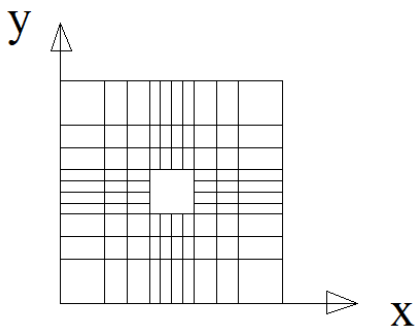

Fig.4.4 Typical 10x10 non-uniform mesh arrangement drawn to scale

4.5 COMPUTER PROGRAM AND INPUT PARAMETERS

To execute the mathematical formulation described in preceding sections, computer code is developed in Fortran language to solve problems of static bending and free vibration response of laminated composite hypar shells with cutout. The program can incorporate various boundary conditions among corner point supported, simply supported and clamped edges. The program can generate uniform and non-uniform meshes once the number of divisions along two directions and length of each division as a fraction of total plan dimension along the respective direction are provided. The program can include the size and position of cut-out along x and y direction as input. The basic input data for the program include a) the geometric dimension of the shell, b) stiffener positions and dimensions, c) cut-out position, d) material properties, e) the load, f) the mesh division, g) the stacking sequences, h) boundary conditions, i) number of frequencies to be evaluated, j) static shell actions to be evaluated. The details of the numerical problems and the results obtained are presented and discussed in the next chapters.

Chapter 5

BENDING BEHAVIOR

5.1 GENERAL

The mathematical formulation given in previous chapter is applicable for static and dynamic analysis of laminated composite unstiffened / stiffened hypar shell with or without cut-out. In this chapter bending behavior of stiffened hypar shell with cut-out has been investigated. Some benchmark problems have been identified in section 5.2 as obtained from available literature, which are close to the scope of present study. Those problems are solved using the present formulation and the results are compared with the previous ones to check the correctness of the present formulation. In section 5.3 some additional examples of laminated composite stiffened hypar shells with cut-out are considered with different parametric variations. The results are analyzed critically from different angles of variations and discussed accurately to show their engineering applications. Results having maximum practical implications are analyzed for the sake of brevity.

5.2 BENCHMARK PROBLEMS

To establish the correctness of the static formulations of the finite element code proposed here, for the analysis of stiffened shells with cutout are compared with pre-established results reported by Rossow and Ibrahimkhail [1978] using constrained method of finite element analysis, by Chang [1973] using conventional method of analysis, by Sinha et al. [1992] and also by using structural packages NASTRAN, STRUDL. Static displacements of simply supported plates are evaluated using the present formulation and a comparison of central displacements obtained by different methods is presented in Table 5.1. The material and geometric properties of the plates are presented with the table as footnote. In order to solve a plate problem with the present formulation, the corner rise of the hypar (c) is made zero. Present composite shell formulation is used for the isotropic material by making the elastic and shear moduli equal in all directions.

To validate the cutout formulation of the present code, additional problem is solved as benchmark. The second problem was solved earlier by Chakravorty et al. [1998] and deals with free vibration of hypar shell with cutouts having simply supported and clamped boundary conditions. The relevant parameters are furnished with Table 5.2 showing the correctness of the cutout formulation. The finite element mesh is refined in steps and a particular grid is chosen to obtain the fundamental frequency when the result does not improve by more than one percent on further refining. Convergence of results is ensured in all the problems taken up here.

Table 5.1 Central deflection of rectangular stiffened plate in inches ($x10^3$).

Source	Concentrated Load		Distributed Load	
	Eccentric	Concentric	Eccentric	Concentric
Rossow and Ibrahimkhail [1978]	1.270	3.464	8.850	24.075
Chang [1973]	1.246	3.464	8.996	24.077
NASTRAN	1.240	-	8.714	-
STRUDL	-	3.463	-	24.120
Sinha et al.[1992]	1.284	3.464	9.322	24.075
Present method	1.313	3.492	8.905	24.011

$E=30x10^6$ psi; $\nu=0.3$; a=30 in; b=60 in; h=0.25 in; x-stiffener 0.5x5.0 in^2; y-stiffener 0.5x3.0 in^2.

Table 5.2: Non-dimensional fundamental frequencies ($\bar{\omega}$) for hypar shells (lamination $(0/90)_4$) with concentric cutouts.

a'/a	Chakravorty et al. [1998]		Present finite element model					
	Simply supported	clamped	Simply supported			clamped		
			8x8	10x10	12x12	8x8	10x10	12x12
0.0	50.829	111.600	50.573	50.821	50.825	111.445	111.592	111.612
0.1	50.769	110.166	50.679	50.758	50.779	109.987	110.057	110.233
0.2	50.434	105.464	50.323	50.421	50.400	105.265	105.444	105.443
0.3	49.165	101.350	49.045	49.157	49.178	101.110	101.340	101.490
0.4	47.244	97.987	47.132	47.242	47.141	97.670	97.985	97.991

a/b=1, a/h=100, a'/b' =1, c/a=0.2; E_{11}/E_{22} = 25, G_{23} = $0.2E_{22}$, G_{13} = G_{12} = $0.5E_{22}$, ν_{12} =ν_{21} =0.25.

Table 5.1 and Table 5.2 show very good agreement of the present results with the established ones and this validate the static formulation of stiffened hypar shell with cutout. Table 5.2 also shows the convergence of fundamental frequencies with increasingly finer mesh and a 10×10 division is taken up for further study since the values do not improve by more than 1% on further refining. Close agreement of present results with benchmark ones establish the fact that the finite element model proposed here is capable of analyzing static problems of stiffened skewed hypar composite shells with cutout.

5.3 BENDING CHARACTERISTICS OF SHELLS WITH CUTOUT

5.3.1 Relative performance of antisymmetric angle-ply shells

Non-dimensional static displacements and stress resultants of composite stiffened hypar shells with cutouts are presented in Table 5.3 to Table 5.15 for different antisymmetric angle ply stacking sequences of graphite-epoxy composite with six different boundary conditions (Fig. 5.1). Orthotropic shells (0^0, 90^0) are also included to study the variation of deflection and stress resultants with change in lamination angle. The boundary conditions are designated as: C for clamped, S for simply supported and F for free edges. The four edges are considered in an anticlockwise order from the edge $x = 0$. For example, a shell with CSCS boundary is clamped along $x = 0$, simply supported along $y = 0$ and clamped along $x = a$ and simply supported along $y = b$. Governing static force and moment resultants (including the deflection, in-plane forces and bending moments which govern the shell thickness) are presented. Performances of the shell combinations in terms of their stress resultants are ranked from 1 to 6. For ranking, only the antisymmetric angle ply stacking sequences are considered. The first rank is given to the shell combination showing least static stress resultant value. Such ranks are very helpful to understand the relative behavior of shell options comprehensively.

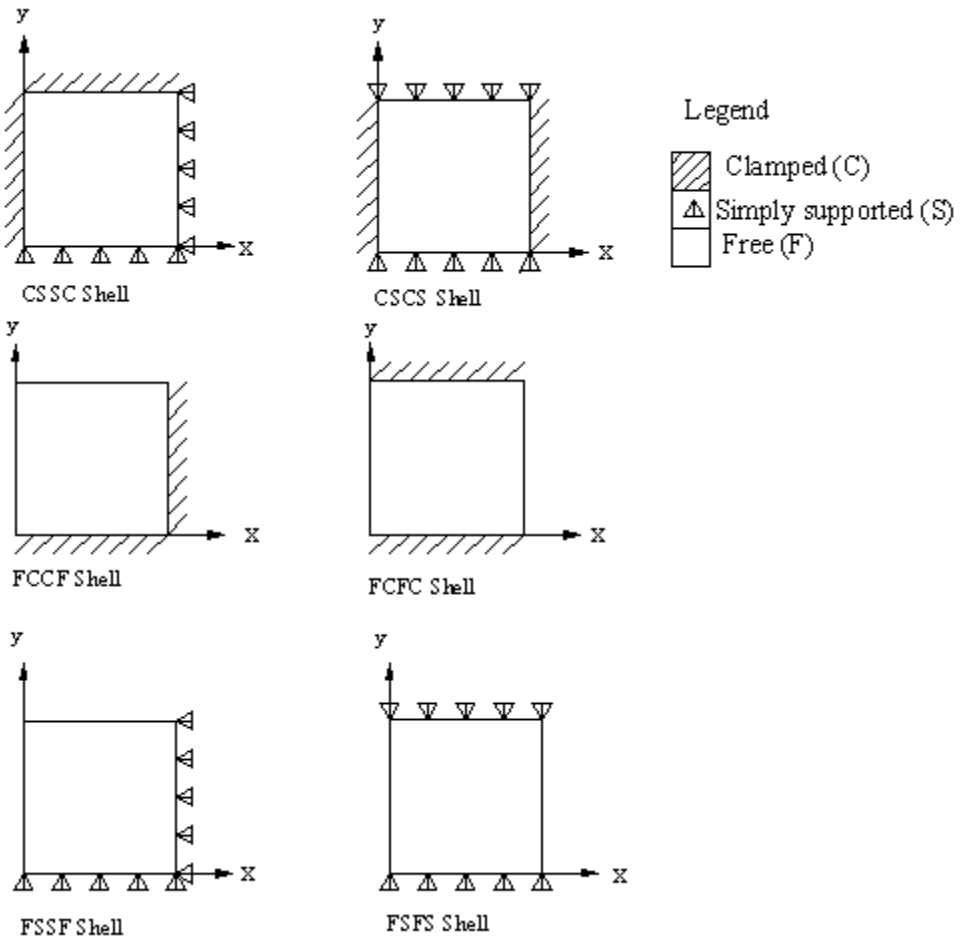

Fig. 5.1 Arrangement of boundary conditions

5.3.1.1 *Effect of boundary conditions on relative performance of composite stiffened hypar shells with cutouts*

Close observation in terms of static deflections from Table 5.3 reveal that Group III shells show lower values when compared to Group I shells for any given lamination. This is quite obvious as in Group I boundary condition, increased number of boundary restraints restrict its possible movements along the boundaries and makes the shell stiffer compared to Group II ones which in turn exhibit lesser deflections than Group III shell, where more number of support degrees of freedom are released. But it is further noted from Table 5.3 that when a free edge is introduced into a shell maximum deflection occurs along the free edges otherwise maximum deflection occur along the periphery of the cutout.

It is further noted from Table 5.3 that deflection increases significantly when a Group IA shell is replaced by a Group IIA shell. However, if a Group IIA shell is replaced by a Group IIIA shell the deflection increases marginally and at times by an insignificant amount. The same trend is noticeable for Group IB, Group IIB and Group IIB shell as well. If Group IB shell is replaced by a Group IIB shell, deflection significantly increases but when a Group IIB shell is replaced by a Group IIIB shell the increase in deflection is not so significant.

A close observation of the results for Group I boundary conditions reveals that the CSSC shells are superior in performance showing lesser deflections than CSCS shells for the antisymmetric angle ply laminates having lamination angle upto 45^0. But reverse is the case for lamination angles greater than 45^0 where CSCS edge shows higher static stiffness than CSSC edge. Thus CSCS shells are better choices than CSSC ones for higher lamination angles.

It is further noted that shells of Group I having CSSC and CSCS boundaries have comparable maximum deflection. But in case of Group II and Group III shells a change in the arrangement of boundary constraints has huge impact on static stiffness. When two opposite free edges are introduced in a shell, it is far stiffer than a shell for which two adjacent edges are free. As a result, FCFC and FSFS shells show less deflection than FCCF and FSSF shells. This is true for all laminations except 45^0 lamination angle, where reverse trend is observed. Thus while keeping the number of support constraints fixed, a change of arrangement of the conditions of individual edges involving free edges markedly influences the maximum deflection.

Comparative study of governing static stress resultants shows that performance of Group I shells is not at all comparable with other groups (Group II and Group III) for in-plane forces and in-plane shear. Only for a few cases in-plane force and in-plane shear shows comparable values. But for sagging, hogging and twisting moment resultants, although Group I shells show lower value than Group II and Group III shells, again a very few exception is there. These findings reinforce the fact that in composite shells, lamination angle plays a very important role along with the support condition to determine resultant stiffness. It is also evident that relative performance study of shells in terms of their deflections cannot be taken as the only basis of comparing their overall performance. A closed scrutiny of the results also reveals that, Group I shells exhibit maximum static stress resultants around the cutout but Group II and Group III shells show towards the free edges.

5.3.1.2 *Relative performance of shells for different lamination angles*

In civil engineering applications among two shell forms the one which exhibits lower deflection is accepted as a better option from serviceability point of view. It is evident from Table 5.3 that, for a given number of boundary constraints, $(+45/-45)_5$ antisymmetric laminate is the best choice. Also number of lamina plays an important role in static deflection consideration. In all the cases considered here, 10 layer antisymmetric laminates are convincingly better than four layer and two-layer angle ply ones. It is interesting to note from Tables 5.4-5.15, that for all the boundary conditions for any two laminations the one which performs better in terms of deflection is not better in terms of other static stress resultants. For static stress resultants like $+\overline{N}_x, -\overline{N}_x, -\overline{M}_x$ lower lamination angle and for $+\overline{N}_y, -\overline{N}_y, -\overline{M}_y$ higher lamination angle is better choices but for other shell actions however, such unified behavior is not found to hold good.

Results of Table 5.3 to Table 5.15 show that in general 10 layer laminates exhibit better performance compared to two and four layered ones in terms of static deflections and static stress resultants with a few exceptions where 4 layer laminates are better than 10 layer laminates.

5.3.1.3 *Performances of Different Boundary Conditions with respect to different Shell Actions*

Now an attempt is made in the present study of antisymmetric angle ply laminates to compare the relative performance of boundary conditions. For each shell action, the best two combinations of lamination and edge condition are selected from each of three groups of boundary conditions. Thus total six combinations are selected from three Groups. These have been furnished in Table 5.16 and Table 5.17 for positive and negative values of shell actions in ascending order of magnitude. For example, the CSCS/(30/-30) shell is the best choice for both positive and negative $\overline{N}_x$ while CSCS (75/-75) shell is the best choice for both positive and negative $\overline{N}_y$. This rank wise arrangement of the shells in terms of lamination along with boundary condition corresponding to the different shell actions will help a design engineer to make a choice among a number of options when it is known that which shell action is critical for a particular situation. It is noteworthy to mention here that superiority of a particular shell combination expressed in terms of lamination and boundary conditions for one particular shell action cannot be used as the guideline of predicting the relative performances for other shell actions.

Based on the results available in Tables 5.3-5.15, it is possible to develop a relative performance matrix of the shells so as to help a design engineer to conclusively decide upon the selection among two different combinations of laminations and boundary conditions. The relative performance matrix of the shells may be developed in the following way. Among two choices of lamination and edge condition, the superior combination is assigned a value of 1 while the inferior combination is assigned 0 with respect to different shell actions. If two combinations show almost equal values of a particular shell action, the number 1 may be assigned to both of them. One such typical performance matrix is shown in Table 5.18 comparing CSCS/$(15/-15)_2$ and CSCS/$(45/-45)_2$ shells. A design engineer can now take a conclusive decision for choice between two shells applying appropriate weightage factors to the different shell actions if such relative performance matrix is made available.

Table 5.3: Values of maximum non-dimensional downward deflections ($-\bar{w}$) x10^4 for different antisymmetric angle ply lamination and boundary conditions of stiffened composite hypar shell with cutout.

Lamination (Degree)	Boundary conditions					
	Group-I		Group-II		Group-III	
	A	B	A	B	A	B
	CSSC	CSCS	FCCF	FCFC	FSSF	FSFS
0	-1.3281 (0.55,0.4)	-1.4671 (0.5,0.6)	-5.3354 (0.5,1.0)	-1.983 (0.0,0.5)	-5.8823 (0.3,1.0)	-2.0482 (0.0,0.5)
(15/-15)	-0.51441 (0.5,0.4)	-0.57554 (0.5,0.4)	-5.7156 (0.7,1.0)	-1.0488 (0.0,0.5)*	-6.2017 (0.3,1.0)	-1.2776 (0.0,0.5)
$(15/-15)_2$	-0.4655 (0.5,0.4)	-0.52171 (0.5,0.4)	-4.432 (0.5,1.0)	-1.0504 (0.0,0.5)	-4.6521 (0.5,1.0)	-1.1396 (0.0,0.5)
$(15/-15)_5$	-0.4495 (0.6,0.45)	-0.50187 (0.5,0.4)	-4.1361 (0.5,1.0)	-1.0614 (0.0,0.5)	-4.2423 (0.5,1.0)	-1.1062 (1.0,0.5)*
(30/-30)	-0.27818 (0.6,0.5)	-0.2863 (0.5,0.6)	-4.1111 (0.7,1.0)	-1.3301 (1.0,0.5)	-4.3846 (0.3,1.0)	-1.4903 (1.0,0.5)

$(30/-30)_2$	-0.2363 (0.6,0.5)	-0.24699 (0.5,0.6)	-3.2274 (0.5,1.0)	-1.2836 (0.0,0.5)*	-3.3642 (0.5,1.0)	-1.3477 (1.0,0.5)
$(30/30)_5$	-0.22063 (0.6,0.5)	-0.2314 (0.5,0.4)	-3.0679 (0.5,1.0)	-1.2895 (0.0,0.5)	-3.1243 (0.5,1.0)	-1.3188 (1.0,0.5)*
(45/-45)	-0.24886 (0.6,0.5)	-0.21628 (0.5,0.6)	-2.4562 (0.0,0.7)	-2.5173 (1.0,0.7)	-3.0157 (0.0,0.7)	-2.6592 (1.0,0.5)
$(45/-45)_2$	-0.20478 (0.6,0.5)	-0.19012 (0.5,0.6)	-2.0948 (0.0,0.5)	-2.2666 (1.0,0.5)	-2.3205 (0.0,0.55)	-2.3752 (1.0,0.5)
$(45/-45)_5$	-0.18956 (0.6,0.5)	-0.17932 (0.5,0.6)*	-2.0522 (0.0,0.5)	-2.222 (0.0,0.5)	-2.216 (0.0,0.5)	-2.3097 (1.0,0.5)
(60/-60)	-0.28683 (0.6,0.5)	-0.24931 (0.4,0.5)	-4.2754 (0.0,0.3)	-3.9971 (0.0,0.3)	-4.5769 (0.0,0.7)	-4.122 (1.0,0.3)
$(60/-60)_2$	-0.24535 (0.6,0.5)	-0.22869 (0.5,0.4)	-3.3999 (0.0,0.5)	-3.196 (0.0,0.3)	-3.5752 (0.0,0.5)	-3.5268 (0.0,0.5)
$(60/-60)_5$	-0.23117 (0.6,0.5)	-0.2197 (0.5,0.6)*	-3.2451 (0.0,0.5)	-3.0483 (0.0,0.5)	-3.3441 (0.0,0.5)	3.3852 (1.0,0.5)
(75/-75)	-0.53 (0.6,0.5)	-0.49 (0.6,0.5)	-5.72 (0.0,0.3)	-5.21 (1.0,0.3)	-6.20 (0.0,0.7)	-5.54 (1.0,0.3)
$(75/-75)_2$	-0.48 (0.6,0.5)	-0.47 (0.5,0.6)	-4.54 (0.0,0.5)	-4.04 (0.0,0.3)	-4.79 (0.0,0.5)	-4.64 (1.0,0.5)
$(75/-75)_5$	-0.47 (0.6,0.5)	-0.46 (0.5,0.6)	-4.24 (0.0,0.5)	-3.70 (1.0,0.3)	-4.39 (0.0,0.5)	-4.39 (1.0,0.5)
90	-1.361 (0.6,0.45)	-1.2916 (0.5,0.6)	-5.3926 (0.0,0.5)	-4.6674 (0.0,0.7)	-5.9227 (0.0,0.65)	-5.4571 (0.0,0.5)

a/b=1, a/h=100, a'/b' =1, c/a=0.2; E_{11}/E_{22} = 25, G_{23} = 0.2E_{22}, G_{13} = G_{12} = 0.5E_{22}, ν_{12} = ν_{21} =0.25.

Values in the parenthesis indicates the location ($\bar{x}, \bar{y}$) of maximum downward deflection in each case.

Asterisk denotes the lowest values of shell actions in each group.

Table 5.4: Values of maximum non-dimensional tensile in-plane forces ($+\overline{N}_x$) for different antisymmetric angle ply lamination and boundary conditions of stiffened composite hypar shell with cutout

Lamination (Degree)	Boundary conditions					
	Group-I		Group-II		Group-III	
	A	B	A	B	A	B
	CSSC	CSCS	FCCF	FCFC	FSSF	FSFS
0	0.31957 (0.0,0.8)	0.23068 (0.6,0.6)	7.6766 (0.0,1.0)	0.072831 (0.3,0.3)	9.7331 (0.0,1.0)	0.42598 (0.0,0.9)
(15/-15)	0.33909 (0.0,0.9)	0.21061 (1.0,0.1)	8.4345 (0.0,1.0)	0.40015 (0.0,1.0)*	9.2218 (0.0,1.0)	1.0713 (0.0,1.0)*
$(15/-15)_2$	0.28265 (0.0,0.9)	0.19707 (0.6,0.6)*	8.2291 (0.0,1.0)	0.4439 (1.0,0.0)	9.2332 (0.0,1.0)	1.0882 (1.0,0.0)
$(15/-15)_5$	0.25797 (0.0,0.9)	0.20857 (0.4,0.4)	8.1402 (0.0,1.0)	0.46501 (0.0,1.0)	9.2351 (0.0,1.0)	1.1021 (0.0,1.0)
(30/-30)	0.34845 (0.0,0.9)	0.19052 (0.6,0.6)*	9.1489 (0.0,1.0)	1.9587 (0.0,1.0)	9.3434 (0.0,1.0)	4.1624 (0.0,1.0) *
$(30/-30)_2$	0.32936 (0.0,0.9)	0.21 (0.6,0.6)	8.9634 (0.0,1.0)	1.9095 (0.0,1.0)	9.3717 (0.0,1.0)	4.2145 (0.0,1.0)
$(30/30)_5$	0.32108 (0.0,0.9)	0.21675 (0.6,0.6)	8.9018 (0.0,1.0)	1.9193 (0.0,1.0)	9.3868 (0.0,1.0)	4.2466 (0.0,1.0)
(45/-45)	0.62534 (1.0,0.0)	0.32589 (0.4,0.4)	10.702 (0.0,1.0)	5.2897 (1.0,0.0)	10.908 (0.0,1.0)	9.6308 (1.0,0.0)
$(45/-45)_2$	0.45906 (0.0,0.9)	0.31976 (0.6,0.6)	10.498 (0.0,1.0)	4.8639 (0.0,1.0)	10.922 (0.0,1.0)	9.9459 (0.0,1.0)
$(45/-45)_5$	0.45662 (0.0,0.9)	0.31743 (0.6,0,.6)	10.431 (0.0,1.0)	4.7968 (0.0,1.0)	10.94 (0.0,1.0)	10.058 (0.0,1.0)
(60/-60)	0.73981 (0.0,0.9)	0.5485 (0.6,0.6)	12.519 (0.0,1.0)	6.9077 (0.0,1.0)	13.657 (0.0,1.0)	15.74 (0.0,1.0)

$(60/-60)_2$	0.74688 (0.0,0.9)	0.52605 (0.6,0.6)	11.802 (0.0,1.0)	5.956 (0.0,1.0)	13.333 (0.0,1.0)	16.843 (0.0,1.0)
$(60/-60)_5$	0.74834 (0.0,0.9)	0.5145 (0.6,0.6)	11.641 (0.0,1.0)	5.7328 (0.0,1.0)	13.298 (0.0,1.0)	17.207 (0.0,1.0)
(75/-75)	1.0767 (0.0,0.9)	0.86053 (0.6,0.6)	10.221 (0.0,1.0)	2.5636 (1.0,0.0)	13.999 (0.0,1.0)	4.9594 (0.0,1.0)
$(75/-75)_2$	1.0893 (0.0,0.9)	0.81437 (0.6,0.6)	9.312 (0.0,1.0)	1.9671 (0.0,1.0)	13.2 (0.0,1.0)	4.4089 (0.0,1.0)
$(75/-75)_5$	1.1045 (0.0,0.9)	0.79251 (0.6,0.6)	9.1627 (0.0,1.0)	1.7865 (0.0,1.0)*	13.117 (0.0,1.0)	4.3593 (0.0,1.0)
90	1.5768 (0.0,0.0)	1.3692 (1.0,1.0)	5.5273 (0.0,1.0)	1.2854 (0.35,0.4)	16.167 (0.0,0.0)	15.315 (0.0,0.0)

a/b=1, a/h=100, a'/b' =1, c/a=0.2; E_{11}/E_{22} = 25, G_{23} = 0.2E_{22}, G_{13} = G_{12} = 0.5E_{22}, ν_{12} = ν_{21} =0.25.

Values in the parenthesis indicates the location ($\bar{x}, \bar{y}$) of maximum tensile in-plane force in each case.

Asterisk denotes the lowest values of shell actions in each group.

Table 5.5: Values of maximum non-dimensional compressive in-plane forces ($-\overline{N}_x$) for different antisymmetric angle ply lamination and boundary conditions of stiffened composite hypar shell with cutout

Lamination (Degree)	Boundary conditions					
	Group-I		Group-II		Group-III	
	A	B	A	B	A	B
	CSSC	CSCS	FCCF	FCFC	FSSF	FSFS
0	-0.2261 (0.6,0.4)	-0.23069 (0.6,0.4)	-3.8372 (1.0,1.0)	-0.072828 (0.7,0.3)	-10.141 (1.0,1.0)	-0.42598 (1.0,0.9)
(15/-15)	-0.22064 (0.0,0.1)	-0.21061 (0.0,0.1)	-4.5277 (1.0,1.0)	-0.40016 (0.0,0.0)*	-9.5148 (1.0,1.0)	-1.0713 (0.0,0.0)*
$(15/-15)_2$	-0.20812 (0.6,0.4)	-0.19707 (0.4,0.6)*	-4.0991 (1.0,1.0)	-0.4439 (0.0,0.0)	-9.4173 (1.0,1.0)	-1.0881 (1.0,1.0)
$(15/-15)_5$	-0.21149 (0.6,0.4)	-0.20856 (0.6,0.4)	-3.9392 (1.0,1.0)	-0.465 (0.0,0.0)	-9.4069 (1.0,1.0)	-1.1021 (0.0,0.0)
(30/-30)	-0.22079 (0.6,0.4)	-0.19052 (0.6,0.4)*	-5.8179 (1.0,1.0)	-1.9587 (0.0,0.0)	-9.5995 (1.0,1.0)	-4.1624 (1.0,1.0)
$(30/-30)_2$	-0.22306 (0.6,0.4)	-0.21 (0.4,0.6)	-5.2345 (1.0,1.0)	-1.9095 (0.0,0.0)*	-9.5102 (1.0,1.0)	-4.2146 (1.0,1.0)
$(30/30)_5$	-0.22126 (0.6,0.4)	-0.21675 (0.6,0.4)	-5.0736 (1.0,1.0)	-1.9192 (0.0,0.0)	-9.494 (1.0,1.0)	-4.2466 (0.0,0.0)
(45/-45)	-0.32889 (0.4,0.6)	-0.32589 (0.6,0.4)	-6.4547 (1.0,1.0)	-5.2902 (1.0,1.0)	-9.8869 (1.0,1.0)	-9.6311 (1.0,1.0)
$(45/-45)_2$	-0.32174 (0.6,0.4)	-0.31976 (0.6,0.4)	-5.9539 (1.0,1.0)	-4.864 (0.0,0.0)	-9.6236 (1.0,1.0)	-9.9462 (0.0,0.0)
$(45/-45)_5$	-0.31743 (0.6,0.4)	-0.31743 (0.4,0.6)	-5.8547 (1.0,1.0)	-4.7967 (1.0,1.0)	-9.568 (1.0,1.0)	-10.058 (0.0,0.0)
(60/-60)	-0.54396 (0.6,0.4)	-0.5485 (0.4,0.6)	-7.4091 (0.0,0.0)	-6.9079 (0.0,0.0)	-15.804 (0.0,0.0)	-15.74 (1.0,1.0)

$(60/-60)_2$	0.52662 (0.6,0.4)	-0.52605 (0.6,0.4)	-6.4334 (0.0,0.0)	-5.9561 (1.0,1.0)	-16.804 (0.0,0.0)	-16.843 (0.0,0.0)
$(60/-60)_5$	-0.51857 (0.6,0.4)	-0.51451 (0.6,0.4)	-6.2067 (0.0,0.0)	-5.733 (1.0,1.0)	-17.2 (0.0,0.0)	-17.207 (0.0,0.0)
(75/-75)	-0.89441 (0.4,0.6)	-0.86053 (0.4,0.6)	-6.08 (1.0,1.0)	-2.5635 (1.0,1.0)	-9.8503 (1.0,1.0)	-4.9592 (0.0,0.0)
$(75/-75)_2$	-0.80972 (0.4,0.6)	-0.81438 (0.4,0.6)	-6.047 (1.0,1.0)	-1.9671 (0.0,0.0)	-9.3426 (1.0,1.0)	-4.4089 (1.0,1.0)
$(75/-75)_5$	-0.81113 (0.6,0.4)	-0.79251 (0.4,0.6)	-6.1081 (1.0,1.0)	-1.7864 (0.0,0.0)	-9.251 (1.0,1.0)	-4.3592 (0.0,0.0) *
90	-1.2582 (0.1,0.1)	-1.3692 (0.0,1.0)	-6.6239 (1.0,1.0)	-1.2853 (0.35,0.6)	-10.557 (0.95,1.0)	-15.316 (0.0,1.0)

a/b=1, a/h=100, a'/b' =1, c/a=0.2; E_{11}/E_{22} = 25, G_{23} = 0.2E_{22}, G_{13} = G_{12} = 0.5E_{22}, ν_{12} = ν_{21} =0.25.

Values in the parenthesis indicates the location ($\bar{x}, \bar{y}$) of maximum compressive in-plane force in each case.

Asterisk denotes the lowest values of shell actions in each group.

Table 5.6: Values of maximum non-dimensional tensile in-plane forces ($+\overline{N}_y$) for different antisymmetric angle ply lamination and boundary conditions of stiffened composite hypar shell with cutout

Lamination (Degree)	Boundary conditions					
	Group-I		Group-II		Group-III	
	A	B	A	B	A	B
	CSSC	CSCS	FCCF	FCFC	FSSF	FSFS
0	1.5703 (0.1,1.0)	0.95337 (0.6,0.6)	8.1249 (0.0,1.0)	7.3326 (0.0,1.0)	13.253 (0.0,1.0)	13.691 (0.0,1.0)
(15/-15)	1.1795 (0.1,1.0)	0.86069 (0.6,0.6)	12.029 (0.0,1.0)	6.584 (0.0,1.0)	14.505 (0.0,1.0)	12.948 (0.0,1.0)
$(15/-15)_2$	1.1585 (0.1,1.0)	0.85032 (0.6,0.6)	10.773 (0.0,1.0)	6.4789 (1.0,0.0)	13.737 (0.0,1.0)	12.842 (1.0,0.0)
$(15/-15)_5$	1.1602 (0.1,1.0)	0.85727 (0.6,0.6)	10.591 (0.0,1.0)	6.5179 (0.0,1.0)	13.687 (0.0,1.0)	12.889 (0.0,1.0)
(30/-30)	0.67986 (1.0,0.0)	0.54083 (0.6,0.6)	12.012 (0.0,1.0)	6.2147 (0.0,1.0)	12.702 (0.0,1.0)	11.539 (0.0,1.0)
$(30/-30)_2$	0.6406 (0.1,1.0)	0.53009 (0.6,0.6)	11.46 (0.0,1.0)	5.8546 (0.0,1.0)	12.517 (0.0,1.0)	11.569 (0.0,1.0)
$(30/30)_5$	0.63949 (0.1,1.0)	0.53243 (0.6,0.6)	11.355 (0.0,1.0)	5.829 (0.0,1.0)	12.524 (0.0,1.0)	11.611 (0.0,1.0)
(45/-45)	0.42775 (1.0,0.0)	0.33923 (0.4,0.4)	9.7855 (0.0,1.0)	5.6655 (0.0,1.0)	10.113 (0.0,1.0)	10.007 (1.0,0.0)
$(45/-45)_2$	0.35756 (0.1,1.0)	0.32619 (0.6,0.6)	9.6464 (0.0,1.0)	5.1692 (0.0,1.0)	10.174 (0.0,1.0)	10.123 (1.0,0.0)
$(45/-45)_5$	0.36093 (0.4,0.4)	0.32003 (0.6,0.6)	9.6076 (0.0,1.0)	5.0771 (0.0,1.0)	10.206 (0.0,1.0)	10.161 (0.0,1.0)
(60/-60)	0.25317 (0.1,1.0)	0.19181 (0.6,0.6)*	8.3981 (0.0,1.0)	4.209 (0.0,1.0)	9.0008 (0.0,1.0)*	9.2695 (0.0,1.0)

$(60/-60)_2$	0.23936 (0.1,1.0)	0.20644 (0.6,0.6)	8.2328 (0.0,1.0)	3.7103 (0.0,1.0)	9.0538 (0.0,1.0)	9.4215 (0.0,1.0)
$(60/-60)_5$	0.23216 (0.1,1.0)	0.20562 (0.6,0.6)	8.1888 (0.0,1.0)	3.5806 (0.0,1.0) *	9.0846 (0.0,1.0)	9.4549 (0.0,1.0)
(75/-75)	0.31007 (0.1,1.0)	0.12527 (1.0,1.0)*	7.9453 (0.0,1.0)	3.5359 (1.0,0.0)	9.2688 (0.0,1.0)	9.2695 (1.0,0.0)
$(75/-75)_2$	0.25629 (0.1,1.0)	0.16415 (0.4,0.4)	7.7264 (0.0,1.0)	3.1525 (0.0,1.0)	9.2364 (0.0,1.0)	9.2189 (1.0,0.0)
$(75/-75)_5$	0.23235 (0.1,1.0)	0.1725 (0.6,0.6)	7.6494 (0.0,1.0)	3.0164 (0.0,1.0)*	9.246 (0.0,1.0)	9.2097 (1.0,0.0)*
90	0.37905 (0.2,1.0)	0.14552 (0.4,0.4)	7.5796 (0.0,1.0)	3.5102 (0.0,1.0)	9.6659 (0.0,1.0)	9.755 (0.0,1.0)

a/b=1, a/h=100, a'/b' =1, c/a=0.2; E_{11}/E_{22} = 25, G_{23} = 0.2E_{22}, G_{13} = G_{12} = 0.5E_{22}, ν_{12} = ν_{21} =0.25.

Values in the parenthesis indicates the location ($\bar{x}$, $\bar{y}$) of maximum tensile in-plane forces in each case.

Asterisk denotes the lowest values of shell actions in each group.

Table 5.7: Values of maximum non-dimensional compressive in-plane forces ($-\overline{N}_y$) for different antisymmetric angle ply lamination and boundary conditions of stiffened composite hypar shell with cutout

Lamination (Degree)	Boundary conditions					
	Group-I		Group-II		Group-III	
	A	B	A	B	A	B
	CSSC	CSCS	FCCF	FCFC	FSSF	FSFS
0	-1.5446 (0.9,1.0)	-0.95336 (0.4,0.6)	-8.2301 (0.0,0.0)	-7.3323 (1.0,1.0)	-11.319 (0.0,0.0)	-13.69 (1.0,1.0)
(15/-15)	-0.96116 (0.4,0.6)	-0.86069 (0.4,0.6)	-6.4601 (0.0,0.0)	-6.584 (0.0,0.0)	-9.8637 (0.0,0.0)	-12.948 (0.0,0.0)
$(15/-15)_2$	-0.87044 (0.4,0.6)	-0.85031 (0.4,0.6)	-6.5404 (0.0,0.0)	-6.4788 (0.0,0.0)	-10.486 (1.0,1.0)	-12.842 (1.0,1.0)
$(15/-15)_5$	-0.84528 (0.4,0.6)	-0.85727 (0.4,0.6)	-6.6268 (0.0,0.0)	-6.5177 (0.0,0.0)	-10.958 (1.0,1.0)	-12.889 (0.0,0.0)
(30/-30)	-0.59335 (0.6,0.4)	-0.54083 (0.4,0.6)	-7.6952 (1.0,1.0)	-6.2147 (0.0,0.0)	-12.178 (1.0,1.0)	-11.539 (1.0,1.0)
$(30/-30)_2$	-0.57468 (0.6,0.4)	-0.5301 (0.4,0.6)	-6.8396 (1.0,1.0)	-5.8546 (0.0,0.0)	-12.911 (1.0,1.0)	-11.569 (1.0,1.0)
$(30/30)_5$	-0.56497 (0.6,0.4)	-0.53242 (0.6,0.4)	-6.645 (1.0,1.0)	-5.8288 (0.0,0.0)	-13.187 (1.0,1.0)	-11.611 (0.0,0.0)
(45/-45)	-0.33559 (0.4,0.4)	-0.33922 (0.6,0.4)	-5.8249 (0.0,0.0)	-5.666 (1.0,1.0)	-9.7042 (0.0,0.0)	-10.007 (1.0,1.0)
$(45/-45)_2$	-0.29996 (0.6,0.4)	-0.32619 (0.6,0.4)	-5.3301 (0.0,0.0)	-5.1693 (0.0,0.0)	-9.569 (0.0,0.0)	-10.124 (1.0,1.0)
$(45/-45)_5$	-0.2952 (0.6,0.4)	-0.32003 (0.6,0.4)	-5.2398 (0.0,0.0)	-5.077 (1.0,1.0)	-9.5481 (0.0,0.0)	-10.161 (1.0,1.0)

(60/-60)	-0.19497 (0.6,0.4)	-0.19181 (0.4,0.6)*	-4.5275 (0.0,0.0)	-4.2091 (0.0,0.0)	-9.4933 (0.0,0.0)	-9.2697 (1.0,1.0)*
$(60/-60)_2$	-0.19597 (0.6,0.4)	-0.20644 (0.6,0.4)	-4.0089 (0.0,0.0)	-3.7104 (1.0,1.0)	-9.4722 (0.0,0.0)	-9.4217 (0.0,0.0)
$(60/-60)_5$	-0.19452 (0.6,0.4)	-0.20562 (0.6,0.4)	-3.8755 (0.0,0.0)	-3.5807 (1.0,1.0)	-9.4768 (0.0,0.0)	-9.4551 (0.0,0.0)
(75/-75)	-0.17365 (0.6,0.4)	-0.12527 (0.0,1.0)*	-4.0322 (0.0,0.1)	-3.5358 (0.0,0.0)	-9.4773 (0.0,0.0)	-9.2261 (0.0,0.0)
$(75/-75)_2$	-0.19411 (0.6,0.4)	-0.16416 (0.4,0.6)	-3.6081 (0.0,0.1)	-3.1525 (0.0,0.0)	-9.3544 (0.0,0.0)	-9.219 (0.0,0.0)
$(75/-75)_5$	-0.19833 (0.6,0.4)	-0.1725 (0.6,0.4)	-3.4788 (0.0,0.1)*	-3.0163 (0.0,0.0)*	-9.3489 (0.0,0.0)	-9.2095 (0.0,0.0)*
90	-0.23827 (0.9,1.0)	-0.14552 (0.6,0.4)	-3.8587 (0.0,0.1)	-3.5101 (0.0,0.0)	-10.191 (0.0,0.0)	-9.7547 (1.0,1.0)

a/b=1, a/h=100, $a^{/}\big/b^{/}$ =1, c/a=0.2; E_{11}/E_{22} = 25, G_{23} = 0.2E_{22}, G_{13} = G_{12} = 0.5E_{22}, ν_{12} = ν_{21} =0.25.

Values in the parenthesis indicates the location ($\bar{x}$, $\bar{y}$) of compressive in-plane forces in each case.

Asterisk denotes the lowest values of shell actions in each group.

Table 5.8: Values of maximum non-dimensional anticlockwise in-plane shear ($+\overline{N}_{xy}$) for different antisymmetric angle ply lamination and boundary conditions of stiffened composite hypar shell with cutout

Lamination (Degree)	Boundary conditions					
	Group-I		Group-II		Group-III	
	A	B	A	B	A	B
	CSSC	CSCS	FCCF	FCFC	FSSF	FSFS
0	0.0 (0.55,0.5)	0.0 (0.55,0.5)	1.0677 (0.1,1.0)	0.029345 (0.6,0.5)	1.475 (0.1,1.0)	0.27826 (0.9,0.0)
(15/-15)	0.0 (0.55,0.5)	0.0 (0.55,0.5)	1.6629 (0.1,1.0)	0.017635 (1.0,0.6) *	1.9098 (0.1,1.0)	0.80412 (0.1,0.0)*
$(15/-15)_2$	0.0 (0.55,0.5)	0.0 (0.55,0.5)	1.6889 (0.1,1.0)	0.0024528 (0.4,0.5)*	1.992 (0.1,1.0)	0.83862 (0.1,1.0)
$(15/-15)_5$	0.0 (0.55,0.5)	0.0 (0.55,0.5)	1.6906 (0.1,1.0)	0.0033569 (0.4,0.5)	2.0144 (0.1,1.0)	0.84946 (0.9,1.0)
(30/-30)	0.060161 (0.5,0.4)	0.049696 (0.5,0.6)	1.9643 (0.1,1.0)	0.21224 (0.9,0.0)	2.0711 (0.1,1.0)	1.8101 (0.1,1.0)
$(30/-30)_2$	0.050709 (0.5,0.4)	0.039623 (0.5,0.6)	1.9164 (0.1,1.0)	0.20183 (0.1,1.0)	2.0612 (0.1,1.0)	1.7764 (0.1,1.0)
$(30/30)_5$	0.048996 (0.5,0.4)	0.039251 (0.5,0.4)	1.9068 (0.1,1.0)	0.19954 (0.0,0.9)	2.0664 (0.1,1.0)	1.7653 (0.9,1.0)
(45/-45)	0.10117 (0.6,0.5)	0.10363 (0.5,0.4)	1.7593 (0.0,0.9)	0.94609 (0.9,1.0)	2.2236 (0.1,0.0)	2.2231 (0.1,0.0)
$(45/-45)_2$	0.10061 (0.5,0.4)	0.099911 (0.5,0.6)	1.7125 (0.0,0.9)	0.75105 (0.1,0.0)	2.034 (0.1,0.0)	2.084 (0.9,1.0)
$(45/-45)_5$	0.10046 (0.5,0.4)	0.098204 (0.5,0.6)	1.7037 (0.0,0.9)	0.71566 (0.0,0.9)	1.9895 (0.1,0.0)	2.0507 (0.9,1.0)
(60/-60)	0.049745 (0.6,0.5)	0.048825 (0.4,0.5)	1.9348 (0.0,0.9)	0.73477 (0.0,0.1)	2.1034 (0.0,0.9)	1.7332 (1.0,0.9)

$(60/-60)_2$	0.039239 (0.6,0.5)	0.038134 (0.6,0.5)	1.8923 (0.0,0.9)	0.68062 (1.0,0.9)	2.1083 (0.0,0.9)	1.675 (0.0,0.9)
$(60/-60)_5$	0.037443 (0.6,0.5)	0.034525 (0.6,0.5)	1.8787 (0.0,0.9)	0.66164 (1.0,0.9)	2.1132 (0.0,0.9)	1.6642 (1.0,0.9) *
(75/-75)	0.0 (0.55,0.5)	0.0 (0.55,0.5)	1.481 (0.0,0.9)	0.11281 (1.0,0.05)	1.8358 (0.0,0.9)	1.7139 (1.0,0.1)
$(75/-75)_2$	0.0038622 (0.0,1.0)*	0.0 (0.55,0.5)	1.5593 (0.0,0.9)	0.081054 (1.0,0.05)	1.9639 (0.0,0.9)	1.7014 (0.0,0.1)
$(75/-75)_5$	0.007586 (0.0,1.0)	0.0 (0.55,0.5)*	1.5639 (0.0,0.9)	0.076102 (1.0,0.05)	1.9895 (0.0,0.9)	1.704 (1.0,0.1)
90	0.012027 (0.0,1.0)	0.0 (0.55,0.5)	1.23 (0.1,1.0)	0.12905 (0.0,0.9)	1.5105 (0.0,0.9)	1.2476 (0.0,0.9)

a/b=1, a/h=100, a'/b' =1, c/a=0.2; E_{11}/E_{22} = 25, G_{23} = 0.2E_{22}, G_{13} = G_{12} = 0.5E_{22}, ν_{12} = ν_{21} =0.25.

Values in the parenthesis indicates the location ($\bar{x}, \bar{y}$) of maximum anticlockwise in-plane shear in each case.

Asterisk denotes the lowest values of shell actions in each group.

Table 5.9: Values of maximum non-dimensional clockwise in-plane shear ($-\overline{N}_{xy}$) for different antisymmetric angle ply lamination and boundary conditions of stiffened composite hypar shell with cutout

Lamination (Degree)	Boundary conditions					
	Group-I		Group-II		Group-III	
	A	B	A	B	A	B
	CSSC	CSCS	FCCF	FCFC	FSSF	FSFS
0	-0.81606 (0.7,0.5)	-0.72411 (0.7,0.5)	-6.4021 (0.0,1.0)	-0.75421 (0.9,0.5)	-8.7467 (0.0,1.0)	-3.1941 (1.0,0.0)
(15/-15)	-0.91201 (0.7,0.5)	-0.82463 (0.7,0.5)*	-8.4393 (0.0,1.0)	-0.8656 (0.2,0.5)	-9.6042 (0.0,1.0)	-4.329 (0.0,0.0)*
$(15/-15)_2$	-0.93954 (0.7,0.5)	-0.86683 (0.3,0.5)	-8.4212 (0.0,1.0)	-0.83944 (0.2,0.5)	-9.8791 (0.0,1.0)	-4.3948 (1.0,0.0)
$(15/-15)_5$	-0.94796 (0.7,0.5)	-0.88329 (0.3,0.5)	-8.3941 (0.0,1.0)	-0.82952 (0.8,0.5)*	-9.9615 (0.0,1.0)	-4.4361 (0.0,1.0)
(30/-30)	-0.96259 (0.7,0.5)	-0.94028 (0.7,0.5)	-9.7512 (0.0,1.0)	-2.0594 (0.0,0.0)	-10.144 (0.0,1.0)	-6.3284 (1.0,1.0) *
$(30/-30)_2$	-0.98367 (0.7,0.5)	-0.95642 (0.3,0.5)	-9.6088 (0.0,1.0)	-2.081 (0.0,0.0)	-10.245 (0.0,1.0)	-6.3365 (1.0,1.0)
$(30/30)_5$	-0.98776 (0.7,0.5)	-0.96097 (0.7,0.5)	-9.5631 (0.0,1.0)	-2.0998 (0.0,1.0)	-10.286 (0.0,1.0)	-6.3508 (0.0,1.0)
(45/-45)	-0.92099 (0.4,0.6)	-0.91662 (0.4,0.4)	-9.8578 (0.0,1.0)	-4.1137 (1.0,1.0)	-10.134 (0.0,1.0)	-8.3716 (1.0,1.0)
$(45/-45)_2$	-0.91888 (0.4,0.4)	-0.90318 (0.7,0.5)	-9.743 (0.0,1.0)	-3.8612 (1.0,1.0)	-10.209 (0.0,1.0)	-8.3429 (1.0,1.0)
$(45/-45)_5$	-0.92326 (0.4,0.4)	-0.89661 (0.7,0.5)	-9.7044 (0.0,1.0)	-3.8051 (0.0,1.0)	-10.247 (0.0,1.0)	-8.3367 (0.0,1.0)
(60/-60)	-0.93505 (0.5,0.3)	-0.95646 (0.5,0.7)	-9.2283 (0.0,1.0)	-3.1476 (0.0,0.0)	-9.9836 (0.0,1.0)	-9.0771 (1.0,1.0)

$(60/-60)_2$	-0.95 (0.5,0.3)	-0.9614 (0.5,0.7)	-9.0971 (0.0,1.0)	-2.853 (1.0,1.0)	-10.121 (0.0,1.0)	-9.0538 (0.0,0.0)
$(60/-60)_5$	-0.95295 (0.5,0.3)	-0.95819 (0.5,0.3)	-9.0465 (0.0,1.0)	-2.7523 (1.0,1.0)	-10.166 (0.0,1.0)	-9.0516 (0.0,0.0)
(75/-75)	-0.88576 (0.5,0.3)	-0.90129 (0.5,0.7)	-7.5545 (0.0,1.0)	-1.0161 (0.5,0.0)	-9.3392 (0.0,1.0)	-8.1809 (1.0,0.0)
$(75/-75)_2$	-0.91152 (0.5,0.3)	-0.90488 (0.5,0.7)	-7.6942 (0.0,1.0)	-1.0141 (0.5,0.7) *	-9.7283 (0.0,1.0)	-8.268 (0.0,0.0)
$(75/-75)_5$	-0.91993 (0.5,0.3)	-0.9019 (0.5,0.7)*	-7.684 (0.0,1.0)	-1.0563 (0.5,0.7)	-9.8266 (0.0,1.0)	-8.3072 (1.0,0.0)
90	-0.79284 (0.5,0.3)	-0.70155 (0.5,0.7)	-6.1053 (0.0,1.0)	-0.83783 (0.3,0.45)	-8.8142 (0.0,1.0)	-7.1506 (0.0,1.0)

a/b=1, a/h=100, a'/b' =1, c/a=0.2; E_{11}/E_{22} = 25, G_{23} = 0.2E_{22}, G_{13} = G_{12} = 0.5E_{22}, ν_{12} = ν_{21} =0.25.

Values in the parenthesis indicates the location ($\bar{x}$, $\bar{y}$) of maximum clockwise in-plane shear in each case.

Asterisk denotes the lowest values of shell actions in each group.

Table 5.10: Values of maximum non-dimensional hogging moments ($+\overline{M}_x$) x10^2 for different antisymmetric angle ply lamination and boundary conditions of stiffened composite hypar shell with cutout

Lamination (Degree)	Boundary conditions					
	Group-I		Group-II		Group-III	
	A	B	A	B	A	B
	CSSC	CSCS	FCCF	FCFC	FSSF	FSFS
0	0.1733 (0.0,0.2)	0.11113 (1.0,0.7)	0.56473 (1.0,1.0)	0.024122 (0.1,0.2)	0.49104 (0.0,1.0)	0.011692 (0.5,0.2)
(15/-15)	0.070218 (0.0,0.8)	0.009076 (0.5,0.6)*	0.58267 (1.0,1.0)	0.018106 (1.0,0.0)*	0.21799 (0.6,1.0)	0.042386 (0.1,1.0)
$(15/-15)_2$	0.073993 (0.0,0.8)	0.020888 (0.0,0.7)	0.47933 (1.0,1.0)	0.054734 (1.0,0.0)	0.17383 (0.0,1.0)	0.014633 (0.9,1.0)
$(15/-15)_5$	0.078154 (0.0,0.8)	0.03203 (1.0,0.3)	0.46034 (1.0,1.0)	0.070948 (0.0,1.0)	0.25984 (0.0,1.0)	0.008737 (0.5,0.9)*
(30/-30)	0.035442 (0.5,0.4)	0.033458 (0.5,0.6)	0.43318 (0.1,1.0)	0.078403 (0.1,0.0) *	0.42881 (0.1,1.0)	0.21199 (0.1,0.0)
$(30/-30)_2$	0.046301 (0.0,0.8)	0.019482 (0.5,0.4)	0.40742 (1.0,0.9)	0.13146 (0.1,1.0)	0.20589 (0.1,1.0)	0.084094 (0.9,0.0)
$(30/30)_5$	0.065945 (0.0,0.8)	0.017297 (1.0,0.8)*	0.40778 (1.0,0.9)	0.18042 (0.0,1.0)	0.16959 (0.1,0.9)	0.022879 (0.0,0.1) *
(45/-45)	0.07068 (0.6,0.5)	0.070597 (0.4,0.5)	0.54376 (0.1,1.0)	0.39356 (0.9,1.0)	0.53034 (0.1,1.0)	0.46518 (0.9,1.0)
$(45/-45)_2$	0.059565 (0.0,0.8)	0.040782 (0.4,0.5)	0.4976 (1.0,0.9)	0.48243 (0.1,1.0)	0.30771 (0.1,1.0)	0.18732 (0.1,0.0)
$(45/-45)_5$	0.10176 (0.0,0.8)	0.04585 (0.0,0.2)	0.48296 (1.0,0.9)	0.47989 (0.1,1.0)	0.3096 (0.1,0.9)	0.088067 (0.1,0.1)
(60/-60)	0.12571 (0.6,0.5)	0.12601 (0.4,0.5)	0.75082 (0.0,0.9)	0.38716 (0.1,0.0)	0.88609 (0.0,0.1)	0.88041 (0.0,0.9)

$(60/-60)_2$	0.093456 (0.0,0.8)	0.068749 (0.6,0.5)	0.76655 (0.1,0.0)	0.66116 (0.1,1.0)	0.37744 (0.0,0.1)	0.40718 (1.0,0.1)
$(60/-60)_5$	0.17278 (0.0,0.8)	0.11344 (1.0,0.2)	0.84427 (0.1,0.0)	0.73403 (0.9,1.0)	0.33143 (0.1,0.95)	0.26611 (0.5,0.7)
(75/-75)	0.17833 (0.4,0.5)	0.17252 (0.6,0.5)	0.45453 (0.0,0.9)	0.22302 (1.0,0.0)	1.4684 (0.0,0.1)	1.4223 (1.0,0.9)
$(75/-75)_2$	0.31203 (0.0,0.85)	0.17805 (1.0,0.8)	0.55158 (0.1,0.0)	0.49388 (0.0,0.0)	0.69868 (0.0,0.1)	0.68733 (1.0,0.1)
$(75/-75)_5$	0.43019 (0.0,0.8)	0.32431 (0.0,0.2)	0.77332 (0.0,1.0)	0.56095 (1.0,0.0)	0.43899 (0.0,1.0)	0.43072 (0.5,0.7)
90	1.2084 (0.0,0.8)	1.1036 (0.0,0.8)	1.6053 (0.0,1.0)	0.83884 (0.5,0.7)	1.5659 (0.0,1.0)	0.63796 (0.5,0.7)

a/b=1, a/h=100, a'/b' =1, c/a=0.2; E_{11}/E_{22} = 25, G_{23} = 0.2E_{22}, G_{13} = G_{12} = 0.5E_{22}, ν_{12} = ν_{21} =0.25.

Values in the parenthesis indicates the location ($\bar{x}$, $\bar{y}$) of maximum hogging moment in each case.

Asterisk denotes the lowest values of shell actions in each group.

Table 5.11: Values of maximum non-dimensional sagging moments ($-\overline{M}_x$) x10^2 for different antisymmetric angle ply lamination and boundary conditions of stiffened composite hypar shell with cutout

Lamination (Degree)	Boundary conditions					
	Group-I		Group-II		Group-III	
	A	B	A	B	A	B
	CSSC	CSCS	FCCF	FCFC	FSSF	FSFS
0	-0.07217 (0.1,0.2)	-0.04077 (0.5,0.8)	-0.15652 (0.1,1.0)	-0.01237 (0.5,0.7)	-0.12979 (0.2,1.0)	-0.02785 (0.1,0.1)
(15/-15)	-0.07661 (0.1,0.8)	-0.05455 (0.7,0.2)	-0.19706 (0.5,1.0)	-0.05043 (0.9,0.4)	-0.19147 (0.8,1.0)	-0.23389 (0.0,1.0)
$(15/-15)_2$	-0.06434 (0.1,0.8)	-0.03983 (0.3,0.2)	-0.11269 (0.5,1.0)	-0.03299 (0.1,0.4)	-0.1124 (0.2,1.0)	-0.09701 (1.0,1.0)
$(15/-15)_5$	-0.05774 (0.1,0.8)	-0.03257 (0.3,0.2)*	-0.09048 (0.5,1.0)	-0.02126 (0.9,0.6)*	-0.09444 (0.2,1.0)	-0.02251 (0.2,0.1)*
(30/-30)	-0.12128 (0.7,0.5)	-0.11661 (0.7,0.5)	-1.1612 (0.0,1.0)	-0.17063 (1.0,0.0)	-1.0995 (0.0,0.0)	-0.87767 (1.0,1.0)
$(30/-30)_2$	-0.0806 (0.1,0.8)	-0.0638 (0.3,0.2)	-0.31795 (0.0,1.0)	-0.07998 (0.8,0.6)	-0.34152 (1.0,1.0)	-0.35251 (1.0,0.0)
$(30/30)_5$	-0.06168 (0.1,0.8)	-0.04251 (0.7,0.2) *	-0.09197 (0.8,0.9)	-0.05672 (0.95,0.5*	-0.09418 (0.3,0.9)	-0.06886 (0.8,0.9) *
(45/-45)	-0.21697 (0.4,0.6)	-0.21721 (0.4,0.4)	-2.4813 (0.0,1.0)	-0.83445 (1.0,1.0)	-2.3619 (0.0,1.0)	-2.1447 (1.0,1.0)
$(45/-45)_2$	-0.1145 (0.6,0.6)	-0.11326 (0.6,0.6)	-0.89639 (0.0,1.0)	-0.16664 (0.5,0.0)	-0.87451 (0.0,1.0)	-0.83756 (0.0,0.0)
$(45/-45)_5$	-0.08484 (0.1,0.9)	-0.0633 (0.3,0.8)	-0.14748 (0.3,0.9)	-0.12532 (0.1,0.8)	-0.16408 (0.3,0.9)	-0.11715 (0.1,0.5)
(60/-60)	-0.34231 (0.5,0.3)	-0.34383 (0.5,0.7)	-3.09 (0.0,1.0)	-1.0957 (1.0,1.0)	-4.1246 (0.0,0.0)	-4.1127 (0.0,1.0)

$(60/-60)_2$	-0.1933 (0.2,0.9)	-0.1738 (0.5,0.7)	-0.95147 (0.0,1.0)	-0.23158 (0.5,0.0)	-1.6648 (0.0,0.0)	-1.8092 (1.0,1.0)
$(60/-60)_5$	-0.143 (0.2,0.9)	-0.1143 (0.8,0.9)	-0.22949 (0.3,1.0)	-0.15333 (0.1,0.2)	-0.30349 (0.0,0.0)	-0.45751 (0.0,1.0)
(75/-75)	-0.57022 (0.5,0.3)	-0.58318 (0.5,0.3)	-1.88 (0.0,0.9)	-0.68 (1.0,1.0)	-5.33 (0.0,0.0)	-5.20 (0.0,1.0)
$(75/-75)_2$	-0.36472 (0.2,0.9)	-0.33128 (0.6,0.7)	-0.67973 (0.2,1.0)	-0.36461 (0.5,0.0)	-2.448 (0.0,0.0)	-2.4407 (0.0,0.0)
$(75/-75)_5$	-0.29287 (0.2,0.9)	-0.2382 (0.8,0.9)	-0.63808 (0.2,1.0)	-0.1734 (0.5,1.0)	-0.89725 (0.0,0.0)	-0.91497 (0.0,0.0)
90	-0.5455 (0.8,0.8)	-0.38428 (0.3,0.9)	-1.105 (0.2,1.0)	-0.11682 (0.6,0.5)	-1.1064 (0.3,1.0)	-0.31231 (0.0,1.0)

a/b=1, a/h=100, a'/b' =1, c/a=0.2; E_{11}/E_{22} = 25, G_{23} = 0.2E_{22}, G_{13} = G_{12} = 0.5E_{22}, ν_{12} = ν_{21} =0.25.

Values in the parenthesis indicates the location ($\bar{x}$, $\bar{y}$) of maximum sagging moment in each case.

Asterisk denotes the lowest values of shell actions in each group.

Table 5.12: Values of maximum non-dimensional hogging moments ($+\overline{M}_y$) x10^2 for different antisymmetric angle ply lamination and boundary conditions of stiffened composite hypar shell with cutout

Lamination (Degree)	Boundary conditions					
	Group-I		Group-II		Group-III	
	A	B	A	B	A	B
	CSSC	CSCS	FCCF	FCFC	FSSF	FSFS
0	1.0989 (0.3,1.0)	0.14567 (0.8,0.4)	1.9282 (0.0,1.0)	1.5501 (1.0,1.0)	1.9577 (0.0,1.0)	0.76568 (0.0,1.0)
(15/-15)	0.18294 (0.5,0.6)	0.17602 (0.5,0.6)	0.60494 (0.1,1.0)	0.49154 (1.0,0.0)	1.4971 (0.9,1.0)	0.43213 (0.1,1.0)
$(15/-15)_2$	0.33502 (0.1,1.0)	0.094348 (0.5,0.4)	0.59732 (0.0,0.0)	0.81579 (1.0,0.0)	0.71556 (0.9,1.0)	0.13878 (0.9,1.0)*
$(15/-15)_5$	0.42442 (0.05,1.0)	0.043018 (0.5,0.6)	0.71295 (0.0,0.0)	0.95353 (0.0,1.0)	0.51698 (0.0,1.0)	0.23817 (1.0,0.2)
(30/-30)	0.13018 (0.5,0.4)	0.12592 (0.5,0.6)	0.65895 (0.1,1.0)	0.29714 (0.1,0.0)*	0.64229 (0.1,1.0)	0.45894 (0.1,0.0)
$(30/-30)_2$	0.12439 (0.2,1.0)	0.068785 (0.5,0.4)	0.68264 (1.0.0.9)	0.68264 (0.05,1.0)	0.39622 (0.0,0.9)	0.23195 (1.0,0.9)
$(30/30)_5$	0.19502 (0.2,1.0)	0.030276 (0.5,0.4)	0.69153 (1.0,0.9)	0.65549 (0.0,1.0)	0.41284 (0.1,0.9)	0.21265 (0.0,0.1)
(45/-45)	0.070755 (0.5,0.4)	0.0715 (0.5,0.6)	0.63083 (0.0,0.9)	0.54743 (0.9,1.0)	0.62673 (0.0,0.9)	0.48471 (1.0,0.9)
$(45/-45)_2$	0.073105 (0.2,1.0)	0.041513 (0.5,0.6)	0.63658 (0.1,0.0)	0.63803 (0.1,1.0)	0.33191 (0.0,0.9)	0.28047 (0.0,0.1)
$(45/-45)_5$	0.11192 (0.2,1.0)	0.03273 (0.0,0.2)	0.62425 (0.1,0.0)	0.63063 (0.1,1.0)	0.42522 (0.1,0.9)	0.17798 (0.05,0.1)
(60/-60)	0.0343 (0.6,0.5)	0.034695 (0.4,0.5)	0.52066 (0.1,0.0)	0.45694 (0.1,0.0)	0.39142 (0.0,0.9)	0.35426 (0.0,0.1)

$(60/-60)_2$	0.054548 (0.2,1.0)	0.020571 (0.4,0.5)*	0.57856 (0.1,0.0)	0.50927 (0.1,1.0)	0.20942 (0.05,0.9)	0.22069 (1.0,0.9)
$(60/-60)_5$	0.071821 (0.2,1.0)	0.032858 (1.0,0.2)	0.58183 (0.1,0.0)	0.51212 (0.9,1.0)	0.24199 (0.1,0.9)	0.17021 (0.1,0.9)
(75/-75)	0.074306 (0.2,1.0)	0.010284 (0.6,0.5)*	0.6692 (0.0,0.0)	0.64125 (1.0,0.0)	0.34954 (0.0,1.0)	0.22477 (1.0,0.4)
$(75/-75)_2$	0.077768 (0.2,1.0)	0.014925 (1.0,0.9)	0.53987 (0.0,0.0)	0.48786 (0.0,0.0)	0.3024 (0.0,1.0)	0.12056 (0.0,0.0)*
$(75/-75)_5$	0.081093 (0.2,1.0)	0.026659 (1.0,0.9)	0.50161 (0.0,0.0)	0.4395 (1.0,0.0) *	0.29251 (0.0,1.0)	0.1519 (1.0,1.0)
90	0.16104 (0.8,1.0)	0.019233 (0.0,0.9)	0.52068 (0.0,1.0)	0.39293 (0.0,1.0)	0.4542 (0.0,1.0)	0.2274 (0.0,1.0)

a/b=1, a/h=100, a'/b' =1, c/a=0.2; E_{11}/E_{22} = 25, G_{23} = 0.2E_{22}, G_{13} = G_{12} = 0.5E_{22}, ν_{12} = ν_{21} =0.25.

Values in the parenthesis indicates the location ($\bar{x}, \bar{y}$) of maximum hogging moments in each case.

Asterisk denotes the lowest values of shell actions in each group.

Table 5.13: Values of maximum non-dimensional sagging moment ($-\overline{M}_y$) x10^2 for different antisymmetric angle ply lamination and boundary conditions of stiffened composite hypar shell with cutout

Lamination (Degree)	Boundary conditions					
	Group-I		Group-II		Group-III	
	A	B	A	B	A	B
	CSSC	CSCS	FCCF	FCFC	FSSF	FSFS
0	-0.5569 (0.2,0.2)	-0.4939 (0.3,0.2)	-1.0872 (0.0,0.8)	-0.53002 (0.0,0.5)	-1.0741 (0.0,0.7)	-0.48039 (1.0,0.5)
(15/-15)	-0.5711 (0.7,0.5)	-0.51574 (0.7,0.5)	-2.5698 (0.0,1.0)	-0.70504 (0.2,0.7)	-6.0338 (1.0,1.0)	-2.274 (0.0,1.0)
$(15/-15)_2$	-0.36225 (0.2,0.2)	-0.33883 (0.3,0.2)	-0.55374 (0.0,0.75)	-0.46423 (0.8,0.4)	-2.797 (1.0,1.0)	-0.86614 (1.0,1.0)
$(15/-15)_5$	-0.27309 (0.2,0.2)	-0.24825 (0.3,0.2)	-0.58115 (0.0,0.75)	-0.31348 (1.0,0.7)	-0.96784 (1.0,1.0)	-0.30621 (0.0,0.5)
(30/-30)	-0.34589 (0.7,0.5)	-0.33118 (0.7,0.5)	-2.7859 (0.0,1.0)	-0.44972 (0.8,0.6)	-3.1552 (1.0,1.0)	-1.9656 (1.0,0.0)
$(30/-30)_2$	-0.19022 (0.2,0.8)	-0.18219 (0.7,0.8)	-0.86671 (0.0,1.0)	-0.26521 (0.8,0.6)	-1.2467 (1.0,1.0)	-0.74163 (1.0,0.0)
$(30/30)_5$	-0.14064 (0.1,0.8)	-0.11837 (0.7,0.2)	-0.21554 (0.0,0.7)	-0.1902 (0.0,0.5)	-0.2256 (0.05,0.7)	-0.19999 (0.0,0.5)
(45/-45)	-0.21819 (0.4,0.6)	-0.21759 (0.4,0.4)	-1.7462 (0.0,1.0)	-0.2829 (0.5,0.0)	-1.6292 (0.0,1.0)	-1.4003 (1.0,1.0)
$(45/-45)_2$	-0.11564 (0.1,0.9)	-0.11318 (0.6,0.6)	-0.5536 (0.0,1.0)	-0.20584 (0.5,1.0)	-0.5317 (0.0,1.0)	-0.4722 (0.0,0.0)
$(45/-45)_5$	-0.09188 (0.1,0.9)	-0.06634 (0.2,0.1)	-0.1338 (0.1,0.7)	-0.14615 (0.5,0.0)	-0.16154 (0.3,0.1)	-0.13433 (0.05,0.5)
(60/-60)	-0.12133 (0.5,0.3)	-0.12091 (0.5,0.7)	-0.4647 (0.0,1.0)	-0.16361 (0.0,0.5)	-0.58686 (0.0,0.0)	-0.64936 (0.0,1.0)

$(60/-60)_2$	-0.083579 (0.2,0.9)	-0.070521 (0.8,0.1)	-0.097655 (0.1,0.2)	-0.10789 (0.5,0.0)	-0.12226 (0.0,0.0)	-0.10789 (1.0,0.0)
$(60/-60)_5$	-0.066557 (0.2,0.9)	-0.049949 (0.8,0.9) *	-0.086694 (0.0,0.3)*	-0.089522 (1.0,0.3)	-0.080367 (0.05,0.7)*	-0.096107 (0.95,0.3)
(75/-75)	-0.07812 (0.2,0.9)	-0.06465 (0.8,0.9)	-0.19869 (0.0,0.5)	-0.20524 (1.0,0.5)	-0.19122 (0.0,0.5)	-0.20417 (0.0,0.5)
$(75/-75)_2$	-0.06825 (0.2,0.9)	-0.05064 (0.8,0.9)	-0.11075 (0.0,0.5)	-0.12232 (0.0,0.5)	-0.10259 (0.0,0.5)	-0.12641 (0.0,0.3)
$(75/-75)_5$	-0.0627 (0.2,0.9)	-0.04301 (0.8,0.9)*	-0.08809 (0.0,0.5)*	-0.10272 (0.0,0.3)	-0.08626 (0.0,0.3)*	-0.11185 (1.0,0.3)
90	-0.071805 (0.2,0.9)	-0.048512 (0.2,0.9)	-0.145 (0.0,0.9)	-0.13011 (1.0,0.7)	-0.13213 (0.0,0.8)	-0.13244 (1.0,0.7)

a/b=1, a/h=100, a'/b' =1, c/a=0.2; E_{11}/E_{22} = 25, G_{23} = 0.2E_{22}, G_{13} = G_{12} = 0.5E_{22}, ν_{12} = ν_{21} =0.25.

Values in the parenthesis indicates the location ($\bar{x}$, $\bar{y}$) of maximum sagging moment in each case.

Asterisk denotes the lowest values of shell actions in each group.

Table 5.14: Values of maximum non-dimensional anticlockwise twisting moments ($+\overline{M}_{xy}$) x10^2 for different antisymmetric angle ply lamination and boundary conditions of stiffened composite hypar shell with cutout

Lamination (Degree)	Boundary conditions					
	Group-I		Group-II		Group-III	
	A	B	A	B	A	B
	CSSC	CSCS	FCCF	FCFC	FSSF	FSFS
0	0.037944 (0.1,0.0)	0.031328 (0.9,1.0)	0.12088 (0.1,1.0)	0.024386 (0.0,0.3)	0.11372 (0.0,0.0)	0.090819 (0.0,0.0)
(15/-15)	0.088735 (0.6,0.6)	0.080738 (0.4,0.4)	0.923 (0.0,1.0)	0.43923 (0.0,1.0)	1.0578 (0.0,1.0)	0.82629 (0.0,1.0)
$(15/-15)_2$	0.057772 (0.4,0.4)	0.052299 (0.4,0.4)	0.35989 (0.1,0.9)	0.24023 (1.0,0.0)	0.37682 (0.1,0.9)	0.35256 (1.0,0.0)
$(15/-15)_5$	0.040785 (1.0,0.9) *	0.031211 (0.4,0.4)*	0.32007 (0.1,0.9)	0.11952 (0.0,1.0) *	0.32814 (0.1,0.9)	0.13407 (1.0,0.1)*
(30/-30)	0.18995 (1.0,0.0)	0.10485 (0.6,0.6)	1.9754 (0.0,1.0)	0.91723 (0.0,1.0)	1.9759 (0.0,1.0)	1.5173 (0.0,1.0)
$(30/-30)_2$	0.07692 (0.4,0.4)	0.068537 (0.6,0.6)	0.70675 (0.0,1.0)	0.48562 (0.0,1.0)	0.7438 (0,1,0.9)	0.65793 (1.0,0.0)
$(30/30)_5$	0.045777 (0.4,0.4)	0.040937 (0.4,0.4)	0.58772 (0.1,0.9)	0.2484 (0.05,0.9)	0.60932 (0.1,0.9)	0.25235 (1.0,0.1)
(45/-45)	0.21947 (1.0,0.0)	0.11146 (0.4,0.4)	2.1835 (0.0,1.0)	1.3376 (1.0,0.0)	2.1452 (0.0,1.0)	1.9668 (1.0,0.0)
$(45/-45)_2$	0.075312 (0.4,0.4)	0.073197 (0.4,0.4)	0.84521 (0.1,0.9)	0.68613 (0.0,1.0)	0.89207 (0.1,0.9)	0.83756 (0.0,1.0)
$(45/-45)_5$	0.045154 (0.4,0.4)	0.043868 (0.6,0.6)	0.68098 (0.1,0.9)	0.43169 (0.1,0.9)	0.707 (0.1,0.9)	0.43052 (0.1,0.9)

(60/-60)	0.11493 (1.0,0.0)	0.1039 (0.4,0.4)	1.5035 (0.0,1.0)	1.0423 (0.0,1.0)	1.5841 (0.0,1.0)	1.6624 (0.0,1.0)
$(60/-60)_2$	0.072134 (0.6,0.6)	0.067079 (0.4,0.4)	0.68201 (0.1,0.9)	0.61209 (0.0,1.0)	0.72278 (0.1,0.9)	0.73891 (1.0,0.0)
$(60/-60)_5$	0.042195 (0.,6,0.6)	0.042783 (0.9,1.0)	0.60475 (0.1,0.9)	0.39865 (0.1,0.9)	0.62474 (0.1,0.9)	0.48929 (0.9,0.1)
(75/-75)	0.08634 (0.4,0.4)	0.084457 (0.9,1.0)	0.42859 (1.0,0.05)	0.35338 (1.0,0.0)	0.54137 (0.05,1.0)	0.29934 (0.95,0.1)
$(75/-75)_2$	0.060973 (0.2,0.0)	0.068926 (0.9,1.0)	0.33476 (0.1,0.9)	0.29418 (0.0,1.0)	0.35635 (0.1,0.9)	0.2705 (0.9,0.1)
$(75/-75)_5$	0.05751 (0.9,0.9)	0.061555 (0.9,1.0)	0.31778 (0.1,0.9)	0.24969 (1.0,0.0) *	0.33055 (0.1,0.9)	0.23722 (0.9,0.1)*
90	0.094868 (0.0,0.85)	0.094647 (0.0,0.9)	0.098128 (0.1,1.0)	0.074555 (0.2,0.9)	0.12883 (0.0,0.0)	0.095647 (0.0,0.0)

a/b=1, a/h=100, a'/b' =1, c/a=0.2; E_{11}/E_{22} = 25, G_{23} = 0.2E_{22}, G_{13} = G_{12} = 0.5E_{22}, ν_{12} = ν_{21} =0.25.

Values in the parenthesis indicates the location ($\bar{x}, \bar{y}$) of maximum anticlockwise twisting moment in each case.

Asterisk denotes the lowest values of shell actions in each group.

Table 5.15: Values of maximum non-dimensional clockwise twisting moments ($-\overline{M}_{xy}$) x10^2 for different antisymmetric angle ply lamination and boundary conditions of stiffened composite hypar shell with cutout

Lamination (Degree)	Boundary conditions					
	Group-I		Group-II		Group-III	
	A	B	A	B	A	B
	CSSC	CSCS	FCCF	FCFC	FSSF	FSFS
0	-0.055845 (1.0,0.0)	-0.031327 (0.9,0.0)	-0.24013 (0.0,1.0)	-0.024384 (0.0,0.7)	-0.23557 (0.0,1.0)	-0.090831 (0.0,1.0)
(15/-15)	-0.082597 (0.4,0.6)	-0.080739 (0.4,0.6)	-0.46078 (1.0,1.0)	-0.43923 (0.0,0.0)	-0.65365 (1.0,1.0)	-0.82627 (0.0,0.0)
$(15/-15)_2$	-0.054896 (0.6,0.4)	-0.052298 (0.4,0.6)	-0.24402 (1.0,1.0)	-0.24022 (0.0,0.0)	-0.32104 (0.9,0.9)	-0.35257 (1.0,1.0)
$(15/-15)_5$	-0.045312 (1.0,0.1)	-0.031211 (0.6,0.4)*	-0.20873 (0.9,0.9)*	-0.11952 (0.0,0.0) *	-0.25284 (0.9,0.9)	-0.13408 (1.0,0.9) *
(30/-30)	-0.11314 (0.6,0.4)	-0.10485 (0.6,0.4)	-1.3121 (1.0,1.0)	-0.91722 (0.0,0.0)	-1.7703 (1.0,1.0)	-1.5173 (0.0,0.0)
$(30/-30)_2$	-0.072684 (0.6,0.4)	-0.068538 (0.6,0.4)	-0.59443 (1.0,1.0)	-0.48561 (0.0,0.0)	-0.70074 (1.0,1.0)	-0.65792 (1.0,1.0)
$(30/30)_5$	-0.043701 (0.4,0.6)	-0.040939 (0.6,0.4) *	-0.42815 (0.9,0.9)	-0.24837 (0.05,0.1)	-0.48183 (0.9,0.9)	-0.25232 (1.0,0.9)
(45/-45)	-0.11261 (0.4,0.6)	-0.11146 (0.6,0.4)	-1.3708 (0.0,0.0)	-1.3377 (1.0,1.0)	-1.8555 (0.0,0.0)	-1.9668 (1.0,1.0)
$(45/-45)_2$	-0.07387 (0.4,0.6)	-0.0732 (0.4,0.6)	-0.70037 (0.0,0.0)	-0.68614 (0.0,0.0)	-0.71911 (0.0,0.0)	-0.8376 (0.0,0.0)
$(45/-45)_5$	-0.05117 (0.1,0.9)	-0.04387 (0.4,0.6)	-0.41485 (0.1,0.1)	-0.43166 (0.1,0.1)	-0.43291 (0.05,0.1)	-0.43053 (0.9,0.9)

(60/-60)	-0.10681 (0.6,0.4)	-0.1039 (0.4,0.6)	-1.0968 (0.0,0.0)	-1.0423 (0.0,0.0)	-1.6311 (0.0,0.0)	-1.6624 (0.0,0.0)
$(60/-60)_2$	-0.069411 (0.6,0.4)	-0.067078 (0.6,0.4)	-0.64052 (0.0,0.0)	-0.61206 (0.0,0.0)	-0.68785 (0.0,0.0)	-0.7389 (1.0,1.0)
$(60/-60)_5$	-0.049518 (0.1,0.9)	-0.042783 (0.9,0.0)	-0.4098 (0.0,0.0)	-0.3987 (0.9,0.9)	-0.50166 (0.1,0.1)	-0.4893 (0.9,0.9)
(75/-75)	-0.08036 (0.4,0.6)	-0.08445 (0.1,1.0)	-0.38089 (1.0,1.0)	-0.35338 (1.0,1.0)	-0.39001 (0.95,1.0)	-0.29929 (0.05,1.0)
$(75/-75)_2$	-0.06047 (0.9,0.0)	-0.06892 (0.9,0.0)	-0.30561 (0.0,0.0)	-0.29418 (0.0,0.0)	-0.27639 (0.05,0.1)	-0.2705 (0.1,0.1)
$(75/-75)_5$	-0.05426 (0.9,0.0)	-0.06155 (0.1,1.0)	-0.26932 (0.0,0.0)	-0.24967 (0.0,0.0)	-0.24089 (0.1,0.1)	-0.23721 (0.9,0.8) *
90	-0.084457 (0.0,0.1)	-0.094646 (0.0,0.1)	-0.18059 (1.0,1.0)	-0.074542 (0.2,0.1)	-0.10505 (0.0,1.0)	-0.095682 (0.0,1.0)

a/b=1, a/h=100, a'/b' =1, c/a=0.2; E_{11}/E_{22} = 25, G_{23} = 0.2E_{22}, G_{13} = G_{12} = 0.5E_{22}, ν_{12} = ν_{21} =0.25.

Values in the parenthesis indicates the location ($\bar{x}, \bar{y}$) of maximum clockwise twisting moment in each case.

Asterisk denotes the lowest values of shell actions in each group.

Table 5.16: Shell options arranged according to ascending order of positive values of shell actions different antisymmetric angle ply lamination and boundary conditions of stiffened composite hypar shell with cutout

Non-dimensional Shell Action	Non-dimensional co-ordinates $(\bar{x}, \bar{y})$	Shell actions at each layer
$\overline{N}_x$	$\bar{x}$ =0.6 $\bar{y}$ =0.6	CSCS/(30/-30)
	$\bar{x}$ =0.6, $\bar{y}$ =0.6	CSCS/ $(15/-15)_2$
	$\bar{x}$ =0.0, $\bar{y}$ =1.0	FCFC/ (15/-15)
	$\bar{x}$ =0.0, $\bar{y}$ =1.0	FCFC/$(75/-75)_5$
	$\bar{x}$ = 0.0, $\bar{y}$ =1.0	FSFS/ (15/-15)
	$\bar{x}$ =0.0, $\bar{y}$ =1.0	FSFS/ (30/-30)
$\overline{N}_y$	$\bar{x}$ =1.0, $\bar{y}$ =1.0	CSCS/ (75/-75)
	$\bar{x}$ =0.6, $\bar{y}$ =0.6	CSCS/ (60/-60)
	$\bar{x}$ =0.0, $\bar{y}$ =1.0	FCFC/$(75/-75)_5$
	$\bar{x}$ = 0.0, $\bar{y}$ =1.0	FCFC/$(60/-60)_5$
	$\bar{x}$ = 0.0, $\bar{y}$ =1.0	FSSF/(60/-60)
	$\bar{x}$ = 1.0, $\bar{y}$ =0.0	FSFS/$(75/-75)_5$
$\overline{N}_{xy}$	$\bar{x}$ =0.55, $\bar{y}$ =0.5	CSCS/$(75/-75)_5$
	$\bar{x}$ = 0.0, $\bar{y}$ =1.0	CSSC/$(75/-75)_2$
	$\bar{x}$ = 0.4, $\bar{y}$ =0.5	FCFC/$(15/-15)_2$
	$\bar{x}$ =1.0, $\bar{y}$ =0.6	FCFC/ (15/-15)
	$\bar{x}$ =0.1, $\bar{y}$ =0.0	FSFS/ (15/-15)
	$\bar{x}$ =1.0, $\bar{y}$ =0.9	FSFS/$(60/-60)_5$
	$\bar{x}$ =0.5, $\bar{y}$ =0.6	CSCS/(15/-15)
	$\bar{x}$ =1.0, $\bar{y}$ =0.8	CSCS/$(30/-30)_5$

$\overline{M}_x$	$\bar{x}$ =1.0, $\bar{y}$ =0.0	FCFC/(15/-15)
	$\bar{x}$ = 0.1, $\bar{y}$ =0.0	FCFC/(30/-30)
	$\bar{x}$ =0.5, $\bar{y}$ =0.9	FSFS/$(15/-15)_5$
	$\bar{x}$ =0.0, $\bar{y}$ =0.1	FSFS/$(30/-30)_5$
$\overline{M}_y$	$\bar{x}$ =0.6, $\bar{y}$ =0.5	CSCS/(75/-75)
	$\bar{x}$ =0.4, $\bar{y}$ =0.5	CSCS/ $(60/-60)_2$
	$\bar{x}$ =0.1, $\bar{y}$ =0.0	FCFC/(30/-30)
	$\bar{x}$ =1.0, $\bar{y}$ =0.0	FCFC/$(75/-75)_5$
	$\bar{x}$ =0.0, $\bar{y}$ =0.0	FSFS/$(75/-75)_2$
	$\bar{x}$ =0.9, $\bar{y}$ =1.0	FSFS/ $(15/-15)_2$
$\overline{M}_{xy}$	$\bar{x}$ =0.4, $\bar{y}$ =0.4	CSCS/$(15/-15)_5$
	$\bar{x}$ =1.0, $\bar{y}$ =0.9	CSSC/ $(15/-15)_5$
	$\bar{x}$ =0.0, $\bar{y}$ =1.0	FCFC/ $(15/-15)_5$
	$\bar{x}$ =1.0, $\bar{y}$ =0.0	FCFC/ $(75/-75)_5$
	$\bar{x}$ =1.0, $\bar{y}$ =0.1	FSFS/ $(15/-15)_5$
	$\bar{x}$ =0.9, $\bar{y}$ =0.1	FSFS/ $(75/-75)_5$

Table 5.17: Shell options arranged according to ascending order of negative values of shell actions of different antisymmetric angle ply lamination and boundary conditions of stiffened composite hypar shell with cutout

Non-dimensional Shell Action	Non-dimensional co-ordinates $(\bar{x}, \bar{y})$	Shell actions at each layer
$\bar{w}$	$\bar{x}$ =0.5, $\bar{y}$ =0.6	CSCS/(45/-45)$_5$
	$\bar{x}$ =0.5, $\bar{y}$ =0.6	CSCS/(60/-60)$_5$
	$\bar{x}$ =0.0, $\bar{y}$ =0.5	FCFC/(15/-15)
	$\bar{x}$ =0.0, $\bar{y}$ =0.5	FCFC/(30/-30)$_2$
	$\bar{x}$ =1.0, $\bar{y}$ =0.5	FSFS/(15/-15)$_5$
	$\bar{x}$ =1.0, $\bar{y}$ =0.5	FSFS/(30/-30)$_5$
$\bar{N}_x$	$\bar{x}$ = 0.6, $\bar{y}$ =0.4	CSCS/(30/-30)
	$\bar{x}$ = 0.4, $\bar{y}$ =0.6	CSCS/(15/-15)$_2$
	$\bar{x}$ =0.0, $\bar{y}$ =0.0	FCFC/(15/-15)
	$\bar{x}$ =0.0, $\bar{y}$ =0.0	FCFC/(30/-30)$_2$
	$\bar{x}$ =0.0, $\bar{y}$ =0.0	FSFS/(15/-15)
	$\bar{x}$ =0.0, $\bar{y}$ =0.0	FSFS/(75/-75)$_5$
$\bar{N}_y$	$\bar{x}$ =0.0, $\bar{y}$ =1.0	CSCS/(75/-75)
	$\bar{x}$ =0.4, $\bar{y}$ =0.6	CSSC/(60/-60)
	$\bar{x}$ =0.0, $\bar{y}$ =0.0	FCFC/(75/-75)$_5$
	$\bar{x}$ =0.0, $\bar{y}$ =0.1	FCCF/(75/-75)$_5$
	$\bar{x}$ =0.0, $\bar{y}$ =0.0	FSFS/(75/-75)$_5$
	$\bar{x}$ =1.0, $\bar{y}$ =1.0	FSSF/(60/-60)
	$\bar{x}$ =0.7, $\bar{y}$ =0.5	CSCS/(15/-15)
	$\bar{x}$ =0.5, $\bar{y}$ =0.7	CSCS/(75/-75)$_5$

$\overline{N}_{xy}$	$\bar{x}$ = 0.8, $\bar{y}$ =0.5	FCFC/(15/-15)$_5$
	$\bar{x}$ =0.5, $\bar{y}$ =0.7	FCFC/(15/-15)
	$\bar{x}$ =0.0, $\bar{y}$ =0.0	FSFS/(15/-15)
	$\bar{x}$ =1.0, $\bar{y}$ =1.0	FSFS/(30/-30)
$\overline{M}_{x}$	$\bar{x}$ =0.3, $\bar{y}$ =0.2	CSCS/(15/-15)$_5$
	$\bar{x}$ =0.7, $\bar{y}$ =0.2	CSCS/(30/-30)$_5$
	$\bar{x}$ = 0.9, $\bar{y}$ =0.6	FCFC/(15/-15)$_5$
	$\bar{x}$ =0.95, $\bar{y}$ =0.5	FCFC/(30/-30)$_5$
	$\bar{x}$ =0.2, $\bar{y}$ =0.1	FSFS/(15/-15)$_5$
	$\bar{x}$ =0.8, $\bar{y}$ =0.9	FSFS/(30/-30)$_5$
$\overline{M}_{y}$	$\bar{x}$ =0.8, $\bar{y}$ =0.9	CSCS/(75/-75)$_5$
	$\bar{x}$ =0.8, $\bar{y}$ =0.9	CSCS/(60/-60)$_5$
	$\bar{x}$ = 0.0, $\bar{y}$ =0.3	FCCF/(60/-60)$_5$
	$\bar{x}$ =0.0, $\bar{y}$ =0.5	FCCF/(75/-75)$_5$
	$\bar{x}$ =0.05, $\bar{y}$ =0.7	FSSF/(60/-60)$_5$
	$\bar{x}$ =0.0, $\bar{y}$ =0.3	FSSF/(75/-75)$_5$
$\overline{M}_{xy}$	$\bar{x}$ =0.6, $\bar{y}$ =0.4	CSCS/(15/-15)$_5$
	$\bar{x}$ =0.6, $\bar{y}$ =0.4	CSSC/(30/-30)$_5$
	$\bar{x}$ =0.0, $\bar{y}$ =0.0	FCFC/(15/-15)$_5$
	$\bar{x}$ =0.9, $\bar{y}$ =0.9	FCCF/(15/-15)$_5$
	$\bar{x}$ =1.0, $\bar{y}$ =0.9	FSFS/ (15/-15)$_5$
	$\bar{x}$ =0.0, $\bar{y}$ =0.8	FSFS/(75/-75)$_5$

Table 5.18: Relative performance matrix considering CSCS/$(15/-15)_2$ and CSCS/$(45/-45)_2$ shells

	Shell actions	CSCS/$(15/-15)_2$	CSCS/$(45/-45)_2$
Positive	$\overline{N}_x$	1	0
	$\overline{N}_y$	0	1
	$\overline{N}_{xy}$	1	1
	$\overline{M}_x$	1	1
	$\overline{M}_y$	1	1
	$\overline{M}_{xy}$	1	1
Negative	$\overline{w}$	0	1
	$\overline{N}_x$	1	0
	$\overline{N}_y$	0	1
	$\overline{N}_{xy}$	1	1
	$\overline{M}_x$	1	0
	$\overline{M}_y$	0	1
	$\overline{M}_{xy}$	1	1
Total		9	10

5.3.2 Shell characteristics along some typical lines of dominating values of the respective shell actions

Ten layered antisymmetric angle ply laminates like $(+15/-15)_5$, $(+30/-30)_5$, $(+45/-45)_5$, $(+60/-60)_5$, $(+75/-75)_5$ are chosen for additional study with graphite epoxy as the material subjected to uniformly distributed load. It has been found from the previous study by the author that as the number of layer increases the shell actions decreases. So ten layered antisymmetric angle ply laminates are chosen for the present study. The shell characteristics along some typical lines of dominating values of the respective shell actions are studied for different lamination angle of antisymmetric angle ply laminates for CSSC and CSCS boundary conditions. The comparative performance of different lamination angle of antisymmetric angle ply lamination in terms of non-dimensional values of static displacements, static stress resultants of different shell combinations are presented systematically in Fig 5.2-5.8. The material and geometric properties of the hypar

shells for these problems are considered as: a/b=1, $a^{/}$ /b $^{/}$=1, a/h=100, c/a=0.2, E_{11}=25E_{22}, G_{12}=G_{13}=0.5E_{22}, G_{23}=0.2E_{22}, v=0.25, ρ=100 N-sec^2/m^4.

Displacement component $\bar{w}$

Figs. 5.2a and 5.2b show that deflection values are highest for cross ply shells (0^0 and 90^0). Fig. 5.2a shows the values of deflection along $\bar{y} = 0.6$ for CSSC shell. It is seen that with the increase in lamination angle deflection increases. It is seen that $(+75/-75)_5$ lamination shows higher deflection than $(+60/-60)_5$ lamination. Whereas the deflection of $(+45/-45)_5$, $(+30/-30)_5$, and $(+15/-15)_5$ laminations are decreasing gradually. This indicates superior performance of the lower lamination angle compared to higher lamination angle On the other hand values of deflection along $\bar{y} = 0.4$ for CSCS boundary condition (Fig. 5.2b) is always higher for 0^0 and 90^0 lamination angle than other lamination angle. The values of deflection of $(+15/-15)_5$ and $(+75/-75)_5$ are close to each other whereas deflection for $(+30/-30)_5$, $(+45/-45)_5$ and $(+60/-60)_5$ laminations are almost same. $(+30/-30)_5$, $(+45/-45)_5$ and $(+60/-60)_5$ laminations and showing lower deflection than $(+15/-15)_5$ and $(+75/-75)_5$ laminations. Comparing Fig. 5.2a and 5.2b, it is noted that the arrangement of boundary constraints have a large impact on deflection.

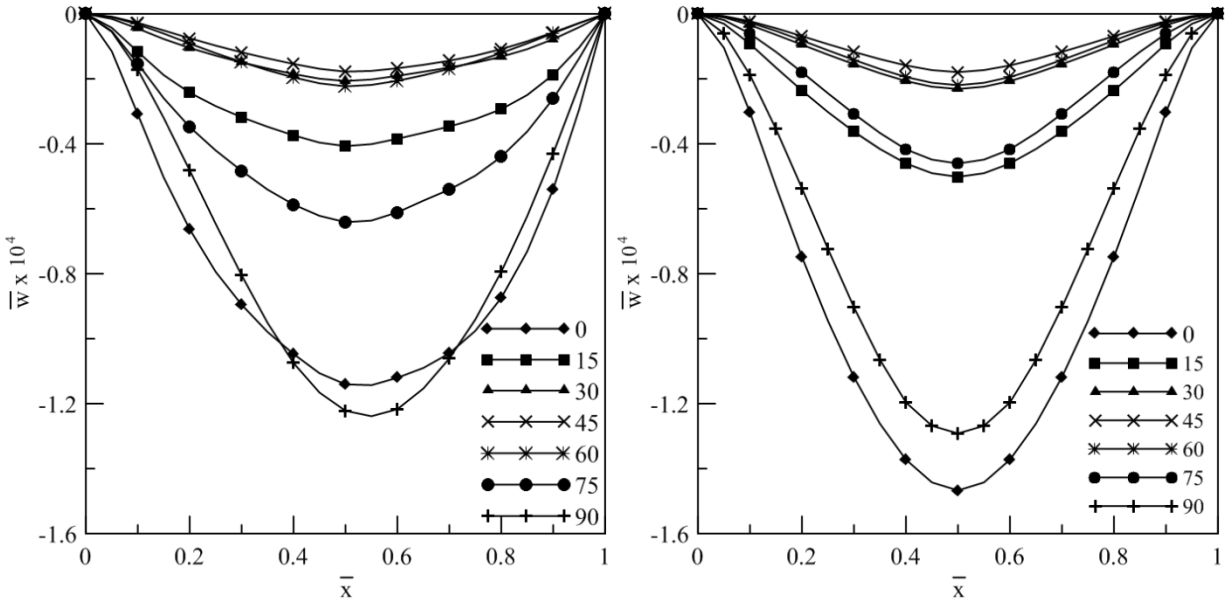

(a) (b)

Fig. 5.2 Variation of $\bar{w}$ (a) along $\bar{y} = 0.6$ for CSSC boundary (b) along $\bar{y} = 0.4$ for CSCS boundary

Stress resultant $\overline{N}_x$

The plots of $\overline{N}_x$ along $\bar{y} = 0.9$ for CSSC boundary condition and $\overline{N}_x$ along $\bar{y} = 0.6$ for CSCS boundary condition (Fig.5.3a and Fig. 5.3b) show that values of $\overline{N}_x$ increase with increase in lamination angle. The rate of increase is higher for higher lamination angle. In case of CSSC shell the peak values of $\overline{N}_x$ are 179% and 206% for $(+60/-60)_5$ and $(+75/-75)_5$ lamination whereas for the $(+30/-30)_5$, $(+45/-45)_5$ and $(+60/-60)_5$ laminations are respectively about -3.7%, 19.8% and 70% more than the maximum value of the 0^0 lamination. For CSCS shells the peak values of $(+60/-60)_5$ and $(+75/-75)_5$ shells are 123% and 243% with respect to 0^0 shell whereas peak values of other lamination angles are within 38%. This indicates superior performance of the lower lamination angle. The peak values of $\overline{N}_x$ for CSSC boundary is occurring along the clamped edge whereas the peak values of CSCS shells are occurring near the cutout of the shell. Here, again the effect of arrangement of boundary constraints upon the shell characteristics is proved.

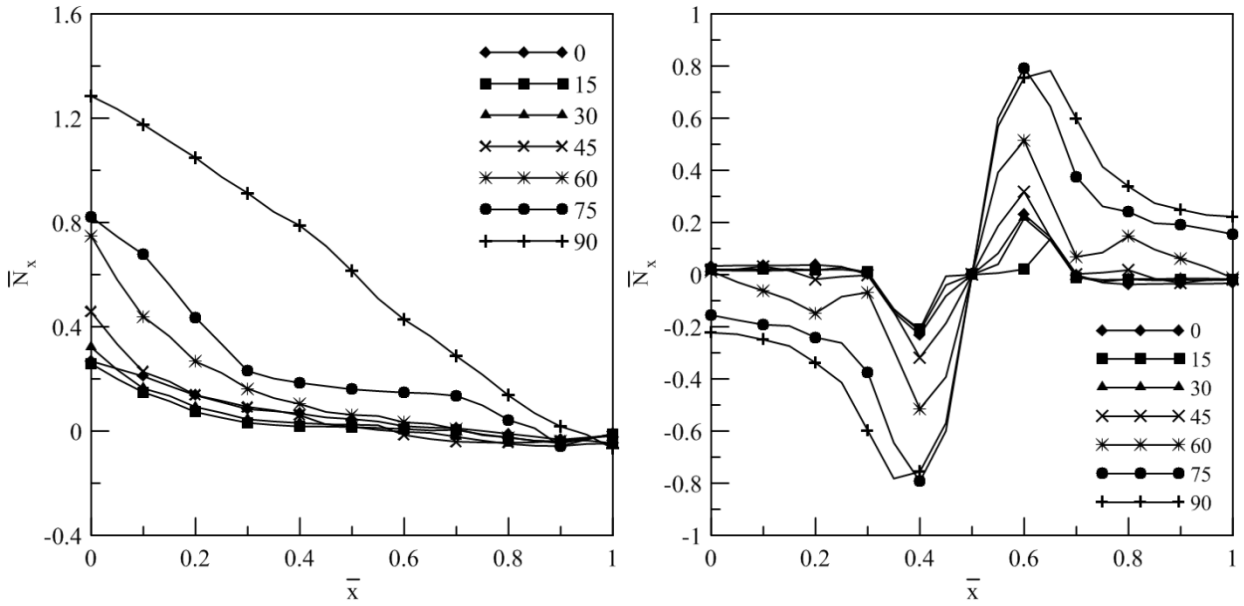

(a) (b)

Fig. 5.3 Variation of $\overline{N}_x$ (a) along $\bar{y} = 0.9$ for CSSC boundary (b) along $\bar{y} = 0.6$ for CSCS boundary

Stress resultant $\overline{N}_y$

The nature and values of $\overline{N}_y$ along $\bar{x} = 0.1$ for CSSC shell (Fig. 5.4a) reveals that the values of $(+75/-75)_5$ and $(+15/-15)_5$ laminations are much higher than the other lamination but lower than 0^0 lamination. The $\overline{N}_y$ values of $(+45/-45)_5$ and $(+60/-60)_5$ laminations are close to each other and showing lowest values. The values are increased at high rate from simply supported edge to a clamped edge. The nature and values of $\overline{N}_y$ along for CSCS boundary condition (Fig.5.4b) shows with the increase in lamination angle shell action decreases gradually with reference to 0^0 lamination. For a CSCS shell there is fluctuation of stress parallel to clamped edge and maximum shell actions occur near the cutout. The effect of arrangement of boundary constraints is once again established.

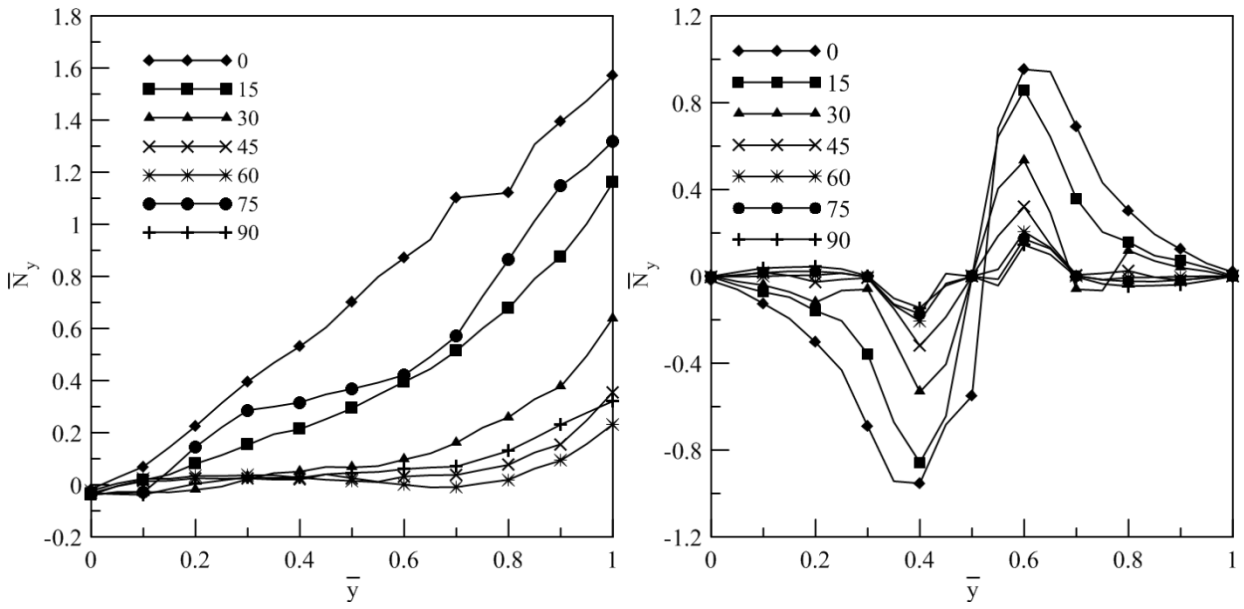

(a) (b)

Fig. 5.4 Variation of $\overline{N}_y$ (a) along $\bar{x} = 0.1$ for CSSC boundary (b) along $\bar{x} = 0.6$ for CSSC boundary

Stress resultant $\overline{N}_{xy}$

The values of $\overline{N}_{xy}$ along $\bar{x} = 0.7$ for CSSC and CSCS boundary (Fig. 5.5a and 5.5b) are found to be wavy in nature. With increase in lamination angle the wavy nature increases.

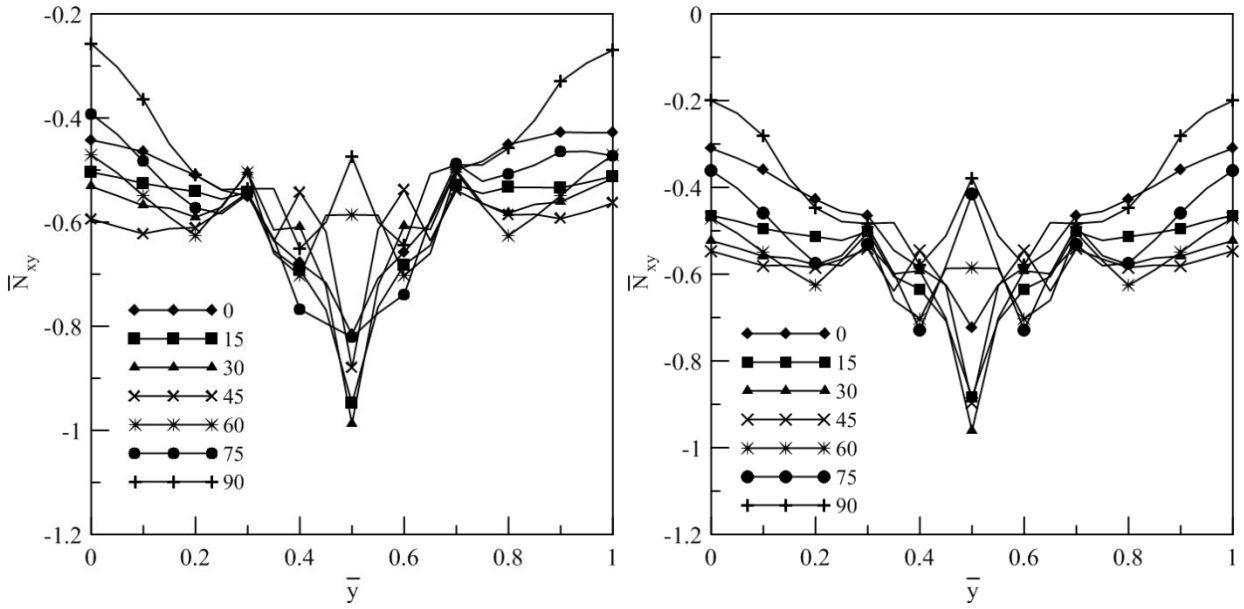

(a) (b)

Fig. 5.5 Variation of $\overline{N}_{xy}$ (a) along $\bar{x} = 0.7$ for CSSC boundary (b) along $\bar{x} = 0.7$ for CSCS boundary

Stress couple $\overline{M}_x$

The plots of $\overline{M}_x$ along $\bar{y} = 0.8$ (Fig 5.6a) for CSSC shell and along $\bar{y} = 0.2$ (Fig.5.6b) for CSCS shell indicates that, for lower lamination angle, increase in lamination angle has marginal effect with respect to nature and magnitude. However, the higher lamination angles show significant increase in the values, the peak values being 25% and 216% more respectively for the $(+60/-60)_5$ and $(+75/-75)_5$, in comparison to cross ply (0) shell. The similar nature of variation and marginal changes of values clearly establishes the superiority of the shell with lower lamination angle over those with higher lamination angle.

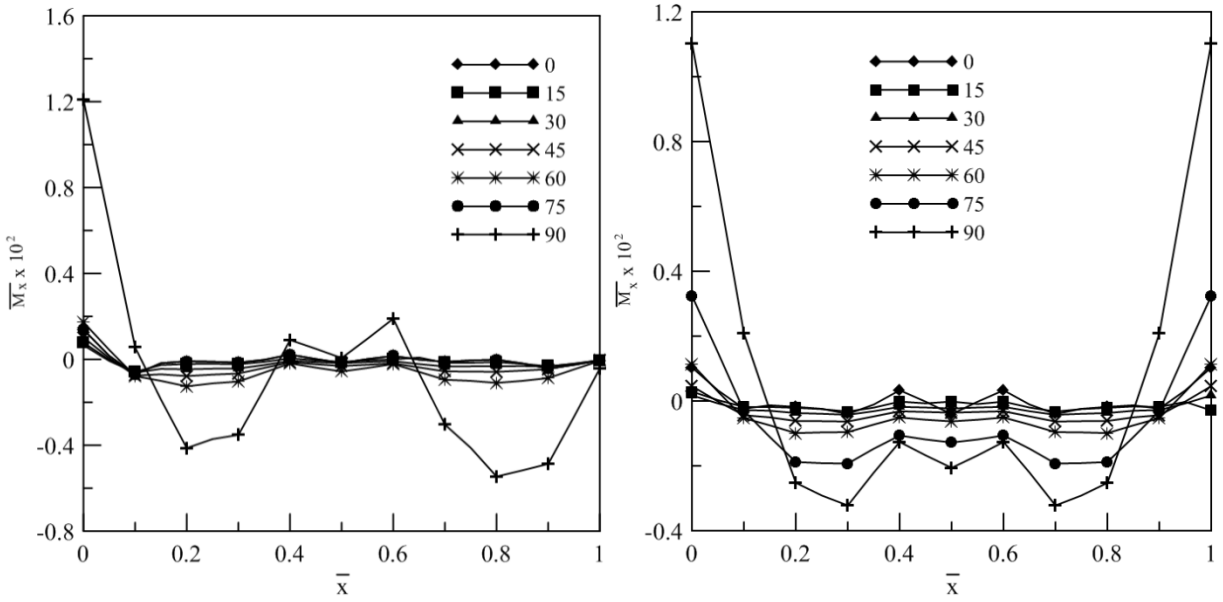

(a) (b)

Fig. 5.6 Variation of $\overline{M}_x$ (a) along $\bar{y} = 0.8$ for CSSC boundary (b) along $\bar{y} = 0.2$ for CSCS boundary

Stress couple $\overline{M}_y$

It is observed from Fig.5.7a that the values of $\overline{M}_y$ hardly changed along $\bar{x} = 0.05$ for CSSC boundary for $(+60/-60)_5$ and $(+45/-45)_5$ lamination. But with increase in lamination angle above 60^0 or decrease in lamination angle below 45^0 there are appreciable changes in the peak values, both positive and negative. For $(+15/-15)_5$, $(+30/-30)_5$ and $(+75/-75)_5$ lamination, the peak values occurring along the clamped edges and plots are wavy in mature. However, from Fig. 5.7b it is found that variation of $\overline{M}_y$ along $\bar{x} = 0.3$ for CSCS boundary condition is significant for lower lamination angle whereas for higher lamination angle the changes are marginal. The peak values are toward the simply supported edges.

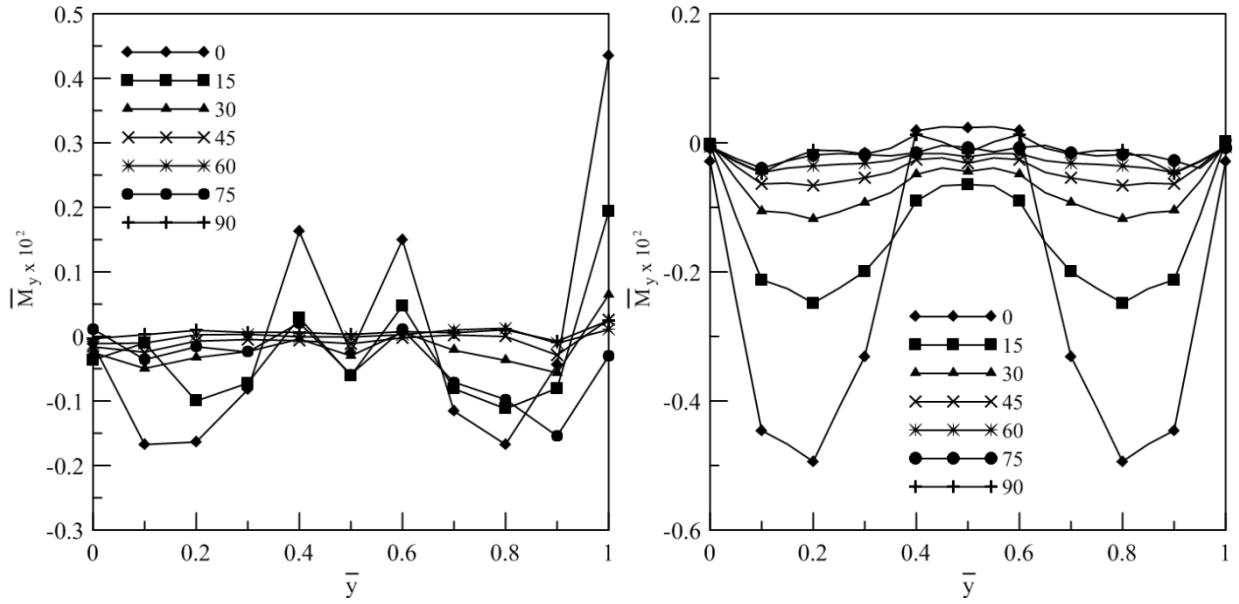

(a) (b)

Fig. 5.7 Variation of $\overline{M}_y$ (a) along $\bar{x} = 0.05$ for CSSC boundary (b) along $\bar{x} = 0.3$ for CSCS boundary

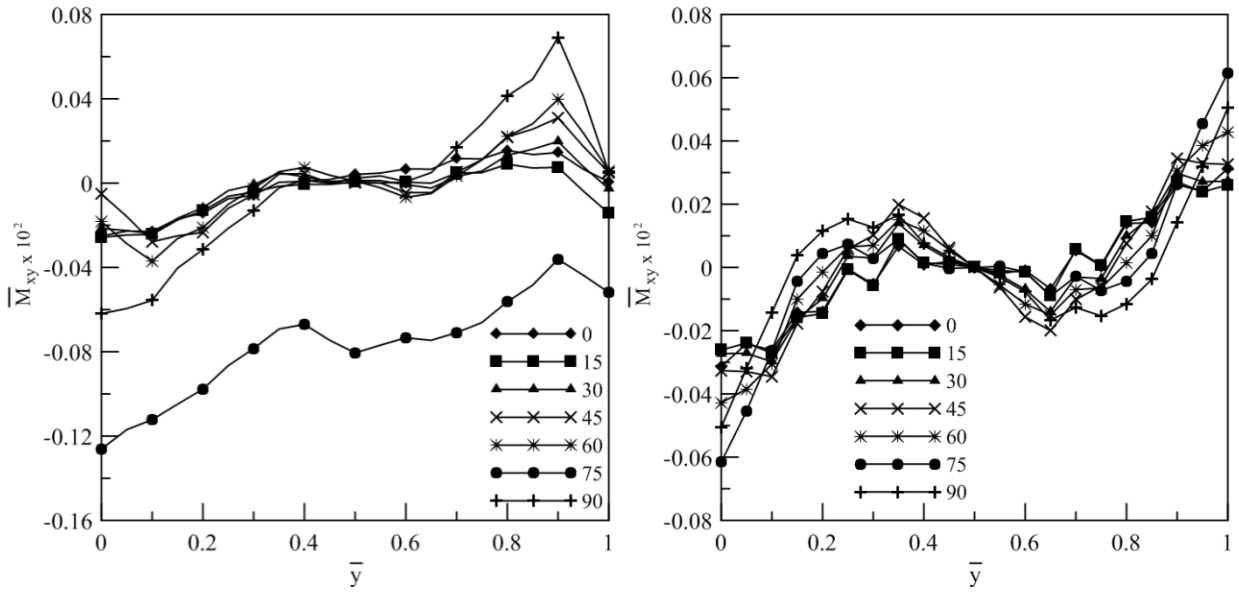

(a) (b)

Fig. 5.8 Variation of $\overline{M}_{xy}$ along $\bar{x} = 0.9$ for (a) CSSC boundary (b) CSCS boundary

Stress couple $\overline{M}_{xy}$

The plots of $\overline{M}_{xy}$ along $\bar{x} = 0.9$ for CSSC and CSCS boundary conditions (Fig. 5.8a and 5.8b) show an identical nature for all the lamination and the values are found to increase uniformly with an increase in lamination angle, except CSSC shell with $(+75/-75)_5$. In both the cases peak values occur along the simply supported edges.

5.3.3 Comparative performance of shell characteristics around the opening

Four layered antisymmetric angle ply laminate $(+45/-45)_2$ is chosen with graphite epoxy as the material subjected to uniformly distributed load. The shell characteristics at the nodal points of different boundary elements around the openings are studied for CSSC boundary conditions. The arrangement of cutout is designated by three characters. The first letter denotes cutout and the next two digits denote the number of elements encompassing cutout along x and y direction respectively. C22, C42 and C62, designated herein as longitudinal cutout. They are increasing in size with 2, 4 and 6 elements removed along the x-direction and 2 elements removed along the y-direction. Similarly, cutout removing 2, 4 and 6 elements along y direction and 2 elements along x direction is designated as transverse cutout and designated as C22, C24 and C26. Thus C22 is common in longitudinal and transverse cutout. Furthermore, cutouts with same number of elements are termed as equivalent. Shell with no cutout is designated as C00. The effect of different sizes of the cutout on shells in terms of non-dimensional values of static displacements, force and moment resultants of different shell combinations are presented systematically in Tables 5.19 and 5.20. The material and geometric properties of the hypar shells for these problems are considered as: a/b=1, a'/b'=1, a/h=100, c/a=0.2, E_{11}=25E_{22}, G_{12}=G_{13}=0.5E_{22}, G_{23}=0.2E_{22}, ν=0.25, ρ=100 N-sec^2/m^4.

5.3.3.1 Displacement around the cutout

The study is concerned with the changes in the values of the shell displacement around the opening for different types of cutouts. The displacement components w are computed at the nodal points of different boundary elements around the openings and typical results are shown in Table 5.19. Five different types of cutouts are considered along with no cutout case. The dash marks in many locations of Table 5.19 indicate the absence of the shell due to cutouts encompassing those locations.

The values of $\bar{w}$ around the cutouts reveal that, in general the cutouts tend to increase the values of w when increasing the size of the openings. The comparative values at the corresponding points, with reference to those for the C00 indicate that the maximum change occurs at the points on the centre line of the shell towards the simply supported end for C22. But reverse is the case for C42 and C62. The absolute maximum is for the C24 shell. For the C24 and the C26, also, the maximum changes occur at the locations of points on the centre line towards the simply supported edges. It is further observed from Table 5.19 that the shell profile along the length of the cutout drastically reverses with the increase in the size of the cutout in the transverse direction, i.e. from the C24 to C26. From Table 5.19 it can be said that the C22 is definitely better than the C42 and C62 respectively. But C26 is better than C24, considering the displacement component w, which is often a major criterion for design.

Table 5.19: Non dimensional displacement component ($\bar{w}$ x10^4) around the cutouts for CSSC shells

$\bar{x}$	$\bar{y}$	C22	C42	C62	C24	C26	C00
0.2	0.35	-	-	-0.0919	-	-	-0.0710
	0.4	-	-	-0.1071	-	-	-0.0662
	0.45	-	-	-0.1203	-	-	-0.0676
	0.5	-	-	-0.1285	-	-	-0.0701
	0.55	-	-	-0.1269	-	-	-0.0685
	0.6	-	-	-0.1202	-	-	-0.0694
	0.65	-	-	-0.1108	-	-	-0.0792
0.3	0.35	-	-0.1365	-0.1459	-	-	-0.1011
	0.4	-	-0.1523	-	-	-	-0.0976
	0.45	-	-0.1650	-	-	-	-0.0971
	0.5	-	-0.1717	-	-	-	-0.0974
	0.55	-	-0.1674	-	-	-	-0.0961

	0.6	-	-0.1563	-	-	-	-0.0962
	0.65	-	-0.1409	-0.1603	-	-	-0.1003
0.4	0.15	-	-	-	-	-0.1155	-0.0833
	0.25	-	-	-	-0.1945	-0.2401	-0.1119
	0.35	-0.1520	-0.1729	-0.1933	-0.3445	-0.2650	-0.1193
	0.4	-	-	-	-0.4031	-0.2433	-0.1188
	0.45	-	-	-	-0.4937	-0.2679	-0.1177
	0.5	-0.1829	-	-	-0.5490	-0.2905	-0.1162
	0.55	-	-	-	-0.4921	-0.2656	-0.1145
	0.6	-	-	-	-0.4020	-0.2387	-0.1122
	0.65	-0.1445	-0.1714	-0.1957	-0.3507	-0.2603	-0.1088
	0.7	-	-	-	-0.2955	-0.2751	-0.1029
	0.75	-	-	-	-0.2069	-0.2336	-0.0934
	0.8	-	-	-	-	-0.1678	-0.0795
	0.85	-	-	-	-	-0.1052	-0.0599

5.3.3.2 Stress resultants and stress couples around the cutout

Table 5.20 presents the values of the stress resultants, $\overline{N}_x, \overline{N}_y$ and $\overline{N}_{xy}$ and stress couples, $\overline{M}_x, \overline{M}_y$ and $\overline{M}_{xy}$ at some selective points of the longitudinal faces of the longitudinal cutout for CSSC boundary conditions. It is observed that shell characteristics changes drastically with changes in sizes of cutout even sometimes shell characteristics reverses with increase in sizes of the cutout. This fluctuation is maximum when C00 shell is converted to C22 and C22 is converted to C42. But when C42 is converted to C62 the changes are not so significant except a few cases. Another interesting observation is that the values of all the shell characteristics are lower for the C62 than C22 and C42; thereby indicating the superiority of C62 type of cutout.

Table 5.20: Shell characteristics along longitudinal faces of longitudinal cut-outs (C00, C22, C42 and C62) for CSSC boundary condition

$\bar{y}$	$\bar{x}$	Cut -out	$\overline{N}_x$	$\overline{N}_y$	$\overline{N}_{xy}$	$\overline{M}_x$	$\overline{M}_y$	$\overline{M}_{xy}$
0.35		C-00	-0.0469	-0.0063	-0.6331	-0.0798	-0.0811	+0.0014
	0.4	C-22	+0.1228	+0.1694	-0.7274	-0.0927	-0.0932	+0.0532
		C-42	-0.0531	-0.1347	-0.5191	-0.0354	-0.0286	+0.0026
		C-62	-0.0480	-0.0248	-0.6026	-0.0396	-0.0295	+0.0033
		C-00	-0.0102	+0.0235	-0.6408	-0.0848	-0.0862	+0.0055
	0.5	C-22	-0.0137	+0.0056	-0.3894	-0.0264	-0.0216	+0.0033
		C-42	-0.0217	-0.0034	-0.5904	-0.0465	-0.0373	0.0000
		C-62	-0.0193	-0.0011	-0.6629	-0.0443	-0.0337	0.0010
		C-00	+0.0165	+0.0424	-0.6334	-0.0823	-0.0834	+0.0076
	0.6	C-22	-0.1502	-0.1332	-0.7074	-0.0943	-0.0945	-0.0459
		C-42	+0.0204	+0.1479	-0.5098	-0.0399	-0.0325	0.0000
		C-62	+0.0021	+0.0241	-0.6087	-0.0426	-0.0319	-0.0031

5.4 CONCLUSIONS

Following conclusions can be drawn from the present study,

1) The close agreement between the results obtained by the present approach and those appearing in the published literature establishes the correctness of the formulation.
2) An increase in support restraints always reduces the deflection and static stress resultants near the boundary.
3) Among shells with two boundaries clamped and other two simply supported, the ones with adjacent boundaries clamped show lesser deflection for all the antisymmetric laminations considered here.
4) Among shells with two free boundaries, one with two adjacent boundaries free shows greater static deflection for all the antisymmetric laminations considered here.
5) Free boundaries bring in higher flexibility in shells and in this respect whether the other boundaries are simply supported or clamped matters to a great extent. Also when a free boundary is introduced to a stiffened shell with cutout, maximum deflection and stress resultants always occur near the free boundary.
6) The superiority of a particular combination in terms of a shell action cannot predict the performance of the shell for other shell actions.
7) For antisymmetric angle ply laminated composite shells lamination angle is a governing criterion to determine the shell characteristics. Also arrangements of boundary constraints have a large impact on deflection and static stress resultants.
8) Though the superiority of the shells with less number of cutouts is clearly established, in some situations it is seen that even cut outs with more openings perform better than shell with fewer openings in terms of all the shell actions.

Chapter 6

FREE VIBRATION BEHAVIOR

6.1 GENERAL

The mathematical formulation for free vibration analysis of laminated composite stiffened hypar shell with cutout is presented in Chapter 4. In Chapter 5, section 5.2, some benchmark problems are identified. In this chapter also some benchmark problems have been identified and presented in section 6.2 which are relevant to the scope of present study. Those problems are solved and the results are compared with the previous ones to check the correctness of the present formulation.

In section 6.3 some additional examples of laminated composite stiffened hypar shells with cut-out are considered with different parametric variations. The results are analyzed critically from different angles of variations and discussed accurately to show their engineering applications. Results having maximum practical implications are analyzed for the sake of brevity. The outcome of this study is presented systematically as conclusions in section 6.4.

6.2 BENCHMARK PROBLEMS

From Table 6.1, the agreement of present results with the earlier ones is excellent and the correctness of the stiffener formulation is established. Free vibration of simply supported and clamped hypar shell with $(0/90)_4$ shell with cut-outs is also considered in section 5.2. The fundamental frequencies of hypar shell with cut-out obtained by the present method agree well with those reported by Chakravorty et al. (1998) as evident from Table 5.2, establishing the correctness of the cut-out formulation. Thus it is evident that the finite element model proposed here can successfully analyze vibration problems of stiffened skewed hypar composite shells with cut-out which is reflected by close agreement of present results with benchmark ones.

Table 6.1: Natural frequencies (Hz) of centrally stiffened clamped square plate

Mode no.	Mukherjee and Mukhopadhyay (1988)	Nayak and Bandyopadhyay (2002a)		Present method
		N8(FEM)	N9(FEM)	
1	711.8	725.2	725.1	733

a=b=0.2032 m, thickness =0.0013716 m, stiffener depth=0.0127 m, stiffener width =0.00635 m, stiffener eccentric at bottom, Material property: E=6.87x10^{10} N/m^2, ν=0.29, ρ=2823 kg/m^3

6.3 HIGHER MODE VIBRATION OF SHELLS

6.3.1 Effect of varying boundary conditions and ply orientation

Laminated composite stiffened hypar shells with cut-out is analysed to study the behavior of the shell under free vibration at higher mode for different parametric variations. The cut-outs are placed concentrically on the shell surface. The stiffeners are placed along the cut-out periphery and extended up-to the edge of the shell. The material and geometric properties of the shells are: a/b=1, a/h=100, a'/b' =1, a'/a =0.2, c/a=0.2, E_{11}/E_{22}=25, G_{23} = 0.2E_{22}, G_{13}= G_{12}= 0.5E_{22}, ν_{12} = ν_{21} =0.25,ρ=100 N-sec^2/m^4 unless otherwise specified. Different type of symmetric and antisymmetric cross and angle ply laminates with different lamination angle is considered.

The different boundary conditions which are used in the present analysis are CCCC, CCSS, SSCC, CSCS, SCSC, SSSS, CCFF, FFCC and CFCF. Numerical analyses are also performed to determine the effect of curvature on non-dimensional frequency by varying c/a = 0.2, 0.15, 0.1 and 0.05.

Table 6.2 presents the non-dimensional frequencies for shells with different laminations and boundary conditions. To facilitate the interpretation of results the boundary conditions are divided into three groups. Group I consists of commonly encountered edge conditions which are clamped and simply supported. Each of the boundary conditions included in either of Group II and Group III has equal number of support constraints. On examining the results, it is evident that the frequencies for all the laminations for all the modes depend on the number of boundary constraints. With increase in number of boundary constraints frequencies increase. Further it is noticed that for

two layered laminates for Group I boundary conditions, angle ply shells show better performance than cross ply laminates but reverse is the case for Group III shells. For Group II shells cross ply shells show better performance on lower mode and angle ply shell shows better performance on higher mode. It is also evident from Table 6.2 that with increase in number of layers angle ply shells perform better than their cross ply counterpart, except some few cases. This is true for Group I and Group II shells but for group III shells except a very few cases cross ply shells are better choices. These are true for both fundamental and higher mode.

Among Group II boundary condition although CCSS and SSCC perform better than CSCS and SCSC shells in lower mode but reverse is the case on higher mode. A more careful observation suggests that among Group III shells when numbers of layers are less CCFF and FFCC perform better but with increase in number of layers, performance of CFCF shells are improved. Hence lamination order may influence the frequency of stiffened composite shell with cutout more significantly than its boundary conditions.

The mode shapes corresponding to the first five modes of vibration are plotted in Fig.6.1 for cross ply and angle ply shells respectively. The normalized displacements are drawn with the shell mid-surface as the reference for all the support condition and for all the lamination used here. The fundamental mode is clearly a bending mode for all the boundary condition for cross ply and angle ply shell. At higher modes of vibration mode shape do not change to a great extent. Most of the mode shapes are in bending mode. It is found that for higher mode, nature of the mode shapes is somewhat similar, only the crest and trough position changes.

Table 6.3 contains the non-dimensional frequency values for different symmetric laminates by varying the lamination angle and boundary conditions. It is observed from the results, with the increase in number of layer frequencies increase marginally from three layered to four layered shells. But with further increase in number of layers does not come to any effective benefit except CSCS and CFCF shells. This is expected as increasing the number of layers will result in reduced bending-stretching coupling and will increase the shell stiffness, till on increasing the number of layers the material becomes quasi-isotropic. Beyond that, increase in the number of layers will not improve the frequency to any extent. Rather, $(0/\theta)_s$ lamination exhibit reasonably good performance and may be adopted for all practical purposes. It is also observed that except for CCCC shells, where $\theta=45^0$ yields the highest values of frequency but for all other boundary conditions frequency increases with θ. For CCSS and CSCS shells $\theta=60^0$ either gives the highest

frequency or yields a frequency value which is marginally less than the highest one. Similarly, for SSSS shells $\theta=75^0$ and for CCFF and CFCF shells $\theta=90^0$ gives the highest results. Fig. 6.2 represents the mode shape corresponding to symmetric cross ply and angle ply laminated composite stiffened shells with cutout for fundamental and higher mode.

The frequencies of four layered symmetric and antisymmetric laminates are furnished in Table 6.4 for various lamination angles and boundary conditions. Since four layered laminates are very common in industrial applications, Table 6.4 is expected to be a good design aid for practicing engineers. Examining the frequencies of shells with four layered symmetric and antisymmetric stacking orders presented in Table 6.4, it is found that for CCFF, CFCF and CCSS shells with $0/\theta/0/\theta$ stacking order the vibrational stiffness increase monotonically with θ. But for CCCC, CSCS, SSSS and $0/\theta/\theta/0$ CCSS shells, the frequency increases with θ upto a certain value but decreases when θ is further increased. Such decreases are quite marginal in all of these cases. All these observations are true for the first five modes shown here except very few cases. Out of twelve cases considered here in four cases (for CCFF, CFCF and CCSS shells with $0/\theta/0/\theta$) highest frequencies are found to be at $\theta=90^0$. In another eight cases highest frequencies are found to be at $\theta=60^0$.

When performances of antisymmetric and symmetric laminates are compared, it is found that considering all the modes performance of antisymmetric laminate is better than its symmetric counterpart. The only exception is symmetrically laminated CCCC shell with lamination angle 15^0. For this shell symmetric laminate perform better than the antisymmetric laminate in all five modes shown here. Fig. 6.3 represents the typical mode shapes corresponding to symmetric and anti-symmetric cross ply and angle ply laminated composite stiffened shells with cutout for fundamental and higher mode.

The frequencies of $0/\theta/\theta/0$ laminates are presented in Table 6.5 for various lamination angles with different c/a ratio for CCSS boundary condition. It is observed in general that frequency of each mode first increases with lamination angle then decrease for all c/a ratios. From Table 6.5 it is also observed that for CCSS boundary condition for a given lamination angle increase in c/a ratio increases the frequency of each mode. Fig. 6.4 represents the typical mode shapes corresponding to fundamental and higher mode for symmetric angle ply laminated composite stiffened shells with cutout for different *c/a* ratio.

Table 6.2: Non-dimensional frequencies $\overline{\omega}$ for different laminations of laminated composite stiffened hypar shell with cut-out for different boundary conditions on higher mode

θ	Mode	Group I		Group II				Group III		
		CCCC	SSSS	CCSS	SSCC	CSCS	SCSC	CCFF	FFCC	CFCF
0/90	1	98.018	26.637	85.438	85.770	49.438	48.964	44.250	44.564	34.587
	2	108.446	26.929	91.838	92.100	76.142	76.592	52.083	52.484	61.940
	3	109.370	39.897	93.835	94.029	97.696	98.754	75.362	75.594	71.091
	4	119.423	42.461	103.232	103.272	102.429	102.454	77.192	76.842	76.053
	5	125.111	57.209	111.447	111.621	105.696	107.404	79.180	79.819	90.241
45/-45	1	120.698	37.986	83.906	84.201	49.165	49.362	27.561	27.473	26.910
	2	124.864	38.107	86.901	88.370	79.967	80.096	31.568	31.527	50.815
	3	125.550	60.215	93.530	94.343	113.990	114.144	54.854	54.747	54.034
	4	142.375	74.380	100.425	102.105	119.097	117.965	58.839	58.823	62.302
	5	180.017	96.224	117.059	118.783	119.229	118.890	66.271	66.178	82.723
0/90/0	1	100.702	40.793	87.276	87.509	47.510	81.413	43.943	45.331	22.040
	2	109.903	56.046	94.274	94.392	66.005	93.511	56.146	56.117	44.861
	3	117.771	57.826	101.721	102.883	90.226	105.734	73.599	73.147	75.056
	4	127.017	76.016	105.475	105.962	95.401	109.393	79.927	81.230	75.230
	5	127.127	88.721	112.081	113.024	108.090	117.934	85.013	85.250	76.614
45/-45/45	1	142.317	53.814	99.785	102.450	72.082	71.489	34.008	33.900	37.830
	2	149.189	55.274	108.133	107.543	113.228	111.680	37.943	37.919	59.124
	3	155.431	83.546	109.827	110.466	138.565	135.739	59.926	59.844	62.084

	4	159.182	106.898	128.808	131.657	143.016	142.474	67.858	67.857	80.642
	5	200.078	129.254	149.427	150.869	144.652	144.137	74.376	74.268	91.550
0/90/0/90	1	101.746	48.701	94.487	95.001	65.309	61.773	49.317	49.639	51.795
	2	117.561	48.995	97.755	98.056	87.723	87.472	59.477	59.877	71.901
	3	118.346	80.970	101.568	101.743	110.525	111.199	81.850	82.181	78.391
	4	134.043	89.063	121.367	121.489	115.587	112.578	85.988	86.129	88.043
	5	151.843	103.765	126.195	126.267	120.032	115.479	87.161	87.134	100.779
45/-45/45/-45	1	143.534	54.131	96.560	98.725	71.356	71.585	31.861	31.761	37.875
	2	157.273	54.182	113.940	114.594	113.115	113.233	36.583	36.527	62.076
	3	158.121	86.637	116.915	116.274	145.381	144.034	62.488	62.371	65.217
	4	165.640	106.252	127.234	128.724	146.878	145.797	68.768	68.728	83.822
	5	216.514	135.294	155.055	155.960	150.707	150.013	77.731	77.595	100.095
0/90/0/90/0	1	102.336	45.490	94.328	94.860	57.234	78.297	48.607	49.332	38.823
	2	114.740	55.612	97.220	97.479	82.655	92.895	59.331	59.712	65.989
	3	125.389	74.322	105.417	105.646	109.061	111.457	81.196	80.333	78.763
	4	138.143	91.929	116.855	117.669	113.620	118.442	83.160	84.523	83.759
	5	138.925	105.747	124.153	124.296	114.241	123.069	91.756	91.689	93.516

Table 6.3: Non-dimensional $\bar{\omega}$ frequencies for symmetric laminated composite stiffened hypar shell with cut-out with different boundary condition

Boundary Condition	θ	(0/θ/0)	$(0/\theta)_S$	$(0/\theta/0)_S$	$[(0/\theta)_2]_S$	$[(0/\theta)_5]_S$
CCCC	0°	92.874	93.093	93.526	93.093	93.094
	15°	110.434	114.779	112.219	115.791	116.266
	30°	120.993	122.546	123.193	123.201	123.311
	45°	121.153	122.941	124.570	124.686	125.341
	60°	117.064	118.771	121.600	121.632	122.930
	75°	111.024	113.132	117.109	116.898	118.736
	90°	100.702	102.030	102.571	102.587	102.679
CCSS	0°	81.037	81.437	82.220	81.437	81.437
	15°	84.473	85.188	86.148	85.424	85.467
	30°	87.443	88.284	89.642	88.863	88.939
	45°	88.839	89.657	91.149	90.260	90.260
	60°	89.033	89.950	91.663	90.757	90.787
	75°	87.885	89.911	92.831	91.997	92.392
	90°	87.276	90.964	95.544	95.333	96.022
CSCS	0°	39.747	39.935	40.302	39.939	39.933
	15°	43.082	43.983	44.378	44.507	44.770
	30°	47.388	49.570	50.896	51.678	52.703
	45°	50.529	54.464	57.362	59.018	61.275
	60°	52.420	58.216	62.162	64.869	68.207
	75°	50.642	57.051	62.272	65.107	69.207
	90°	47.510	53.208	60.222	62.180	66.728
SSSS	0°	32.418	32.543	32.837	32.547	32.542
	15°	34.688	35.396	35.853	35.964	36.243
	30°	37.607	39.215	40.577	41.047	41.929
	45°	39.729	42.274	44.529	45.304	46.724
	60°	41.439	44.707	47.165	48.213	49.682
	75°	41.779	45.213	47.682	48.892	50.322
	90°	40.793	43.804	46.898	47.958	50.116

CCFF	0°	29.312	29.409	29.596	29.413	29.415
	15°	29.948	30.167	30.551	30.419	30.530
	30°	31.211	31.548	32.023	31.936	32.067
	45°	33.377	33.876	34.284	34.270	34.313
	60°	37.124	37.918	38.165	38.315	38.234
	75°	42.187	43.812	44.531	45.191	45.166
	90°	43.943	45.859	49.123	49.343	50.178
CFCF	0°	16.299	16.419	16.797	16.426	16.422
	15°	16.320	16.558	17.036	16.765	16.812
	30°	16.670	17.841	19.477	19.572	20.447
	45°	17.877	21.341	25.710	26.560	29.037
	60°	19.715	26.198	33.831	35.551	39.845
	75°	21.358	30.343	40.613	43.025	48.863
	90°	22.040	31.967	43.256	45.952	52.412

Table 6.4: Non-dimensional frequencies $\bar{\omega}$ for composite stiffened hypar shell with cut-out with 0/θ/0/θ and 0/θ/θ/0 lamination scheme and different boundary conditions on higher mode

θ	Mode	BOUNDARY CONDITION											
		CCCC		CCSS		CSCS		SSSS		CCFF		CFCF	
		0/θ/0/θ	0/θ/θ/0	0/θ/0/θ	0/θ/θ/0	0/θ/0/θ	0/θ/θ/0	0/θ/0/θ	0/θ/θ/0	0/θ/0/θ	0/θ/θ/0	0/θ/0/θ	0/θ/θ/0
0°	1	93.093	93.093	81.437	81.437	39.935	39.935	32.543	32.543	29.409	29.409	16.419	16.419
	2	106.371	106.371	84.595	84.595	55.034	55.034	48.270	48.270	44.947	44.947	33.066	33.066
	3	109.995	109.995	88.777	88.777	73.047	73.047	56.092	56.092	57.358	57.358	48.250	48.250
	4	110.260	110.260	95.973	95.973	87.515	87.515	62.595	62.595	65.815	65.815	48.520	48.520
	5	116.956	116.956	103.540	103.540	95.965	95.965	84.479	84.479	70.574	70.574	56.071	56.071
15°	1	111.960	114.779	81.785	85.188	45.478	43.983	36.699	35.396	30.995	30.167	16.844	16.558
	2	115.687	116.295	90.856	90.133	61.772	59.971	54.530	52.559	47.231	46.336	34.766	33.921
	3	128.878	130.301	98.844	99.544	81.674	78.304	56.864	57.909	62.764	60.978	50.135	50.021
	4	130.427	133.877	112.802	112.599	100.026	101.648	71.059	67.853	69.912	69.097	52.497	51.119
	5	140.496	142.419	120.095	119.977	102.962	106.987	92.798	94.828	72.897	73.089	57.662	56.664
30°	1	118.349	122.546	84.994	88.284	53.234	49.570	42.253	39.215	32.250	31.548	20.373	17.841
	2	132.432	129.103	104.341	97.437	75.344	67.956	58.233	58.848	50.919	47.307	41.158	36.867
	3	146.421	140.195	110.837	108.153	101.662	88.629	64.897	59.485	66.516	64.557	55.465	53.783
	4	148.276	152.635	127.119	125.869	118.461	116.438	87.613	76.774	73.115	72.637	56.016	55.531
	5	160.833	161.266	136.646	135.310	122.698	122.225	105.810	103.934	78.731	77.092	69.109	61.080
45°	1	121.010	122.941	86.838	89.657	61.578	54.464	46.469	42.274	34.025	33.876	28.739	21.341
	2	136.675	130.152	113.312	102.168	92.408	76.412	57.809	59.411	54.637	49.174	52.006	43.288
	3	156.322	140.900	121.090	111.560	125.669	100.876	75.658	64.370	68.258	67.738	60.782	60.975

	4	156.944	159.237	123.486	127.559	128.633	125.125	102.074	85.970	76.027	76.098	67.482	61.683
	5	166.305	171.106	147.745	141.559	133.669	132.857	108.272	106.353	83.907	82.828	85.023	72.540
60°	1	119.538	118.771	87.736	89.950	68.120	58.216	48.447	44.707	37.302	37.918	39.328	26.198
	2	136.911	126.372	109.540	102.446	106.292	83.176	56.160	58.318	57.007	51.014	63.872	52.105
	3	151.622	141.852	120.116	113.423	123.653	111.838	84.490	68.661	70.234	71.436	68.950	71.193
	4	163.179	158.797	127.936	121.051	138.385	123.093	93.730	93.617	79.787	78.587	84.106	71.841
	5	165.697	161.590	144.223	143.545	149.906	137.592	119.474	102.556	86.733	88.843	91.687	85.248
75°	1	116.354	113.132	89.720	89.911	68.504	57.051	48.332	45.213	43.808	43.812	48.283	30.343
	2	124.902	119.546	101.523	99.165	106.126	83.470	53.117	56.868	58.053	53.884	74.826	59.516
	3	138.661	140.262	115.751	110.513	117.868	115.616	84.436	69.285	75.700	76.759	79.476	82.918
	4	148.999	143.832	121.725	117.273	131.935	118.242	89.881	95.616	84.933	79.158	96.764	82.980
	5	155.419	145.424	129.441	127.497	132.464	126.783	108.352	97.490	87.615	91.991	97.422	89.354
90°	1	101.746	102.030	94.487	90.964	65.309	53.208	48.701	43.804	49.317	45.859	51.795	31.967
	2	117.561	111.696	97.755	96.054	87.723	77.722	48.995	56.080	59.477	60.454	71.901	60.044
	3	118.346	127.711	101.568	107.634	110.525	102.523	80.970	68.019	81.850	77.566	78.391	80.826
	4	134.043	128.893	121.367	108.858	115.587	111.379	89.063	90.758	85.988	81.456	88.043	82.361
	5	151.843	138.257	126.195	123.965	120.032	114.690	103.765	98.610	87.161	92.388	100.779	89.747

Table 6.5: Non-dimensional frequencies $\bar{\omega}$ for 0/θ/θ/0 stiffened hypar shell with cut-out with different c/a ratio for CCSS boundary condition on higher mode

θ	Mode	c/a			
		0.2	0.15	0.1	0.05
0°	1	81.437	68.926	50.845	33.025
	2	84.595	70.089	52.940	36.752
	3	88.777	77.733	62.553	50.804
	4	95.973	80.442	74.440	66.119
	5	103.540	87.336	75.331	71.641
15°	1	85.188	76.139	60.664	38.424
	2	90.133	80.995	61.326	41.498
	3	99.544	82.078	73.217	55.059
	4	112.599	94.783	77.307	69.290
	5	119.977	102.417	82.645	72.224
30°	1	88.284	80.280	67.962	47.013
	2	97.437	87.112	71.727	48.636
	3	108.153	91.259	79.937	61.777
	4	125.869	112.832	90.117	73.096
	5	135.310	116.351	93.836	76.124
45°	1	89.657	80.509	68.059	47.720
	2	102.168	89.685	75.140	52.607
	3	111.560	97.278	83.203	65.001
	4	127.559	112.103	92.107	74.601
	5	141.559	125.170	101.364	83.599
60°	1	89.950	78.548	63.700	43.078
	2	102.446	88.382	71.985	49.824
	3	113.423	97.166	80.544	68.703
	4	121.051	108.805	95.209	75.920
	5	143.545	122.901	100.398	83.882
75°	1	89.911	75.713	58.137	37.119

	2	99.165	81.321	62.024	45.068
	3	110.513	94.973	81.766	71.083
	4	117.273	102.476	85.903	74.848
	5	127.497	110.154	93.761	80.592
90°	1	90.964	74.507	54.050	34.489
	2	96.054	75.982	58.420	44.005
	3	107.634	92.748	79.692	70.108
	4	108.858	95.015	83.706	75.919
	5	123.965	105.420	89.772	79.067

θ	Mode	Group I		Group II				Group III		
		CCCC	SSSS	CCSS	SSCC	CSCS	SCSC	CCFF	FFCC	CFCF
0/90	1			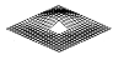	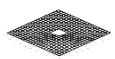		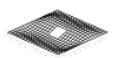			
	2	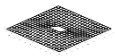						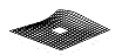		
	3	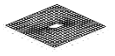								
	4									
	5									
45/-45	1									
	2									
	3									
	4									
	5									

Fig.6.1 Mode shapes for cross ply and angle ply shells for different boundary conditions for first five modes.

Boundary Condition	θ	Mode	$(0/\theta/0)$	$(0/\theta)_S$	$(0/\theta/0)_S$	$[(0/\theta)_2]_S$	$[(0/\theta)_5]_S$
CCCC	45°	1	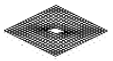	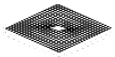		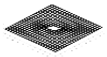	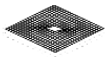
		2		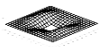			
		3		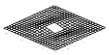			
		4	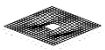		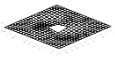	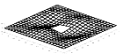	
		5					
CCSS		1	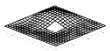	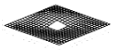	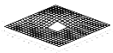	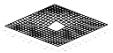	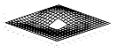
		2		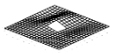	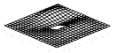		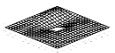
		3	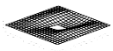				
		4					
		5					
CCCC	90°	1					
		2					
		3					
		4					
		5					
CCSS		1					
		2					
		3					

		4	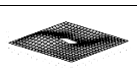	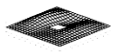		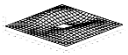	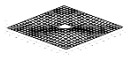
		5		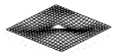	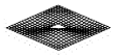	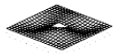	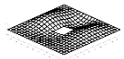

Fig. 6.2 Mode shapes of symmetric cross ply and angle ply shells with cut-out for first five modes.

θ	Mode	CCCC		CCFF		CCSS		CFCF		CSCS		SSSS	
		0/θ/0/θ	0/θ/θ/0	0/θ/0/θ	0/θ/θ/0	0/θ/0/θ	0/θ/θ/0	0/θ/0/θ	0/θ/θ/0	0/θ/0/θ	0/θ/θ/0	0/θ/0/θ	0/θ/θ/0
45º	1	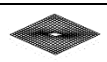		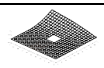	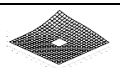	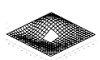			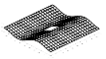	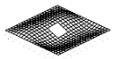	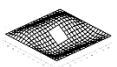	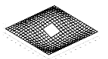	
	2		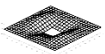	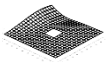	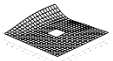	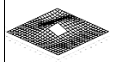	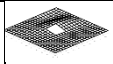					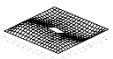	
	3		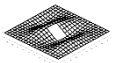	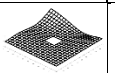	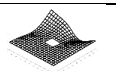				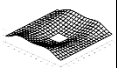		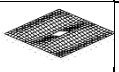		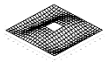
	4	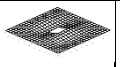		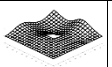									
	5												
90º	1												
	2												
	3												
	4												
	5												

Fig. 6.3 Mode shapes corresponding to anti symmetric and symmetric laminated composite stiffened hypar shell with cut-out for different boundary conditions for first five modes

Mode	*c/a*			
	0.2	0.15	0.1	0.05
1	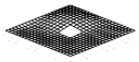	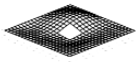	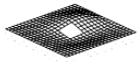	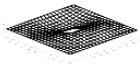
2	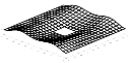		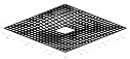	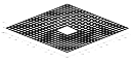
3	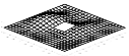	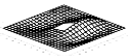	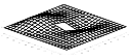	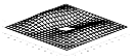
4	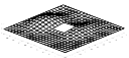			
5	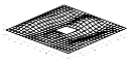	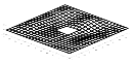	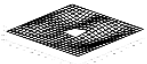	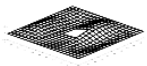

Fig. 6.4 Mode shapes corresponding to 0/45/45/0 laminated composite stiffened hypar shell with cut-out for CCSS boundary condition for different *c/a* ratio for first five modes.

6.3.2 Effect of other parametric variations

Anti-symmetric angle-ply laminated composite stiffened hypar shells with cutout are analyzed to study the behavior of the shell under free vibration at higher mode for different parametric variation. The cutouts are placed concentrically on the shell surface. The stiffeners are placed along the cutout periphery and extended upto the edge of the shell. The material and geometric properties of the shells are: a/b=1, a/h=100, a'/b' =1, a'/a =0.2, c/a=0.2, E_{11}/E_{22} =25, G_{23} = 0.2E_{22}, G_{13} = G_{12} = 0.5E_{22}, ν_{12} = ν_{21} =0.25, ρ =100 N-sec^2/m^4 unless otherwise specified.

Seven laminate stacking sequences, viz. anti-symmetric angle-ply $(0/-0)_{10}$, $(15/-15)_{10}$, $(30/-30)_{10}$, $(45/-45)_{10}$, $(60/-60)_{10}$, $(75/-75)_{10}$ and $(90/-90)_{10}$ are considered. Numerical analyses are performed to determine the effect of fibre orientation angle (θ= 0^0, 15^0, 30^0, 45^0, 60^0, 75^0 and 90^0), degree of orthotropy (E_{11}/E_{22} = 5, 10, 20, 25, 30, 40 and 50) and width to thickness ratio (b/h=10,

20, 50, 100) on non-dimensional natural frequency. The different boundary conditions which are used in the present analysis are CSCS, CSSC, FCCF, FCFC, FSFS and FSSF.

Table 6.6 gives the non-dimensional fundamental frequency (first mode frequencies) for 2 layer, 4 layer and 10 layered anti-symmetric angle-ply laminated composite stiffened hypar shells with cutout with the fibre orientation angle varying between 0^0 and 90^0. In each column, the maximum value is indicated by an asterisk. It is seen that for 2 layer hypar shell, maximum fundamental frequency occurs for lamination angle either 0^0 or 90^0 except CSSC shell. For CSSC shell, maximum fundamental frequency occurs for lamination angle 45^0. It is also observed that for all the boundary conditions considered here, 4 layer and 10 layer laminates exhibit maximum value of frequency parameter for same lamination angle. For CSCS and CSSC shells, maximum fundamental frequency occurs at lamination angle θ=75^0 and 45^0 respectively, for FCFC shells at θ =0^0 and for FCCF, FSFS and FSSF shells at θ =30^0. This observation is valid for both 4 layer and 10 layer hypar shells. According to the number of boundary constraints, boundary conditions can be grouped as: CSCS & CSSC; FCCF & FCFC; FSFS & FSSF. For all the layers considered here, as the number of boundary constraint increases fundamental frequency increases. Thus CSCS & CSSC perform better than FCCF & FCFC which in turn perform better than FSFS & FSSF shells. It is also seen from Table 6.6 that with the increase in layer, frequency parameter increases. The increments are sharper from two layer to 4 layer compared to 4 layer to 10 layer, in which a mild increase in the frequency parameter is observed. As 10 layer laminates exhibit best performance so far the fundamental frequency is concerned, 10 layer laminates are considered for further studies.

6.3.2.1 *Effect of fibre orientation*

The total thickness of the laminate was maintained constant and the number of layers being 10. Fig. 6.5 shows the variation of non-dimensional frequency with boundary conditions and lamination angle. Seven laminate stacking sequences, viz. anti-symmetric angle-ply $(0/-0)_{10}$, $(15/-15)_{10}$, $(30/-30)_{10}$, $(45/-45)_{10}$, $(60/-60)_{10}$ $(75/-75)_{10}$ and $(90/-90)_{10}$ are considered. The non-dimensional frequency parameter for the first, second, third, fourth and fifth mode increases with an increase in fibre orientation angle from 0^0 to 45^0 for CSSC, FCCF and FSFS shells but for further increase in lamination angle, fundamental frequency decreases. Similarly, for CSCS shell,

Table 6.6: Non-dimensional fundamental frequency of anti-symmetric angle-ply multilayered laminated composite stiffened hypar shell with cutout

Angle-ply	Boundary Condition	2 Layer	4 Layer	10 Layer
0°	CSCS	6.356	6.356	6.356
15°		6.056	7.467	7.892
30°		6.787	9.399	10.121
45°		7.825	11.356	12.324
60°		8.914	12.622	13.631
75°		10.196	12.919	13.642*
90°		13.254*	13.254*	13.254
0°	CSSC	13.017	13.016	13.016
15°		12.449	13.979	14.307
30°		12.607	14.954	15.547
45°		13.356*	15.369*	15.799*
60°		12.526	14.928	15.549
75°		12.402	13.998	14.362
90°		13.008	13.008	13.008
0°	FCCF	6.539	6.539	6.539
15°		6.011	6.855	7.082
30°		6.263	7.327*	7.555*
45°		6.233	7.161	7.377
60°		6.196	7.212	7.436
75°		6.000	6.806	7.024
90°		6.548*	6.548	6.548
0°	FCFC	11.707*	11.706*	11.708*
15°		8.031	10.746	11.394
30°		5.875	8.628	9.246
45°		4.283	6.033	6.435
60°		3.147	3.795	3.958
75°		2.674	2.741	2.759
90°		2.604	2.604	2.604
0°	FSFS	4.367*	4.367	4.367
15°		4.041	4.732	4.882
30°		3.974	4.984*	5.204*
45°		2.941	4.038	4.293
60°		2.194	2.583	2.679
75°		1.860	1.905	1.918
90°		1.806	1.806	1.806
0°	FSSF	3.628*	3.628	3.628
15°		3.310	3.945	4.127
30°		3.349	4.190*	4.403*
45°		3.290	4.166	4.380
60°		3.304	4.104	4.307
75°		3.268	3.860	4.027
90°		3.560	3.560	3.560

fundamental frequency increases upto 60^0 then decreases. Again for FCFC shell, fundamental frequency decreases with increase in lamination angle. On the other hand, for FSSF shell, the change in frequency with change in lamination angle is very insignificant. For all the laminations and boundary conditions shown here, frequency parameter increases from first mode to fifth mode except few cases, where frequency parameter is almost same in two consecutive modes. The lamination and boundary conditions interact in a complex manner so that no unified conclusion can be reached. The reason behind is that the frequencies depend upon the contribution made by extensional stiffness, coupling stiffness and bending stiffness term in addition to the boundary conditions and panel geometry among others. However, for all the lamination angles considered here, CSCS, CSSC perform better than FCCF, FCFC which in turn perform better than FSFS, FSSF. So it can be concluded that number of boundary constraints plays a great role for free vibration. CSSC perform better than CSCS for lower lamination angles but for higher lamination angle CSCS perform better than CSSC. But reverse trend is observed when free edges are involved. FCFC and FSFS perform better in lower lamination angle but FCCF and FSSF perform better in higher lamination angle.

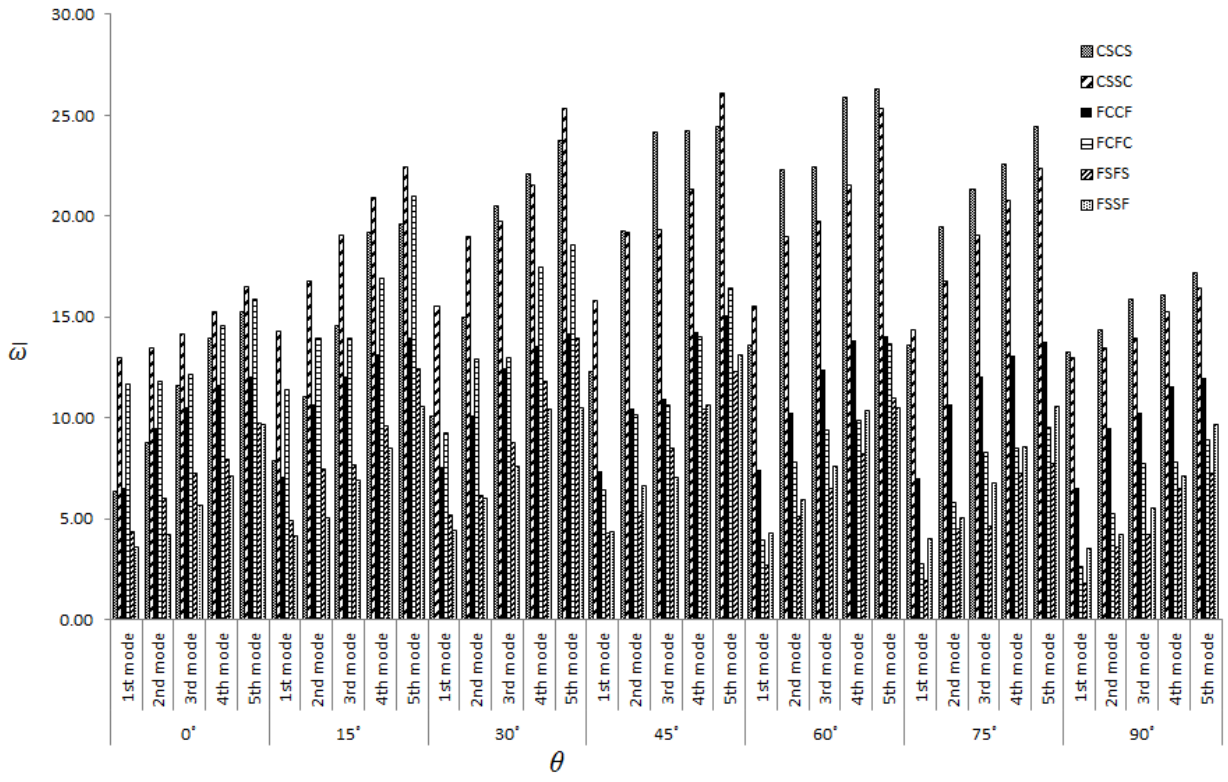

Fig.6.5 Variation of non-dimensional fundamental frequency with fibre orientation angle

6.3.2.2 *Effect of material anisotropy*

The effects of material anisotropy on the frequencies of ten-layer anti-symmetric angle-ply square shells with fibre orientation angles 0^0, 15^0, 30^0, 45^0, 60^0, 75^0 and 90^0 for CSCS, CSSC, FCCF, FCFC, FSFS and FSSF edge boundary conditions are demonstrated in Figs. 6.6-6.12. These results are obtained by keeping the material properties constant as G_{12}/E_{22} =0.5 and ν_{12} =0.25, and changing the E_{11}/E_{22} ratio. As seen from these figures, the first, second, third, fourth and fifth frequency parameter increases monotonically for all the laminations and boundary conditions considered here as the degree of orthotropy increases. These increments are sharper for CSSC shell. FCFC shell shows better performance for lower lamination angle but with the increase in lamination angle performance of CSCS shell is better. For other boundary conditions mild increase in the frequency parameter is observed. It is also observed that for almost all the cases frequency parameter increases from first mode to fifth mode. In a few cases frequency remains almost same between two consecutive modes.

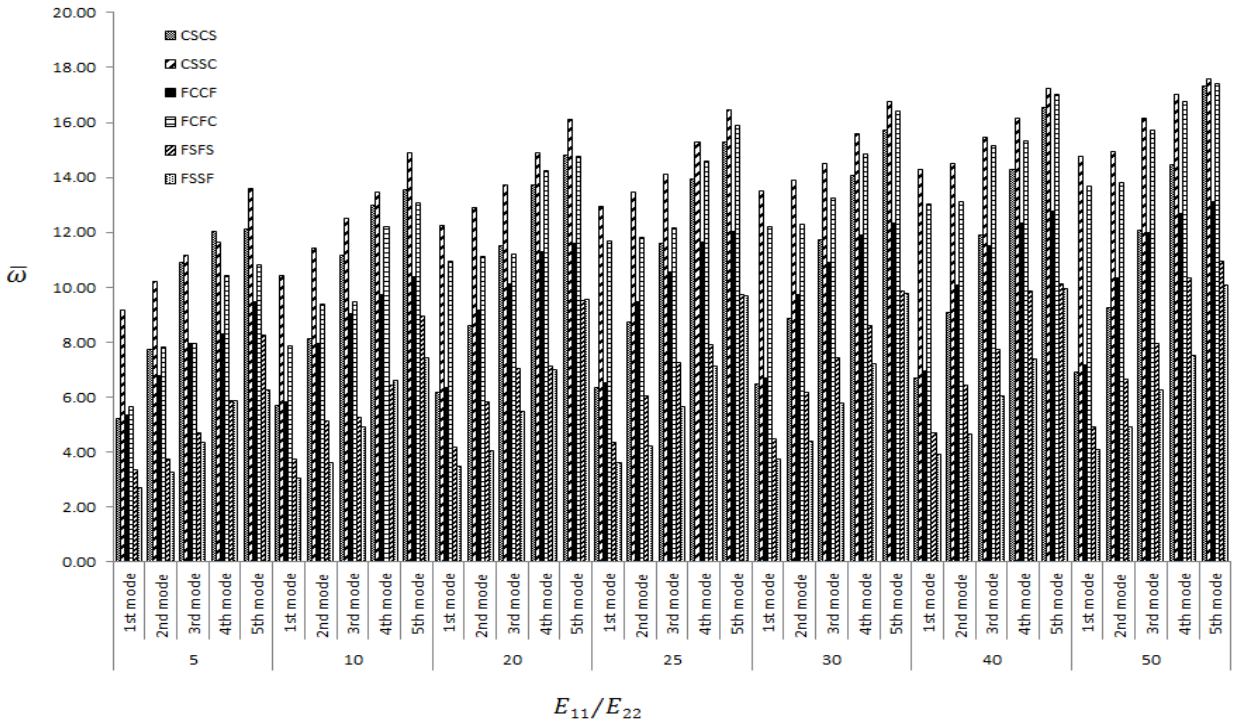

Fig.6.6 Variation of non-dimensional fundamental frequency with material anisotropy for $(0/-0)_{10}$ lamination

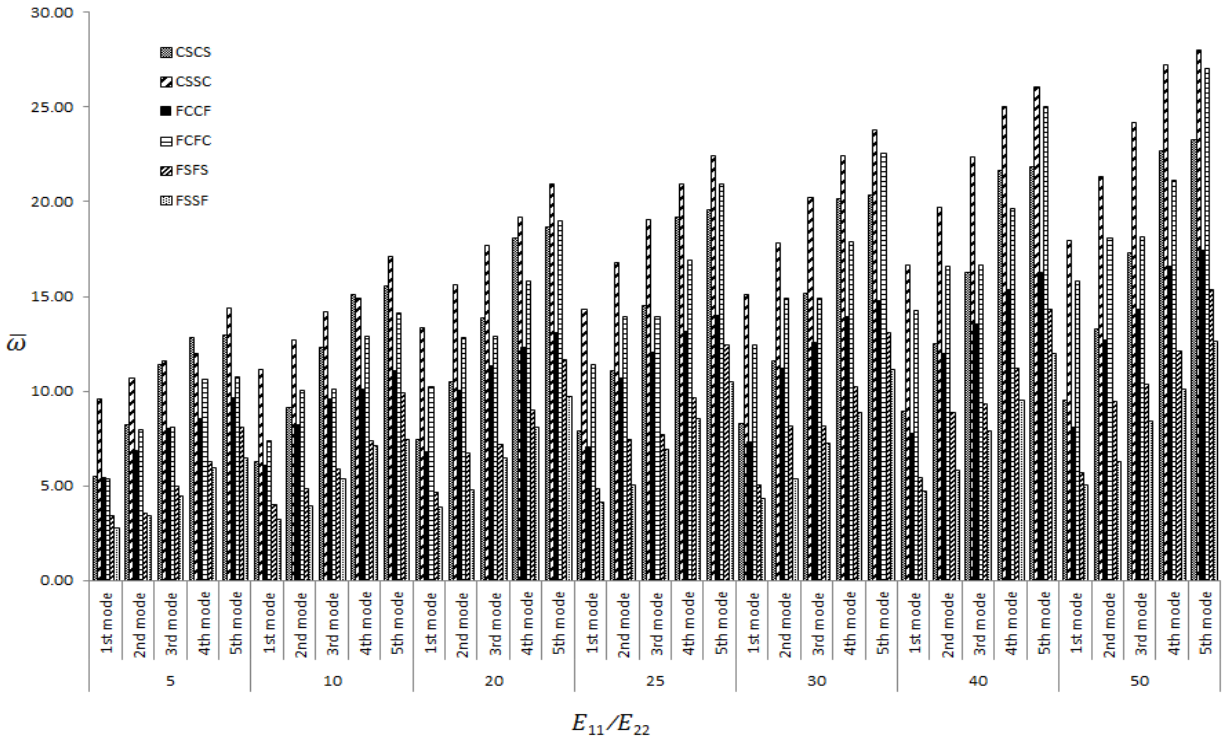

Fig.6.7 Variation of non-dimensional fundamental frequency with material anisotropy for $(15/-15)_{10}$ lamination

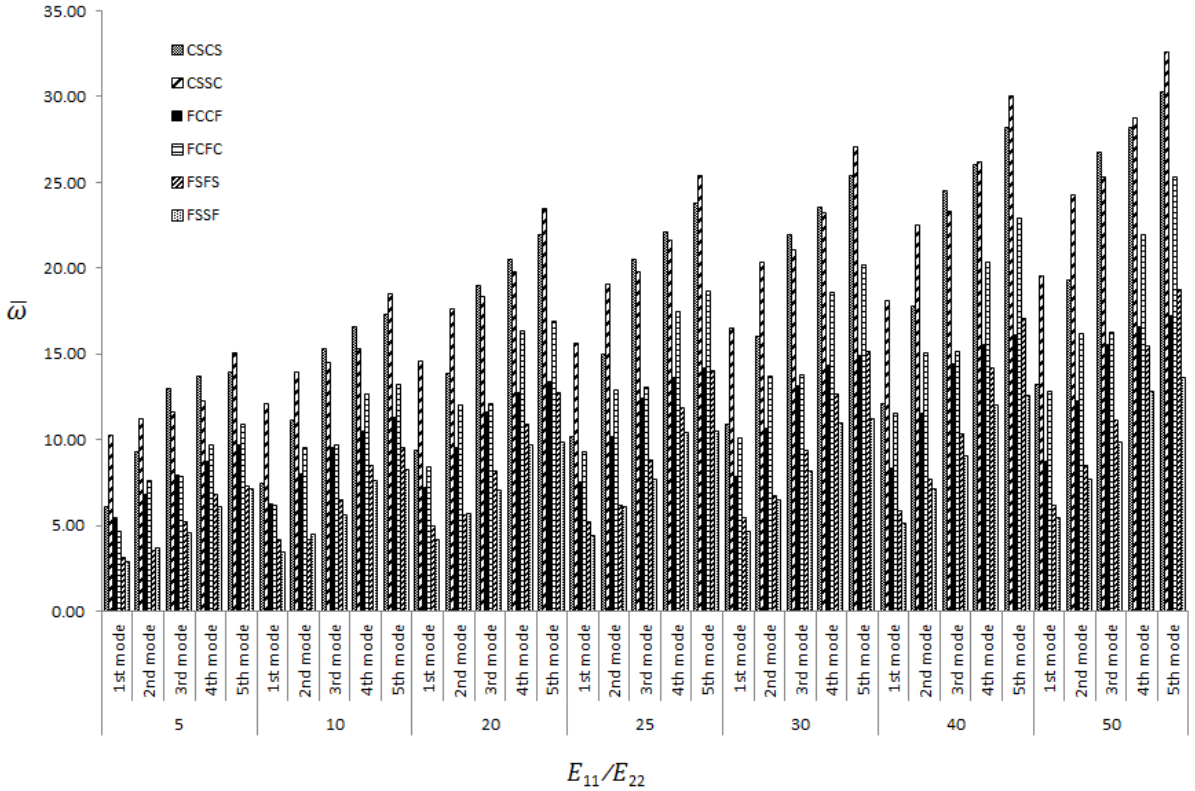

Fig.6.8 Variation of non-dimensional fundamental frequency with material anisotropy for $(30/-30)_{10}$ lamination

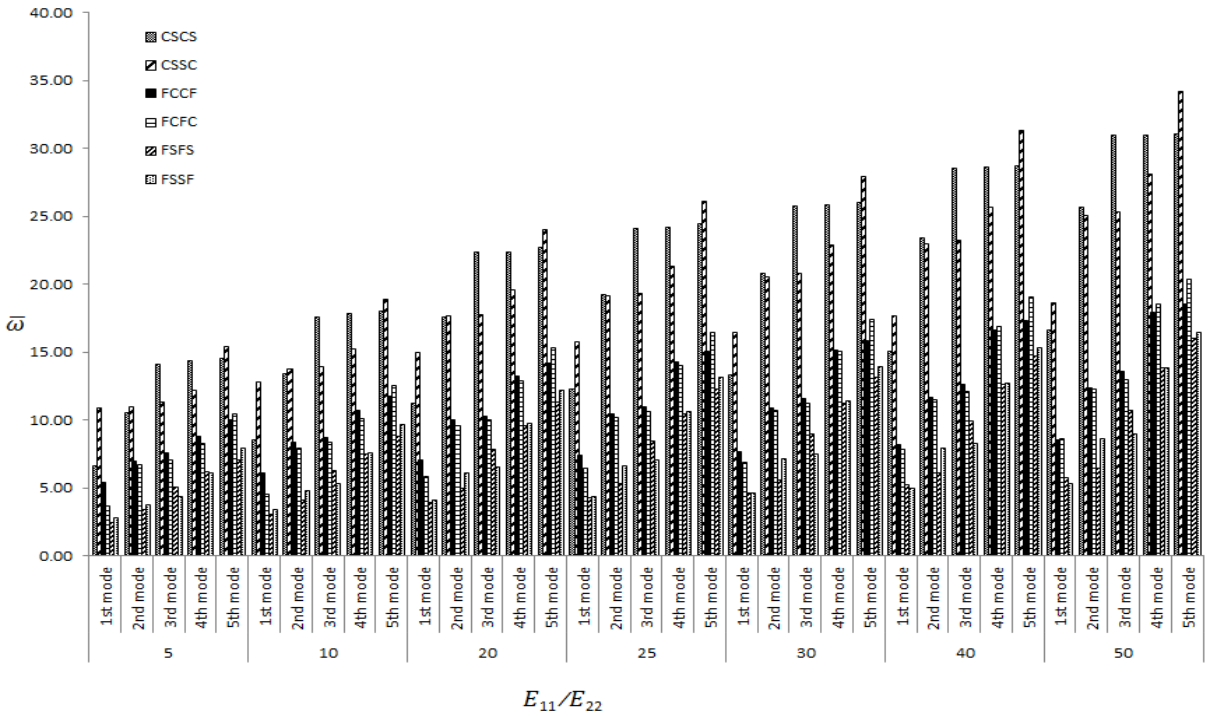

Fig.6.9 Variation of non-dimensional fundamental frequency with material anisotropy for $(45/-45)_{10}$ lamination

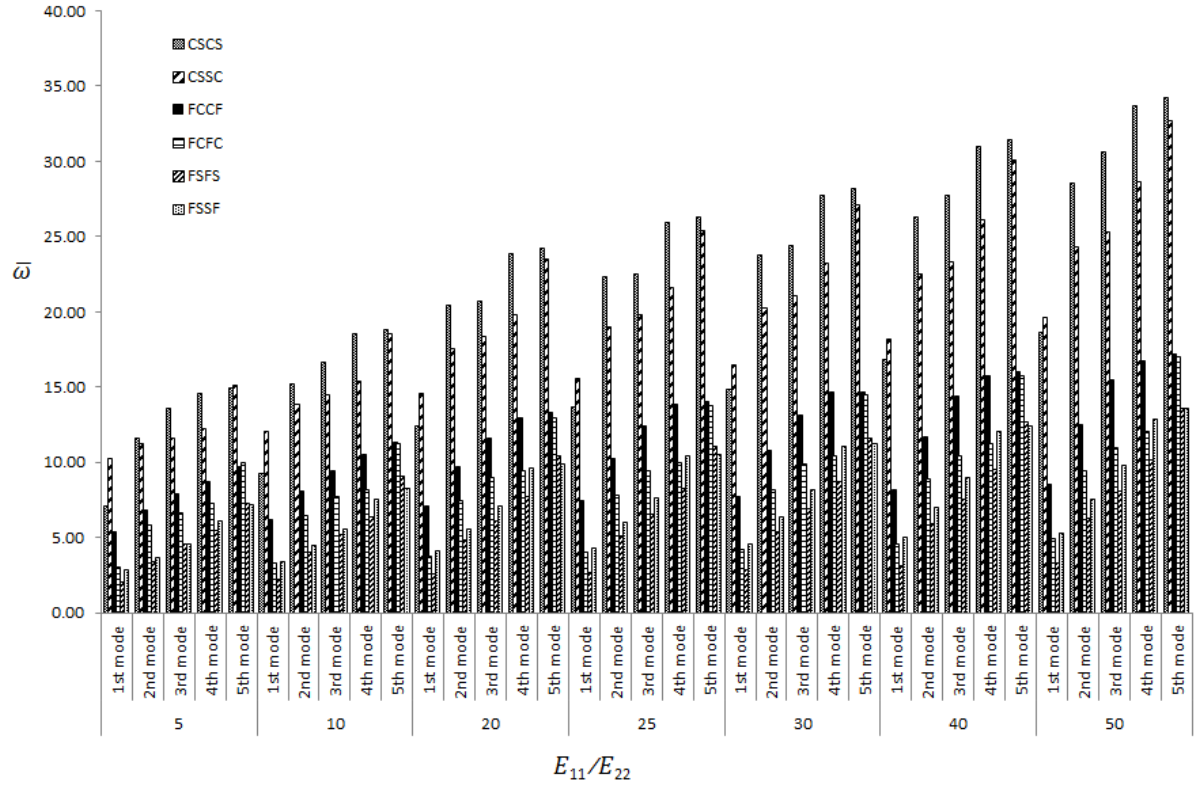

Fig.6.10 Variation of non-dimensional fundamental frequency with material anisotropy for $(60/-60)_{10}$ lamination

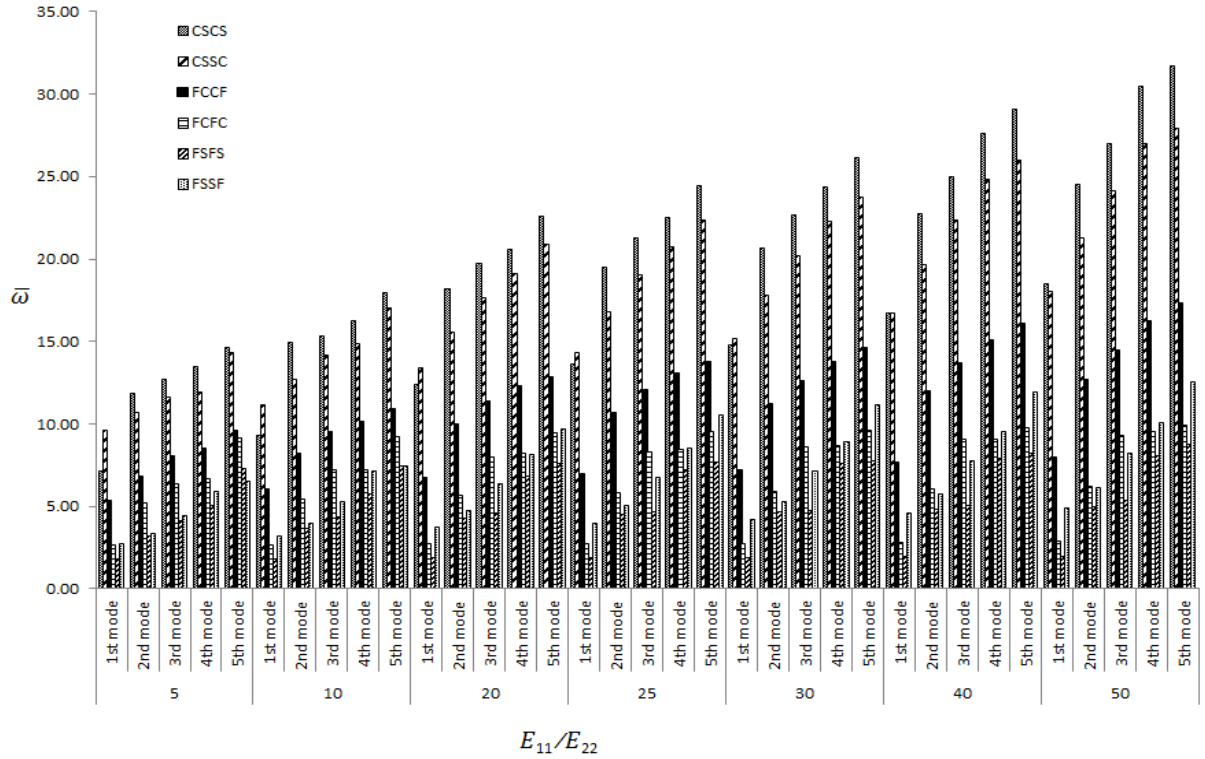

Fig.6.11 Variation of non-dimensional fundamental frequency with material anisotropy for $(75/-75)_{10}$ lamination

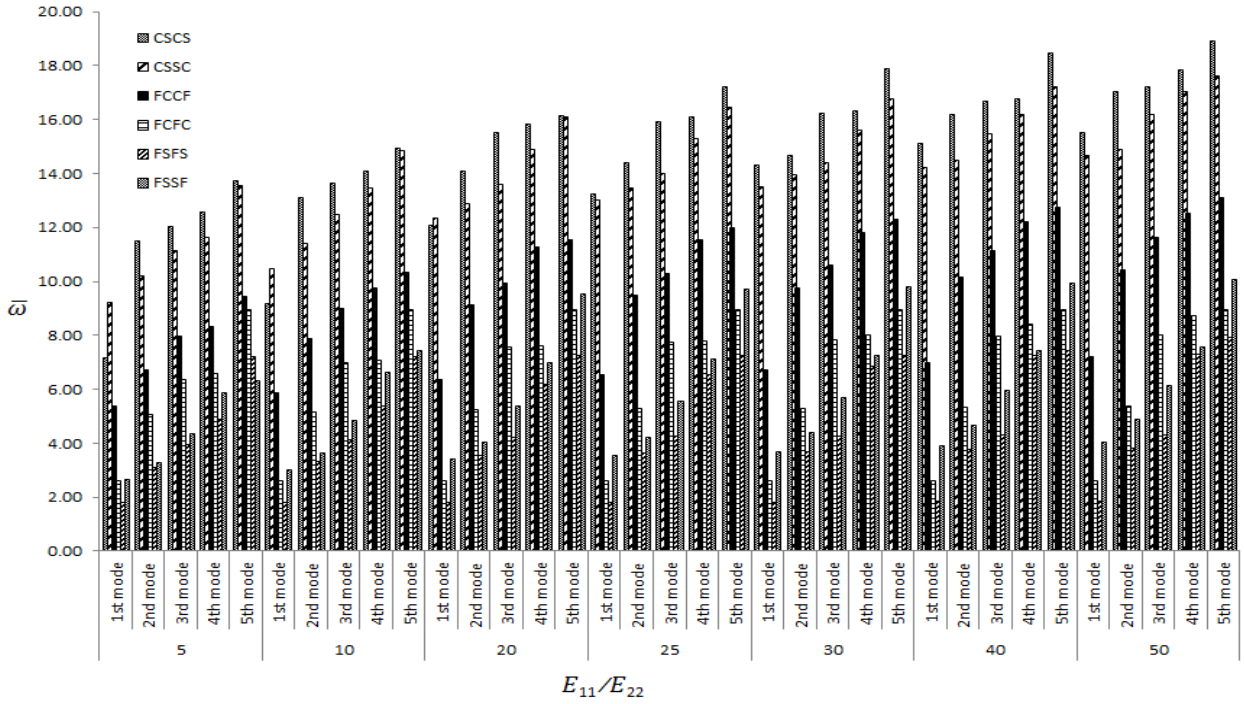

Fig.6.12 Variation of non-dimensional fundamental frequency with material anisotropy for $(90/-90)_{10}$ lamination

6.3.2.3 *Effect of width to thickness ratio*

If the width to thickness ratio is increased while maintaining the width of the laminate a constant and the number of layers being fixed at 10, the thickness of the shell is decreased. Figs. 6.13-6.19 show the variation of the non-dimensional frequency for the first, second, third, fourth and fifth mode with variation of width to thickness ratio and boundary conditions for various values of lamination angles. Ten layered anti-symmetric angle-ply laminates with fibre orientation angle varying as 0°, 15°, 30°, 45°, 60°, 75^0 and 90° having different width to thickness ratios (b/h=10, 20, 50, 100) are analyzed. It is evident from Figs. 6.13-6.19 that with increase in width to thickness ratio dimensionless frequencies decrease. This decrease in frequency is very much significant in case of CSSC, CSCS and FCFC shells. For other boundary conditions these decrease in dimensionless frequency is significant at higher value of width to thickness ratio. These are true for all the five modes. Here also for all the combination of stacking sequences, boundary conditions and width to thickness ratios, the non-dimensional frequency increases from first mode to fifth mode except few cases.

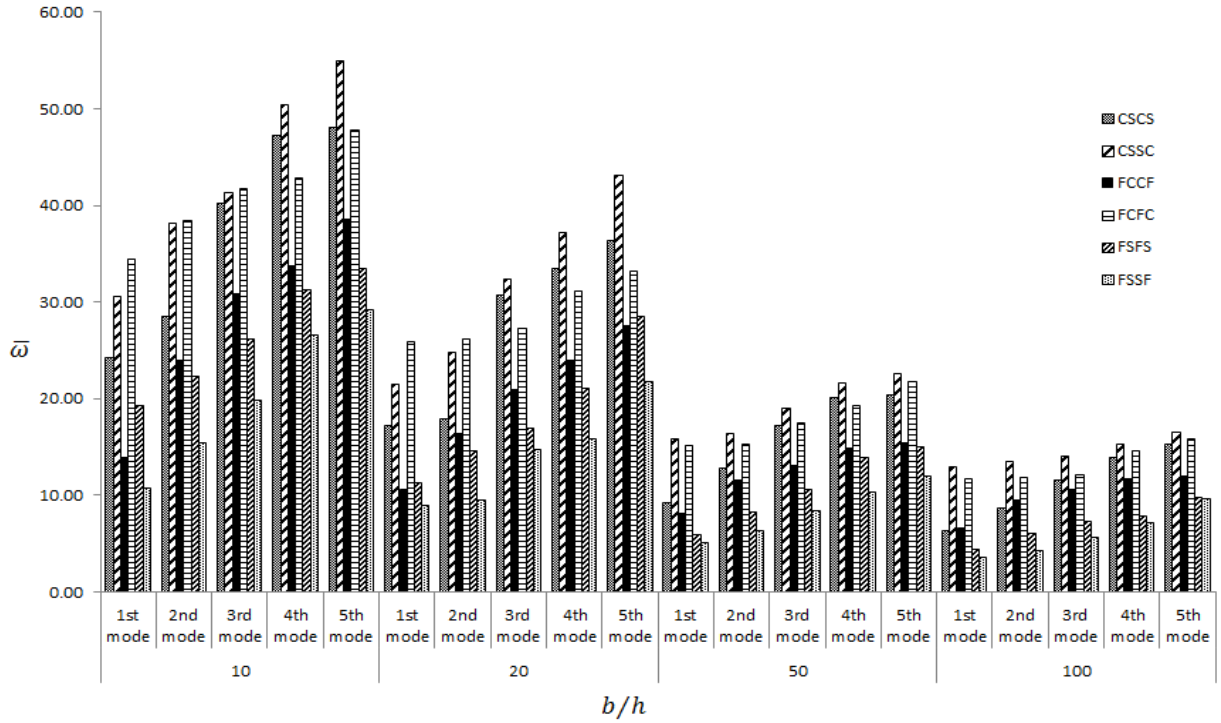

Fig.6.13 Variation of non-dimensional fundamental frequency with b/h ratio for $(0/-0)_{10}$ lamination

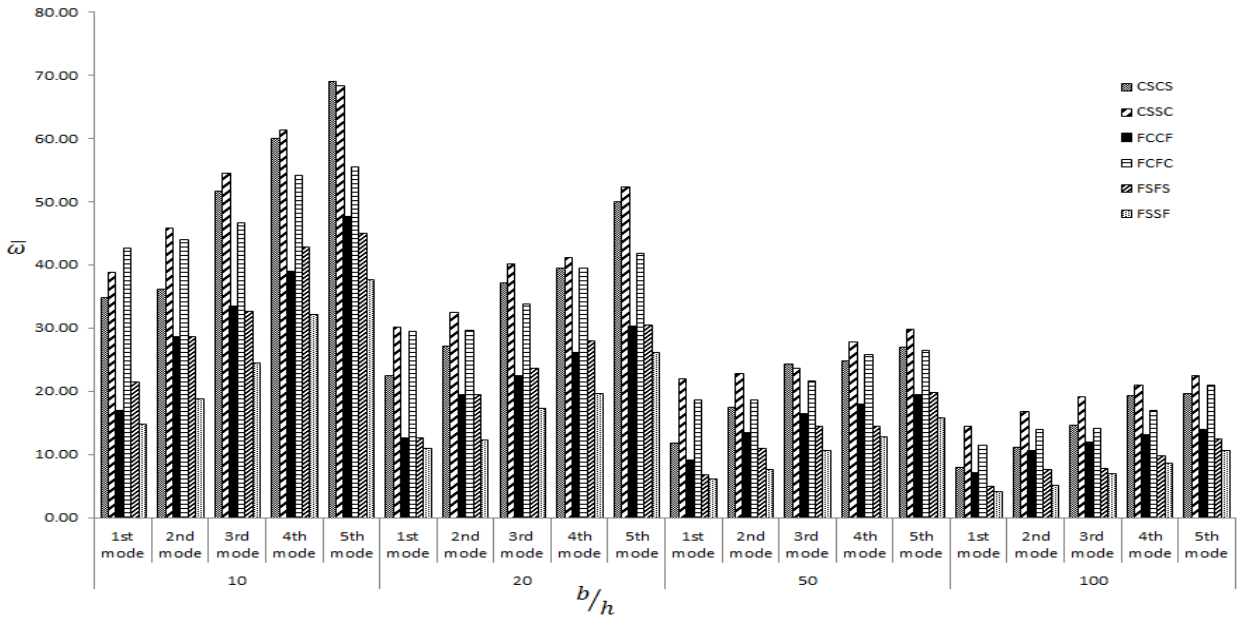

Fig.6.14 Variation of non-dimensional fundamental frequency with *b/h* ratio for $(15/-15)_{10}$ lamination

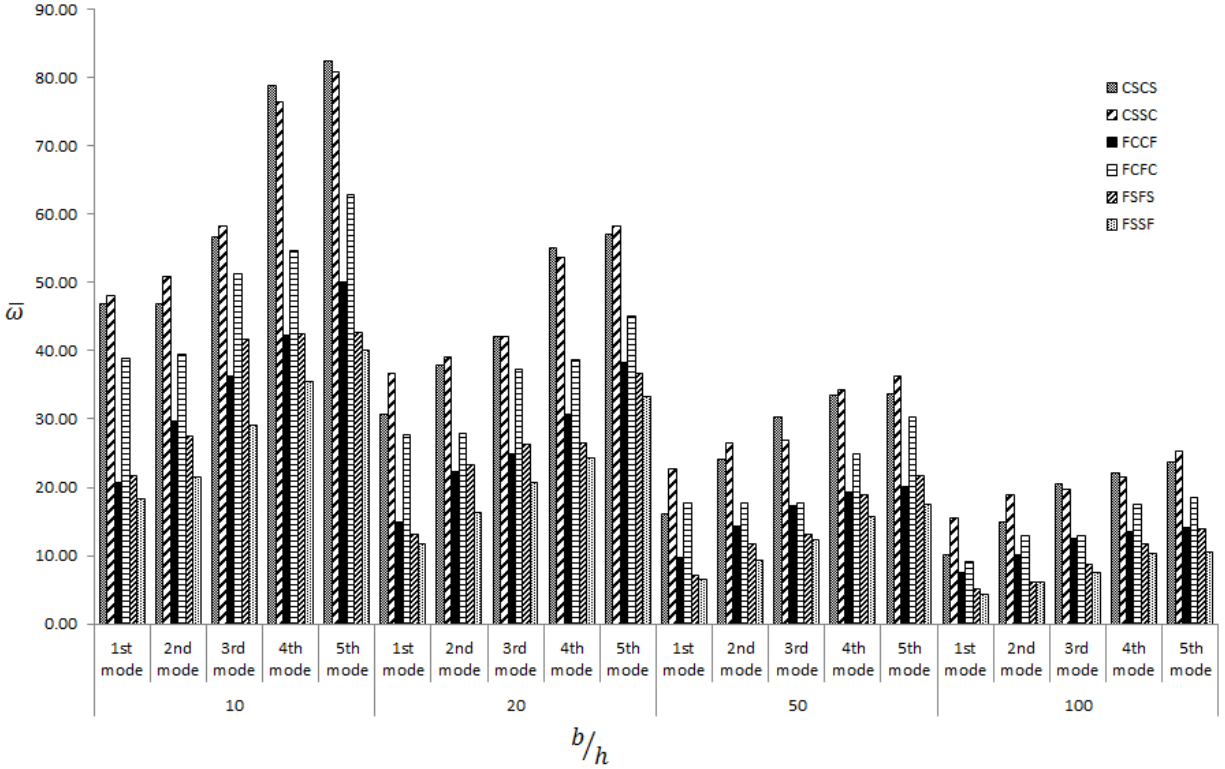

Fig.6.15 Variation of non-dimensional fundamental frequency with *b/h* ratio for $(30/-30)_{10}$ lamination

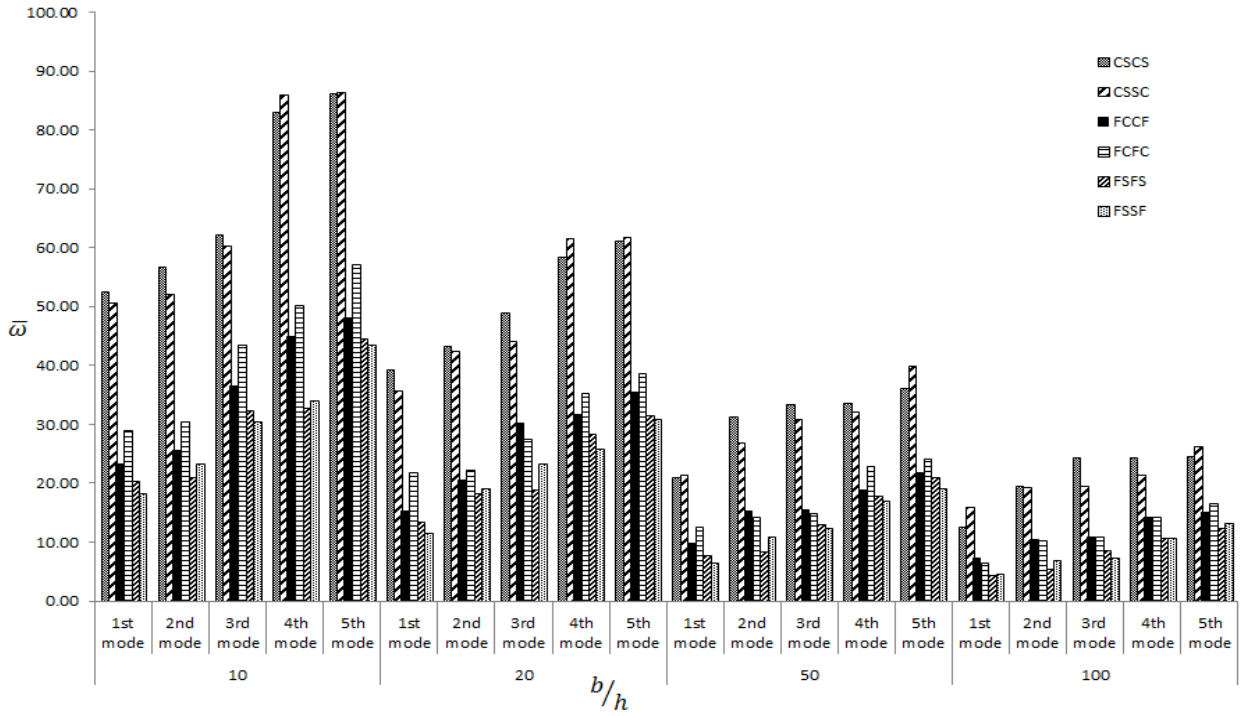

Fig.6.16 Variation of non-dimensional fundamental frequency with *b/h* ratio for $(45/-45)_{10}$ lamination

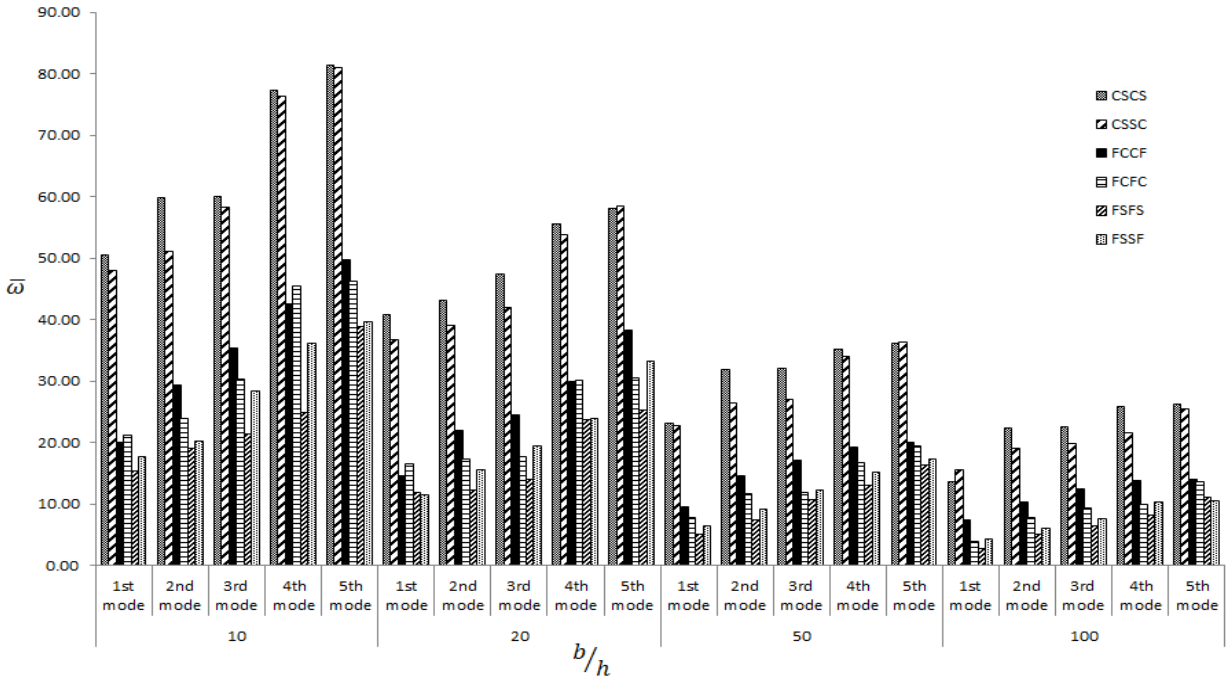

Fig.6.17 Variation of non-dimensional fundamental frequency with *b/h* ratio for $(60/-60)_{10}$ lamination

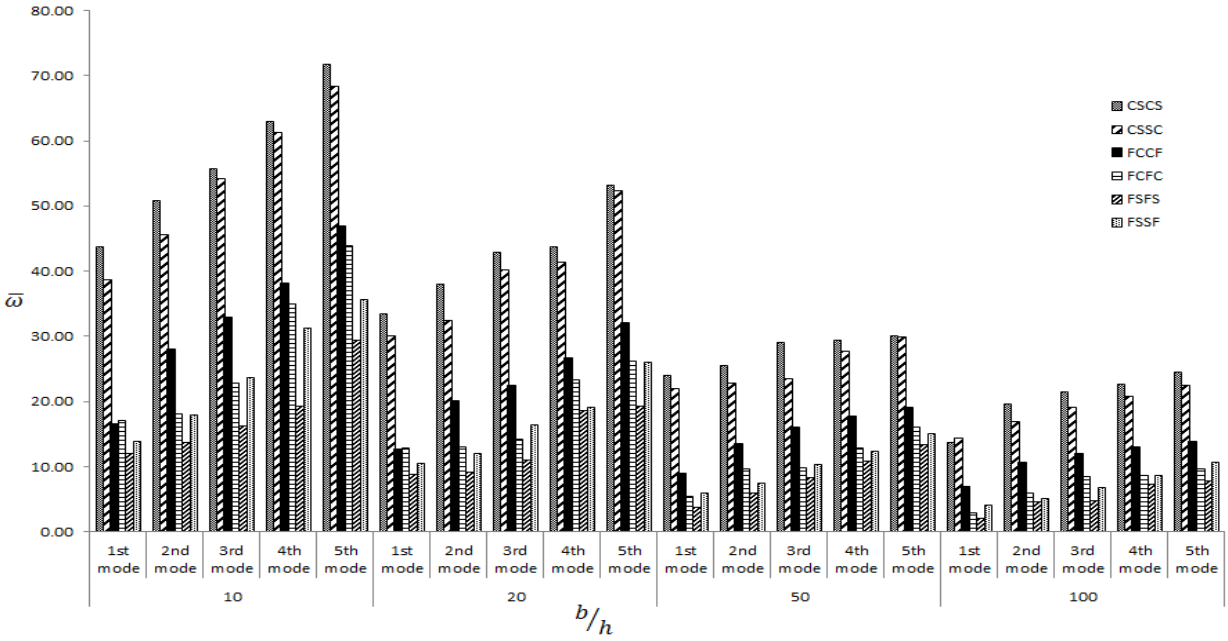

Fig.6.18 Variation of non-dimensional fundamental frequency with *b/h* ratio for $(75/-75)_{10}$ lamination

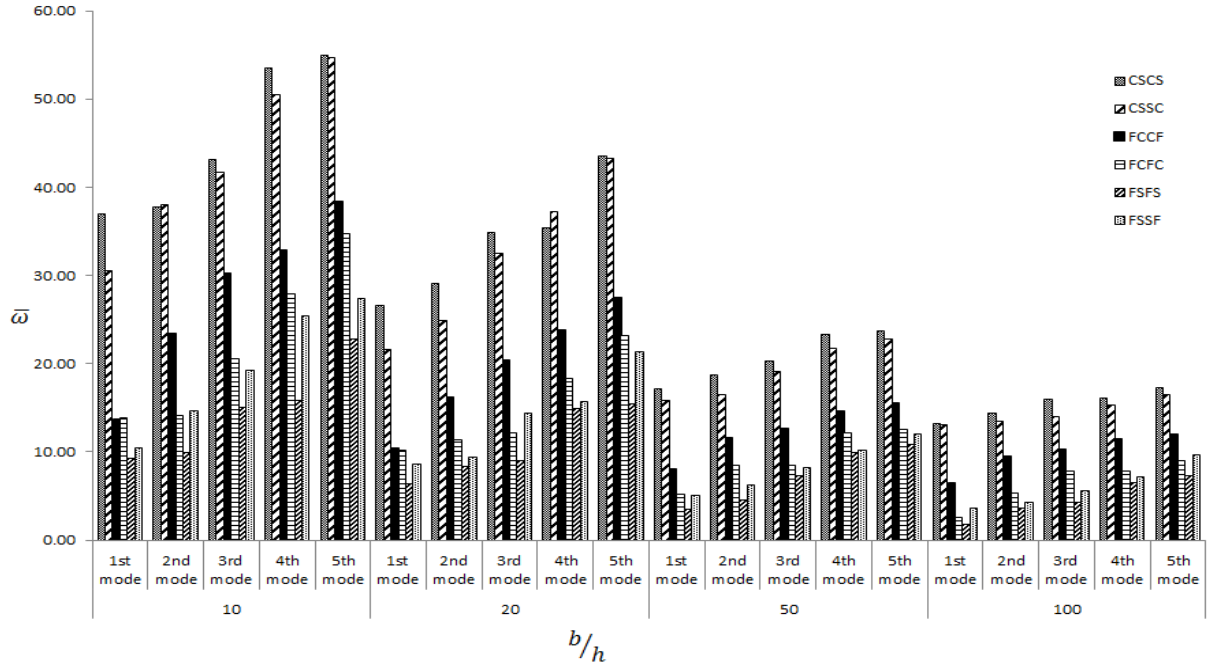

Fig.6.19 Variation of non-dimensional fundamental frequency with *b/h* ratio for $(90/-90)_{10}$ lamination

6.4 CONCLUSIONS

Higher mode free vibration analysis of composite hypar shells is presented using finite element method based on first order shear deformation theory and including the effect of cross curvature. The following conclusions are drawn from the present study:

1. In general, fundamental frequency increases with the increase in the number of support constraints. There are, however, few departures from this general tendency when two shells of different laminations are compared. Sometimes lamination order may influence the frequency of stiffened composite shell with cut-out more significantly than its boundary conditions.
2. (0/θ)s lamination exhibit reasonably good performance and may be adopted for all practical purposes.
3. For four layered laminates the frequency either increases monotonically with θ or increases with θ upto a certain value of θ then decreases. For CCCC, CSCS, SSSS and 0/ θ/ θ/0 CCSS shells, the frequency increases with θ upto a certain value but decreases when θ is further increased. For each of these shells the values of θ yielding highest frequencies are to be found out by numerical experimentation. All these observations are true for the first five modes except very few cases.
4. Considering all the modes performance of four layered antisymmetric laminate is better than its symmetric counterpart, except CCCC shell with lamination angle 15^0.
5. For shell with CCSS boundary condition for a given lamination angle increase in c/a ratio increases the frequency of each mode.
6. As the number of layers increase, fundamental frequency increases. With the increase in lamination angle non-dimensional natural frequency may increase or decrease but from first mode to fifth mode natural frequency always increase or remain same in very few cases.
7. The first, second, third, fourth and fifth non-dimensional frequency parameter increases monotonically for all the laminations and boundary conditions as the degree of orthotropy increases.
8. With increase in width to thickness ratios, dimensionless frequencies decrease from first mode to fifth mode.

9. Free vibration behavior mainly depends on the number of boundary constraints whatever may be the other parametric variation like change in fibre orientation angle, increase in degree of orthotropy and width to thickness ratio etc.

Chapter 7

OPTIMIZATION OF VIBRATION BEHAVIOR

7.1 GENERAL

In previous chapters, the static and free vibration behavior of laminated stiffened hypar shell with cutout at different boundary conditions has been discussed. In this chapter, a method of analysis has been presented to optimize the value of fundamental frequency at different parametric variations such as effect of lamination angle (A), width to thickness ratio (B), cutout location along x-direction and cutout location along y-direction using Taguchi robust design concept.

Vibration frequencies of laminated panels depend on laminations, edge conditions, shell dimensions (thickness, length) and cutout (size and position). Therefore, for cutout borne stiffened hypar shells with various material system and geometric shape, obtaining an appropriate combination of lamination angle, thickness, cutout position and end conditions for maximization of the fundamental frequency becomes an interesting problem. This is more so because fundamental frequency needs to be higher to skip any resonance effect occurring from ground vibrations and other natural disturbances. However, there has not been much of an activity in this respect perhaps due to the complexities involving so many shell parameters and complicated algorithm flow as well.

Despite of good number of studies on maximization of fundamental frequency by appropriate design of stacking sequence, extensive scrutiny of literature reveals paucity of reports on optimization of the fiber orientation, dimension, thickness, material orthotropy and position of the cutout for different edge constraints leading to maximum fundamental frequency of laminated shells. This study of stiffened hypar shells considers the application of the Taguchi method along with an efficient finite element formulation to determine the suitable combination of multi-parametric design optimization to yield maximum frequency of cutout borne shell. Taguchi

orthogonal design is applied with four design factors namely, fiber orientation, width-to-thickness, level of orthotropy of the composite and position of the cutout as independent variables. Taguchi analysis is performed to obtain the suitable combination of factors that results maximum fundamental frequency. A confirmation analysis verified the optimal parametric combination obtained from Taguchi approach. Analysis of variance (ANOVA) was performed to get the significant design factors and the level of significance of their interactions.

7.2 TAGUCHI METHOD

Taguchi method [Taguchi, 1990; Ross, 1996] employs orthogonal array (OA) based experiments that help in reducing the variance with optimum combination of control factors. For achieving the same, it integrates design of experiments (DOE) technique with optimization of control factors. For performance analysis, traditional experimental designs use the average of characteristics while Taguchi method is based on the effect of variation of the characteristics. In essence, the performance of the system becomes insensitive to the variation of noise factors. Standard OA helps to evaluate the ability of design parameters in controlling the variability of a particular characteristic by performing least number of tests.

Thus, Taguchi method considers the total design space using reduced number of experiments to evaluate all of the design factors and interactions. The optimal setting of the design factors for maximizing the objective function is thus obtained. The factor trends and noise sensitivities are also obtained. The flow-chart in Taguchi design is shown in Fig. 7.1.

Taguchi optimization uses signal-to-noise (S/N) ratio as the objective function. S/N ratio considers the mean (signal) as well as the variability (noise). It depends on the type of the design. Three types of S/N ratios are defined: Type LB: lower is better, Type HB: higher is better and Type NB: nominal is best. The combination of factor levels that yields the maximum value of the S/N ratio is the optimal condition. For the current study, fundamental frequency needs to be maximized, thus HB characteristic is to be used. Moreover, ANOVA [Montgomery, 2001] is performed to obtain the significant factors. S/N ratio analysis and ANOVA together yield the suitable setting of the design factors that optimizes the objective function. Finally, confirmatory run verifies the optimal setting of factors obtained from the analysis.

The main advantage of Taguchi method is that it considers a mean performance characteristic value close to the target rather than a value within specified limits. Taguchi method is simple and

easy to apply. Thus it is a powerful yet simple tool for optimization without requirement for large amount of experimentation. Hence it is cost effective and less time consuming. On the other hand, the main demerit of the method is that the results obtained are only relative and do not exactly point out which parameter has the highest effect on the performance characteristic. Moreover, since orthogonal arrays do not test all variable combinations, this method is not recommended if relationships between all variables are sought for. Also, Taguchi method fails to account for all interactions between parameters. The other demerit of the method is its offline nature. Thus it cannot be applied for dynamically varying situations. Since Taguchi approach deals with designing quality rather than correcting for poor quality, it is most effective and also recommended for early stages of process development only. According, in the present study, Taguchi methodology is applied to determine the combination of parameters that yield the maximum fundamental frequency of composite stiffened hypar shell in presence of perforations in the form of cutout.

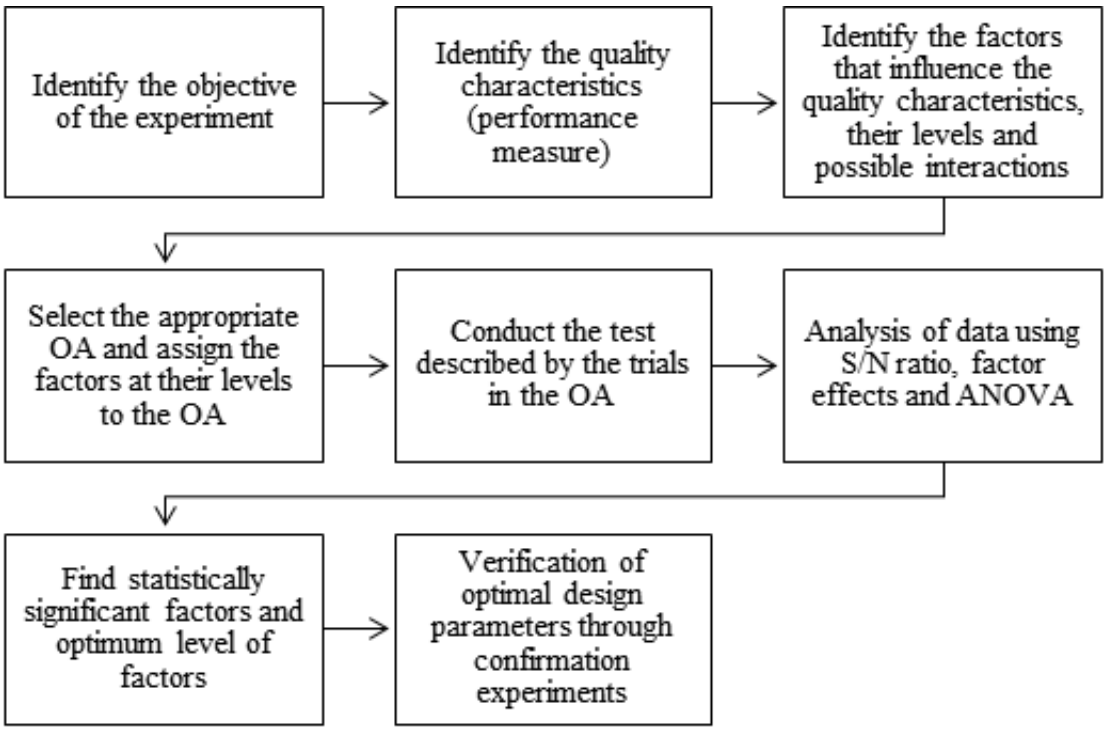

Fig. 7.1 Flow chart in Taguchi design

7.3 DESIGN OF EXPERIMENTS

DOE helps in analyzing of the effect of design factors on the response characteristics. Here, response is fundamental frequency of the shell which is an unknown function of design factors. A

large number of factors may influence the fundamental frequency. However, existing literature reveals that the fundamental frequency of laminated shell is mostly influenced by lamination angle (A), width/thickness factor of shell (B) and degree of orthotropy of the material (C). The shell material considered here is orthotropic and the degree of orthotropy is defined as the ratio of longitudinal to transverse Young's modulus (E_{11}/E_{22}). Thus these are taken as design factors along with their interaction. Also, it is well documented in literature that position of cutout (D) influences the fundamental frequency of cutout borne shells. Thus position of cutout (D) is taken as the fourth design factor. Table 7.1 exhibits the levels of design factors within the operating range of the factors. The purpose of choosing three levels is to consider the curvature or non-linearity effects. This study is employed to consider free vibration of laminated hypars with stiffeners and cutout. The response variable here is the fundamental frequency. The design factors are optimized with the aim to have maximum fundamental frequency of shell.

Table 7.1: Design factors along with level settings

Design factors	Notation in OA	Levels		
		1	2	3
Lamination angle (θ degree)	A	30	45	60
Width/thickness factor, b/h	B	20	50	100
Degree of orthotropy, E_{11}/E_{22}	C	10	25	40
Position of cutout $(\bar{x}, \bar{y})$	D	(0.2, 0.2)	(0.3, 0.3)	(0.4, 0.4)

According to Taguchi philosophy, the choice of suitable OA is governed by consideration of degrees of freedom (DOFs). DOF of chosen OA needs to be larger than or at least equal to the total DOFs needed for the analysis. In the present study, there are four design factors and each factor has three levels. For this three level run, each main factor has (3-1) DOF. Thus, DOF of four main factors is 4x(3-1), i.e., 8. The DOF for three two-way interactions (AxB, AxC, BxC) is 3x (3-1) x(3-1), i.e., 12. Hence, the total DOFs required for the analysis is 20. Accordingly, an L27 OA is chosen as It has 26 degrees of freedom (DOF). It contains 27 rows; each row corresponds to a test run. There are total 13 columns (all are not shown here in Table 7.1 for brevity). 1st column is allotted to lamination angle (A), 2nd column is allotted to b/h ratio (B), 5th column is allotted to

Table 7.2: Experimental layout based on L27 OA

Trial No.	Lamination angle (A)	Width/thickness factor of shell (B)	Degree of orthotropy (C)	Position of cutout (D)
1	1	1	1	1
2	1	1	2	2
3	1	1	3	3
4	1	2	1	2
5	1	2	2	3
6	1	2	3	1
7	1	3	1	3
8	1	3	2	1
9	1	3	3	2
10	2	1	1	2
11	2	1	2	3
12	2	1	3	1
13	2	2	1	3
14	2	2	2	1
15	2	2	3	2
16	2	3	1	1
17	2	3	2	2
18	2	3	3	3
19	3	1	1	3
20	3	1	2	1
21	3	1	3	2
22	3	2	1	1
23	3	2	2	2
24	3	2	3	3
25	3	3	1	2
26	3	3	2	3
27	3	3	3	1

material orthotropy (C), and 9th column is allotted to position of cutout (D). Six columns (3rd, 4th, 6th, 7th, 8th, 9th and 11th) are considered for two-way interactions and the rest three columns (10th, 12th and 13th) are considered for error terms. The trial run is governed by the combination of the design factors and the same is shown in Table 7.2. It may be noted that for a full factorial design that considers four factors at three levels, the number of trial run required is 3x3x3x3 =81. On the other hand, L27 OA needs only 27 runs, i.e., a part of full factorial design. Moreover, the array is orthogonal; and thus factor levels carry equal weights throughout the design space.

7.4 NUMERICAL ANALYSIS

In this section, laminated stiffened hypars with cutout is considered with eight types of end conditions, viz., SSSS, CCCC, CSCS, CSSC, FCCF, FCFC, FSFS and FSSF. However, for brevity, results of SSSS boundary condition are explained in details. The laminate layups of the shells are $[(\theta/-\theta)_{10}]$, i.e., a twenty-layer anti-symmetric angle ply laminate is selected for analysis. The non-dimensional coordinates of the cutout centre is denoted by ($\bar{x} = x/a, \bar{y}$= y/a,). Shell dimensions are taken as: a/b=1, a/h=100, a'/b'=1, c/a=0.2; while material properties are chosen as: E_{11}/E_{22} = 25, $G_{23} = 0.2E_{22}$, $G_{13} = G_{12} = 0.5E_{22}$, $\nu_{12} = \nu_{21}$ =0.25. Fundamental frequency of stiffened hypars with cutout is obtained as per the trial run mentioned in L27 OA based on the combination of design factors. The same is then subjected to S/N ratio analysis, ANOVA analysis and validation study. S/N ratio analysis of test data is done using Minitab [2001]. As fundamental frequency needs to be maximized, higher is better (HB) criterion of S/N ratio analysis is chosen here. S/N ratios of data (fundamental frequency) are calculated by the following relation (n is number of observations, y_i is examined data):

$$\frac{S}{N} = -10\log\left[\frac{1}{n}\sum\left(\frac{1}{y_i^2}\right)\right] \tag{7.1}$$

7.5 RESULTS AND DISCUSSION

Table 7.3 shows the fundamental frequency for SSSS shell obtained from finite element analysis following sequential trials as per L27 OA and the corresponding S/N ratios. DOE being orthogonal, the effect of each parameter can easily be separated at different levels. Thus, the mean S/N ratio for factor A at level 1 is obtained by taking the average of S/N ratios for the experiments

Table 7.3: Non-dimensional fundamental frequencies and S/N ratios for SSSS shell

Trial No.	Fundamental frequency	S/N Ratio
1	18.037	25.12
2	25.804	28.23
3	31.116	29.85
4	10.211	20.18
5	14.667	23.32
6	16.453	24.32
7	8.535	18.62
8	10.624	20.52
9	14.269	23.08
10	21.563	26.67
11	30.612	29.71
12	36.373	31.21
13	11.609	21.29
14	15.778	23.96
15	19.746	25.90
16	8.35	18.43
17	12.806	22.14
18	15.747	23.94
19	18.516	25.35
20	25.184	28.02
21	31.301	29.91
22	9.74	19.77
23	14.508	23.23
24	17.858	25.03
25	8.458	18.54
26	12.157	21.69
27	12.587	21.99

1-9 and so on. Mean S/N ratio for all levels of each factor A-D is presented in response table (Table 7.4). Total mean of S/N ratio is obtained as 24.08 for SSSS shell. Table 7.4 also includes delta value of every design factor. Depending on the delta value, design factors are given ranks that help to decide the impact of factors on fundamental frequency. Table 7.4 shows that depending on delta value, width/thickness parameter (B) gets the rank 1, Degree of orthotropy (C) gets the rank 2, lamination angle (A) gets rank 3 and cut-out location (D) gets rank 4. Thus, B has the maximum influence in determining the fundamental frequency for SSSS shell.

Table 7.4: Response table for SSSS shell

Level	A	B	C	D
1	23.7	28.23	21.56	23.71
2	24.81	23	24.54	24.21
3	23.73	21	26.14	24.32
Delta	1.11	7.23	4.59	0.61
Rank	3	1	2	4

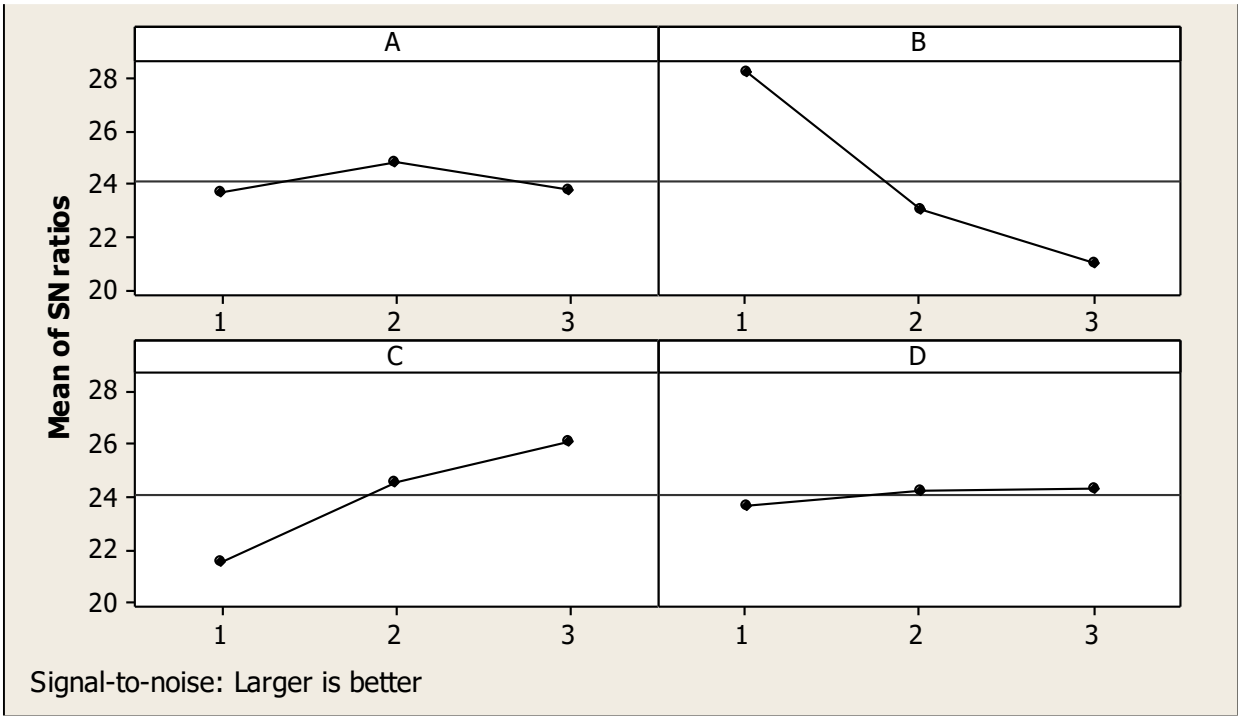

Fig. 7.2: Main effects plot of S/N ratios for SSSS shell

Main effect plot helps to observe the effect of design factors on fundamental frequency of the concerned structure. It also identifies the optimal parametric combination that yields the maximum frequency. Figure 7.2 shows the main effect plot for SSSS shell. The type of the plots explains the significance of the factors and their level of significance. If inclination of plot of a factor is the highest, then that factor has greater influence while gentle slope of a factor means less influence. Figure 7.2 shows that plot of factor B yields the highest inclination while that of factors C, A and D are in decreasing order. Hence factor B is the most influencing one and other factors have little influence. It is evident from Fig. 7.2 that B has the highest S/N ratio at lowest level whereas factor C has the highest S/N ratio at its highest level, factor A contains the highest S/N ratio at middle level, and factor D yields the highest S/N ratio value at its highest level.

The optimal parametric combination is the one where S/N ratio achieves the maximum value. Accordingly, the optimal combination for highest fundamental frequency is A2B1C3D3, i.e., 45^0 lamination angle, width/thickness value 20, E_{11}/E_{22} ratio 40 and cut-out location (0.4, 0.4). Figure 7.3 represents the two-way interaction plot for SSSS shells. In interaction graph, non-parallelism between lines means occurrence of some level of interaction while intersecting lines indicate occurrence of significant interaction. In Fig. 7.3, non-parallel lines are obtained for (A×B) and (A×C) which implies that interaction is present for SSSS shells.

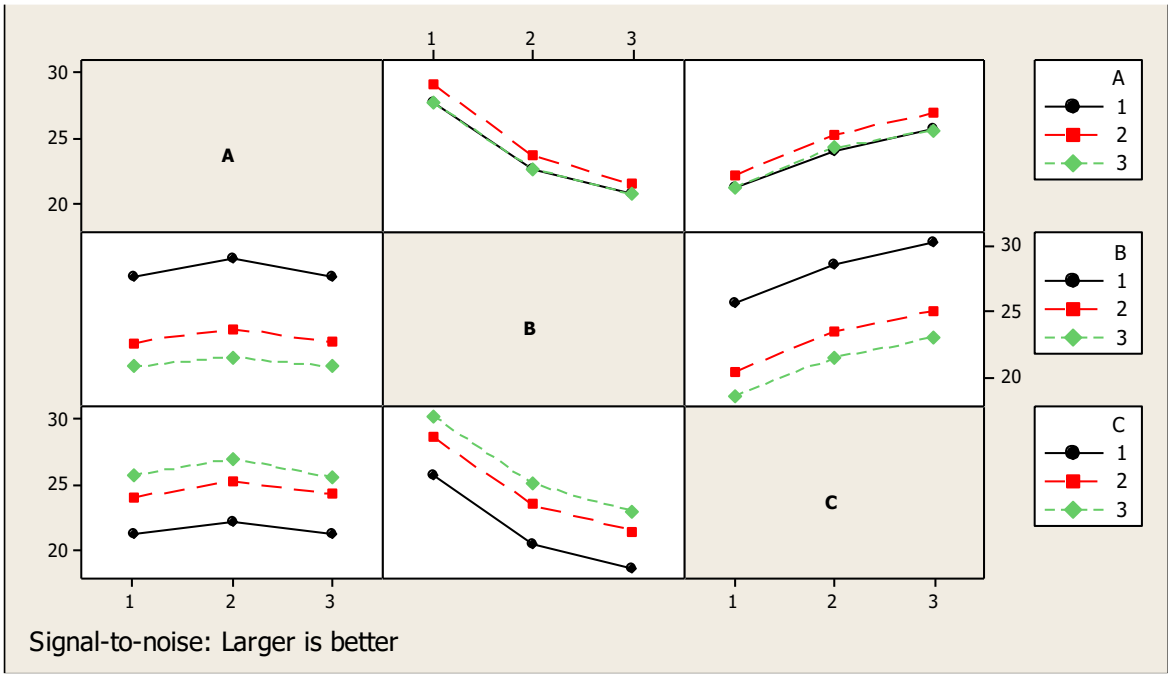

Fig. 7.3: Interaction plot of S/N ratios for SSSS shell

ANOVA provides the significant design factors and interactions which mostly impact total variance of obtained data. Results of ANOVA for SSSS shells is included as Table 7.5. Along with F-ratio and P-value, ANOVA table includes % contribution of design factors. F-ratio justifies whether a factor or interaction is significant or not. Factor having Higher F-ratio value for a factor indicates that the factor has higher impact. For SSSS shells, B receives the highest F-ratio value. Factors C and A follow the same. This implies that width-to-thickness factor (B) is the most dominating factor while degree of orthotropy (C) and lamination angle (A) have some significance. Among the interaction parameters, (A×B) and (A×C) have some significance. P-values of all the factors (except D) are below 0.005, which indicates that A, B, C all are significant factors in controlling the fundamental frequency of SSSS shells. Table 7.5 also includes the percentage contribution of each factor and interactions. Here B has 69.91% contribution and C has 27.16% contribution whereas other factors and interactions contribute little.

Table 7.5: ANOVA result for SSSS shell

Source	DF	Seq SS	Adj SS	MS	F	P	%
A	2	7.226	7.226	3.613	46.77	0	2.01
B	2	251.091	251.091	125.545	1625.25	0	69.91
C	2	97.571	97.571	48.786	631.56	0	27.16
D	2	1.908	1.908	0.954	12.35	0.007	0.53
A*B	4	0.481	0.481	0.12	1.56	0.299	0.13
A*C	4	0.353	0.353	0.088	1.14	0.42	0.09
B*C	4	0.045	0.045	0.011	0.15	0.958	0.01
Error	6	0.463	0.463	0.077			
Total	26	359.139					
S=0.277933		R-Sq=99.87%		R-Sq (adj.)=96.64%			

Coefficient of determination value for the present analysis of SSSS shells is 99.87%. The normal probability plot in Fig. 7.4 verifies that the model is adequate. It correlates the predicted values with the data obtained from numerical analysis (finite element procedure). Figure. 7.4 reveals that all these data approximately lie on a straight line. Thus it establishes the adequacy of

the analysis. The residual versus the fitted value of frequency is plotted in Fig. 7.4 and it can be seen that fitted values do not form any definite pattern, in other words, these are scattered. Thus adequacy of the model is confirmed from this. The data independency is checked by plotting residuals against test order, as included in Fig. 7.4. The residuals plot justified that no predictive pattern can be seen and all the residuals are scattered within allowable limits.

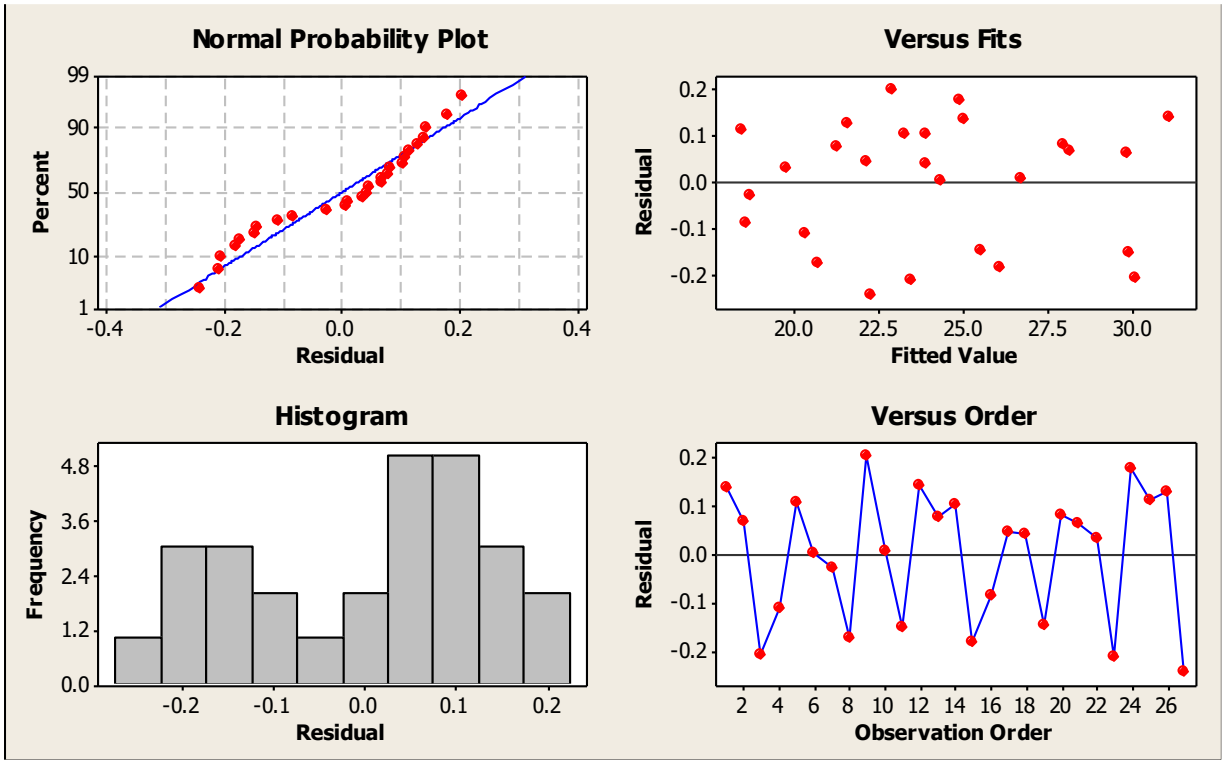

Fig. 7.4: Residual plots for SSSS shell

Lastly, a confirmatory test compares the initial factor setting with optimal factor setting. It helps in obtaining the improvement in final optimal result. Optimal setting of design factors is obtained using the following equation:

$$\overline{\eta} = \eta_m + \sum_{i=1}^{o} (\overline{\eta}_i - \eta_m) \qquad (7.2)$$

Here, η_m represents total mean of data, η_i denotes mean of data at optimal combination, while o denotes the number of design factors with significant influence on fundamental frequency. Table

7.6 provides the results of the confirmation test for SSSS shells. S/N ratio gets improved by 7.04 dB (29.03%) compared to the initial condition. Thus, significant improvement is obtained through this procedure.

Table 7.6: Confirmation table for SSSS shell

	Initial setting	Predicted setting	FE Analysis
Level	A2B2C2D2	A2B1C3D3	A2B1C3D3
Fundamental frequency	16.305		36.698
S/N ratio (dB)	24.25	29.8	31.29

Table 7.7: Summary of contribution (%) of design factors for different shell boundaries

Shell boundaries	Lamination angle (A)	Width/thickness factor (B)	Degree of orthotropy (C)	Position of cutout (D)
CCCC	1.29	39.58	57.45	0.21
CSCS	5.67	64.81	28.44	0.33
CSSC	0.44	66.31	32.22	0.02
SSSS	2.01	69.91	27.17	0.53
FCCF	0.13	69.41	29.81	0.11
FCFC	18.99	53.45	25.71	0.51
FSFS	0.24	77.80	21.27	0.03
FSSF	0.16	72.12	27.45	0.02

For other boundary conditions (CCCC, CSCS, CSSC, FCCF, FCFC, FSFS and FSSF), similar analysis is performed, however details are omitted for brevity. Instead, salient observations are mentioned here. From ANOVA analysis results for all these boundary conditions, summary of contribution of the design factors on fundamental frequency of shells is shown in Table 7.7. It is seen from the present study that in general with number of boundary constraints play a pivotal role in controlling the fundamental frequency. Width/thickness factor (B) is the most dominating factor for deciding the frequency of all shell boundary conditions except CCCC shells. In CCCC shell, degree of orthotropy (C) is the most effective one. As the number of edge constraints is maximum in CCCC shell, the stiffness of the shell is also maximum. So for shells with increased number of

e constraints, rate of change of stiffness due to change in material orthotropy is higher than rate of change of stiffness with lamination thickness. It is also found from the present study that arrangement of boundary constrains has significant influence on fundamental frequency.

For CCCC shells, contributions of B and C are 39.58% and 57.45%. For CSCS shells, the same contributions are 64.81% and 28.44% while for CSSC shells these are 66.31% and 32.22% respectively. Similarly, for FCCF shells, contributions of B and C are 69.41% and 29.81%; for FCFC shells, contributions of A, B and C are 18.99%, 53.45% and 25.71% respectively. For FSFS shells, contributions of B and C are 77.80% and 21.27% and for FSSF shells, these are 72.12% and 27.45% respectively. It is interesting to note here that when two opposite boundaries are clamped and other two are free (FCFC shell), lamination angle significantly influence the fundamental frequency. This is because with variation in lamination angle, the direction of fiber lay changes. Accordingly, the stiffness of shell is high when the fibers are laid in the direction of clamped edges, compared to case when the fibers are laid in the direction of free edges. Regarding interactions, it is found from the present analysis that for shells with boundary conditions like CCCC, CSCS, CSSC, FCCF, FCFC, FSFS and FSSF have interaction at (A×B) and (A×C), while FCFC shells have also some interaction at (B×C).

Table 7.8: Optimal condition for different shell boundaries

Shell boundaries	Optimal condition
CCCC	A2B1C3D3
CSCS	A3B1C3D2
CSSC	A3B1C3D3
SSSS	A2B1C3D3
FCCF	A1B1C3D3
FCFC	A1B1C3D3
FSFS	A2B1C3D1
FSSF	A3B1C3D3

For different edge supports, the optimal conditions for maximum fundamental frequency are tabulated in Table 7.8. As already discussed earlier, the optimal condition for SSSS shells is A2B1C3D3. Similarly, for shells with CCCC, CSCS, CSSC, FCCF, FCFC, FSFS and FSSF

boundary conditions, the optimal predictions are A2B1C3D3, A3B1C3D2, A3B1C3D3, A1B1C3D3, A1B1C3D3, A2B1C3D1 and A3B1C3D3 respectively. Thus, it is observed that maximum fundamental frequency is obtained at the lowest level of width/thickness r of shell (i.e., at b/h =20) and the highest level of degree of orthotropy (i.e., at E_{11}/E_{22} =40) for all the shell boundaries considered here.

The present approach of using Taguchi based DOE method in design optimization of structural response is new of its kind in literature. Though similar methodology is well established in process optimization of machining methods and tribology of materials. It is believed that the present analysis will greatly help the structural engineers who design and analyze shell structures made of laminated composite materials. In the current study, dynamic response is taken up for optimization. However, future studies may be attempted considering other structural issues like bending, buckling, post-buckling etc. adopting similar approach.

7.6 CONCLUSION

In this study, fundamental frequency of cutout borne stiffened hypars made of laminated composites are obtained by numerical approach (finite element method). Taguchi technique is used for optimizing shell attributes like lamination angle, width/thickness, degree of orthotropy, and cutout location in order to have the maximum fundamental frequency. Significant shell parameters are obtained by performing analysis of variance (ANOVA). Residual analyses testify the adequacy of the model. Confirmatory test is conducted for comparison of the initial combination with optimal combination of factors in order to determine the improvement in final optimal result. From this design of experiment analysis, the following conclusions are made:

1) For SSSS shell, optimum combination for highest fundamental frequency is A2B1C3D3, i.e., 45^0 lamination angle, width/thickness factor 20, E_{11}/E_{22} ratio 40 and cut-out location (0.4, 0.4).
2) Similarly, for CCCC, CSCS, CSSC, FCCF, FCFC, FSFS and FSSF boundary conditions, the optimal predictions are A2B1C3D3, A3B1C3D2, A3B1C3D3, A1B1C3D3, A1B1C3D3, A2B1C3D1 and A3B1C3D3 respectively.

3) For SSSS shell, interaction (A×B) and (A×C) have some significance. Similarly, for other shells with boundary conditions like CCCC, CSCS, CSSC, FCCF, FCFC, FSFS and FSSF have interaction at (A×B) and (A×C). FCFC shell has some interaction at (B×C).
4) For different shell boundaries considered here, width/thickness factor (B) is the most dominating factor followed by degree of orthotropy (C). Only in case of CCCC shells, degree of orthotropy (C) is the most dominating factor followed by width/thickness factor of shell (B). Lamination angle (A) plays significant contribution in case of FCFC shells.
5) Position of cutout has very little impact for all the shell boundaries considered here.
6) Maximum fundamental frequency is obtained at the lowest level of width/thickness factor (i.e., at b/h =20) and the highest level of degree of orthotropy (i.e., at E_{11}/E_{22} =40) for all the shell boundaries considered here.

CONCLUSIONS

8.1 GENERAL

The engineering conclusions from numerical and parametric studies presented in Chapters 5 to 7 are included at respective chapters. In this chapter, the generalized conclusions and future scope of research are presented.

8.2 CONCLUSIONS

The mathematical formulation proposed for static and free vibration problems of laminated composite skewed hypar shells is successfully validated from the results of the benchmark problems. Static analysis of antisymmetric angle ply laminated composite stiffened hypar shells with cut-out for different type of practical boundary conditions reveals a lot of interesting conclusions. An increase in support restraints always reduces deflection and static stress resultants near the boundary. Among shells with two boundaries clamped and other two simply supported, the ones with adjacent boundaries clamped show lesser deflection for all antisymmetric laminations considered in the present study. For shells with free boundaries, one with two adjacent boundaries free shows greater static deflection for all antisymmetric laminations considered. Free boundaries bring high flexibility in shells with respect to other boundaries (clamped or simply supported). Also, when a free boundary is introduced to stiffened shell with cutout maximum deflection and stress resultant always occur near free boundary. Thus arrangement of boundary constraints has a large impact on deflection and static stress resultants.

Higher mode free vibration of laminated composite skewed hypar shell with cutout at various boundary conditions has been studied. The non-dimensional fundamental frequency varies with the variation of parameters like material anisotropy, width to thickness ratio and fibre orientation angle. In some cases, non-dimensional frequency increases with fibre orientation angle

and material anisotropy and decreases in few cases. With increase in width to thickness ratio fundamental frequency decreases from first mode to fifth mode. Mode frequency analysis has been discussed for laminated composite skewed hypar shell with cutout. The first five non-dimensional fundamental frequency parameter increases monotonically for all laminations and boundary constraints as the degree of orthotropy increases. It has been noticed that free vibration behavior mainly depends on the number of support constraints whatever be the parametric variations in terms of fibre orientation angle, degree of orthotropy, width-to-thickness ratio etc.

Taguchi robust design has been presented to optimize shell parameters (lamination angle, width-thickness ratio, cutout location along x-direction and cutout along y-direction) to maximize the fundamental frequency of the shell structure. Significant shell parameters and their interactions are obtained by testing analysis of variance (ANOVA). Adequacy of the present model is verified by the residual plots. Confirmation test is implemented to compare the initial condition with optimal condition so that improvement in final optimal result can be understood. From the design of experiment investigation, subsequent interpretations are made considering numerical trials with respect to various types of boundary conditions. The results obtained for each trial shows the improvement in final results for the boundary conditions considered here for analysis. Position of cutout has less impact on optimum condition for all shell boundaries considered here. Maximum fundamental frequency is obtainable at the lowest level of width-to-thickness ratio and the highest level of degree of orthotropy for all shell boundaries considered here.

8.3 FUTURE SCOPE

The present study clearly explains the static and free vibration behavior of composite stiffened hypar shell with cutout. But still some parametric behavior of static and dynamic analysis of hypar shell with cut out at various support constraints and cutout positions are yet to be studied. Buckling and stability aspects and optimization behavior for critical buckling load of stiffened hypar shells with cutout may be studied in future. The above topics are only suggestive topics of research.

REFERENCES

Acharyya, A.K., Chakravorty, D. and Karmakar, A., 2008, Bending characteristics of delaminated composite cylindrical shells—a finite element approach, *Journal of Reinforced Plastics and Composites*, 28(8), pp.965-978.

Almeida, F.S.D., 2016, Stacking sequence optimization for maximum buckling load of composite plates using harmony search algorithm, *Composite Structures*, 143, pp. 287–299.

Ashwinkumar, A., Sivakumar, P. and Lakshmikandhan, K.N., 2015, Parametric study of thin cylindrical shells, *International Journal of Engineering Research and Technology*, 3, pp.1-5.

Aymerich, F. and Serra, M., 2008, Optimization of laminate stacking sequence for maximum buckling load using the ant colony optimization (ACO) metaheuristic, *Composites Part A: Applied Science and Manufacturing*, 39, pp. 262–72.

Barroso, E.S., Parente, E. and Cartaxo de Melo, A.M., 2017, A hybrid PSO-GA algorithm for optimization of laminated composites, *Structural and Multidisciplinary. Optimization*, 55(6), pp. 2111–2130.

Biswal, M., Sahu, S.K. and Asha, A.V., 2015, Experimental and numerical studies on free vibration of laminated composite shallow shells in hygrothermal environment, *Composite Structures*, 127, pp.165-174.

Chakravorty D., Bandyopadhyay J.N. and Sinha P.K., 1995, Finite element free vibration analysis of point supported laminated composite cylindrical shells, *Journal of Sound and Vibration*, 181(1), pp.43-52.

Chakravorty D., Bandyopadhyay J.N. and Sinha P.K., 1998, Applications of FEM on free and forced vibrations of laminated shells, *ASCE Journal of Engineering Mechanics*, 124(1), 1–8.

Chang, S.P., 1973, Analysis of eccentrically stiffened plates, Ph. D. Thesis, University of Missouri, Columbia, MO.

Chen, Y., Jin, G. and Liu, Z., 2013, Free vibration analysis of circular cylindrical shell with non-uniform elastic boundary constraints, *International Journal of Mechanical Sciences*, 74, pp.120-132.

Civalek, O, 2006, An efficient method for free vibration analysis of rotating truncated conical shells, *International Journal of Pressure Vessels and Piping*, 83(10, pp.1-12

Das, H.S. and Chakravorty, D., 2011, Bending analysis of stiffened composite conoidal shell roofs through finite element application, *Journal of Composite Materials*, 45(5), pp.525-542.

Dennis S.T. and Palazotto A.N., 1990, Static response of a cylindrical composite panel with cutouts using a geometrically nonlinear theory, *AIAA J*, 28, pp.1082-1108.

Dey, S., Mukhopadhyay, T. and Adhikari, S., 2014, Stochastic free vibration analysis of composite shallow doubly curved shells- A Kriging model approach, *Composites: Part B*, 70, pp.99-112.

Dey, S., Mukhopadhyay, T. and Adhikari, S., 2015, Stochastic free vibration analyses of composite shallow doubly curved shells-A Kriging model approach, *Composite: Part B*, 70, pp.99-112.

Dey, S., Mukhopadhyay, T., Sahu, S.K. and Adhikari, S., 2016, Effect of cut-out on stochastic natural frequency of composite curved panels, *Composites Part B: Engineering*, 105, pp.188-202.

Duc, N.D., 2014. Nonlinear Static and Dynamic Stability of Functionally Graded Plates and Shells. Vietnam National University Press, Hanoi.

Erdal, O. and Sonmez, F.O., 2005, Optimum design of composite laminates for maximum buckling load capacity using simulated annealing. *Composite Structures*, 71(1), pp. 45–52.

Ergin, A. and Temarel, P, 2002, Free vibration of a partially liquid-filled and submerged horizontal cylindrical shell, *Journal of Sound and Vibration*, 254(5), pp.951-965.

Ferreira, A.J.M, Roque, C.M.C and Jorge, R.M.N., 2006, Static and free vibration analysis of composite shells by radial basis functions, *Engineering Analysis with Boundary Elements*, 30(9), pp.719-733.

Gholami, M., Fathi, A. and Baghestani, A.M., 2021, Multi-objective optimal structural design of composite superstructure using a novel MONMPSO algorithm, *International Journal of Mechanical Sciences*, 193, ID:106149.

Ghosh B. and Bandyopadhyay J.N., 1994, Bending analysis of conical shells with cutouts, *Computers & Structures*, 53, pp.9-18.

GulshanTaj, M.N.A. and Chakraborty, A., 2013, Dynamic response of functionally graded skew shell panel, *Latin American Journal of Solids and Structures*, 10, pp.1243-1266.

Halder, S., 2008, Free vibration of composite skewed cylindrical shell panel by finite element method, *Journal of Sound and Vibration*, 311, pp.9-19.

Halder, S., Majumdar, A. and Kalita, K., 2019, Bending analysis of composite skew cylindrical shell panel, *International Journal of Computer Applications*, 1(8), pp.82-86.

Halder, S., Majumdar, A. and Manna, M.C, 2010, Bending of skewed cylindrical shell panels, *International Journal of Computer Applications*, 1(8), pp.89-93.

Hota, S.S. and Chakravorty, D., 2007, Free vibration of stiffened conoidal shell roofs with cut-outs, *Journal of vibration and Control*, 13(3), pp.221-240.

Hufenbach, W., Holste, C. and Kroll, L., 2002, Vibration and damping behavior of multi-layered composite cylindrical shells, *Composite Structures*, 58, pp. 165-174.

Hwang D.Y. and Foster Jr. W.A., 1992, Analysis of axisymmetric free vibration of isotropic shallow spherical shells with a circular hole, *J. Sound Vib*. 157, pp.331-343.

Jin G., Ye T., Jia X. and Gao S., 2014, A general Fourier solution for the vibration analysis of composite laminated structure elements of revolution with general elastic restraints, *Composite Structures*, 109, pp.150–168.

Kamarian, S., Salim, M. and Dimitri, R. and Tornabene, F. 2016, Free vibration analysis of conical shells reinforced with agglomerated carbon nanotubes, *International Journal of Mechanical Sciences*, 108, pp.157-165.

Kandasamy, S. and Singh, A.V., 2006, Free vibration analysis of skewed open circular cylindrical shells, *Journal of Sound and Vibration*, 290, pp. 1100-1118.

Kang, J.H. and Leissa, A.W., 2005, Free vibrations of thick, complete conical shells of revolution from a three-dimensional theory, *Journal of Applied Mechanics*, 72(5), pp.797-800.

Kaveh, A., Dadras, A. and Malek, N.G., 2018, Buckling load of laminated composite plates using three variants of the biogeography-based optimization algorithm. *Acta Mechanica*, 229(4), pp. 1551–1566.

Kumar A., Bhargava P. and Chakrabarti A., 2012, Natural Frequencies and mode shape of laminated composite skew hypar shells with complicated boundary conditions using finite element method, *Advanced Material Research*, 585, pp.44-48.

Kumar A., Bhargava P. and Chakrabarti A., 2013, Vibration of laminated composite skew hypar shells using higher order theory, *Thin Walled Structures*, 63, pp.82-90.

Kumar A., Chakrabarti A. and Bhargava P., 2013a, Finite element analysis of laminated composite and sandwich shells using higher order zigzag theory, *Composite Structures*, 106, pp.270-281.

Kumar A., Chakrabarti A. and Bhargava P., 2013b, Vibration of laminated composites and sandwich shells based on higher order zigzag theory, *Engineering Structures*, 56, pp.880-888.

Kumar A., Chakrabarti A. and Bhargava P., 2013c, Vibration of laminated composite shells with cutouts using higher order shear deformation theory, *International Journal of Scientific & Engineering Research*, 4(5), pp.199-202.

Kumar A., Chakrabarti A. and Bhargava P., 2014, Accurate dynamic response of laminated composites and sandwich shells using higher order zigzag theory, *Thin Walled Structures*, 77, pp.174-186.

Kumar A., Chakrabarti A. and Bhargava P., 2015, Vibration analysis of laminated composite skew cylindrical shells using higher order shear deformation theory, *Journal of Vibration and Control*, 21(4), pp.725-735.

Kumar, R., Mishra, B.K. and Jain, S.C., 2008, Static and dynamic analysis of smart cylindrical shell, *Finite Element in Analysis and Design*, 45, pp.13-24.

Kumari, S. and Chakravorty, D., 2010, On the bending characteristics of damaged composite conoidal shells-a finite element approach, *Journal of Reinforced Plastics and Composites*, 29(21), pp.3287-3296.

Labans, E., Bisagni, C., Celebi, M., Tatting, B., Gurdal, Z, Blomschieber, A., Rassain, M. and Wanthal, S., 2019, Bending of composite cylindrical shells with circular cut-out: Experimental Validation, *Journal of Aircrafts*, 56(4), pp.1-17.

Lal, A., Singh, B.N. and Anand, S., 2011, Nonlinear bending response of laminated composite spherical shell panel with system randomness subjected to hygro-thermo-mechanical loading, *International Journal of Mechanical Sciences*, 53(10), pp.855-866.

Lee, H. and Kwak, M.K., 2015, Free vibration analysis of a circular cylindrical shell using the Rayleigh–Ritz method and comparison of different shell theories, *Journal of Sound and Vibration*, 353, pp.344-377.

Lee, Y.S., Yang, M.S., Kim, H.S. and Kim, J.H, 2002, A study on the free vibration of the joined cylindrical–spherical shell structures, *Computers and Structures*, 80. pp.2405-2414.

Liew K.M. and Lim C.W., 1994a, Vibration of perforated doubly curved shallow shells with rounded corners, International Journal of Solids and Structures, 31(11), pp.1519-1536.

Liew K.M. and Lim C.W., 1994b, A Pb-2 Ritz formulation for flexural vibration of shallow cylindrical shells of rectangular planform, *Journal of Sound and Vibration*,173(3), pp.343-375.

Liew K.M. and Lim C.W., 1994c, Vibratory characteristics of cantilever rectangular shallow shells of variable thickness, *AIJJ Journal*, 32(2), pp.387-396.

Liew K.M. and Lim C.W., 1995a, A Ritz vibration analysis of doubly curved rectangular shallow shells using a refined first-order theory, *Computer Methods in Applied Mechanics and Engineering*, 127(1-4), pp.145-162.

Liew K.M. and Lim C.W., 1995b, Vibratory behavior of shallow conical shells by a global Ritz formulation, *Engineering Structures*, 17(1), pp.63-70.

Liew K.M. and Lim C.W., 1995c, Higher-order theory for vibration analysis of cantilever thick shallow shells with constrained boundaries, *Journal of Vibration and Control*, 1(1), pp.15-39.

Liew K.M. and Lim C.W., 1996, Vibratory characteristics of pre-twisted cantilever trapezoids of unsymmetric laminates, *AIJJ Journal*, 34(5), pp.1041-1050.

Liew K.M., Kirtiporanchai S. and Wang C.M., 1993, Research developments in analyses of plates and shells, *Journal of Construction Steel Research*, 26(2-3), pp.231-248.

Liew K.M., Lim C.W. and Kitiporanchai S., 1997, Vibration of shallow shells: a review with bibliography, *Applied Mechanics Reviews*, 50(8), pp.431-444.

Liew K.M., Lim C.W. and Ong L.S., 1994d, Vibration of pre-twisted shallow conical shells, *International Journal of Solids and Structures*, 31(18), pp. 2463-2476.

Liew K.M., Lim C.W. and Ong L.S., 1994e, Flexural vibration of doubly-tapered cylindrical shallow shells, *International Journal of Mechanical Sciences*, 36(6), pp. 547-565.

Lim C.W. and Liew K.M., 1995d, Vibration of pre-twisted cantilever trapezoidal symmetric laminates, *ActaMechanica*, 111, pp. 193-208.

Madenci E. and Barut A., 1994, Pre and post-buckling response of curved thin composite panels with cutouts under compression, *Int J Numer Meth Engrg*, 37, pp. 1499-1510.

Maghami, S.A., and Tahani, M, 2015, Thermal bending analysis of doubly curved composite laminated shell panels with general boundary conditions and laminations, *Journal of Thermal Stresses*, 38(2), pp.250-270.

Mantari, J.L., Oktem, A.S. and Soares, C.G., 2012, Bending and free vibration analysis of isotropic and multilayered plates and shells by using a new accurate higher-order shear deformation theory, *Composites Part B: Engineering*, 43(8), pp.3348-3360.

Minitab User Manual (Release 13.2), 2001, Making Data Analysis Easier. MINITAB Inc., State college, PA, USA.

Mokhtar, B., Fodil, H. and Mostapha, K., 2010, Bending analysis of symmetrically laminated plates, *Leonardo Journal of Sciences*, 16, pp.105-116.

Monge, J., Mantari, J., Yarasca, J and Arciniega, R., 2018, Bending response of doubly curved laminated composite shells using hybrid refined models, *IOP: Conference series: Material Science and Engineering*, 473, pp.1-6.

Montgomery, D.C., 2001, Design and Analysis of Experiments. New York: Wiley.

Mukherjee A. and Mukhopadhyay M., 1988, Finite element free vibration of eccentrically stiffened plates, *Computers and Structures*, 30, pp. 1303-1317.

Naghsh, A. and Azhari, M., 2015, Non-linear free vibration analysis of point supported laminated composite skew plates, *International Journal of Non-linear Mechanics*, 76, pp.64-76.

Naghsh, A., Saadatpour, M.M and Azhari, M, 2015, Free vibration analysis of stringer stiffened general shells of revolution using meridional finite strip method, *Thin Walled Structures*, 94, pp.651-662.

Nanda, N. and Bandyopadhyay, J.N., 2007, Non-linear free vibration analysis of laminated composite cylindrical shells with cut-out, *Journal of Reinforced Plastics and Composites*, 26(14), pp.1413-1427.

Nanda, N. and Bandyopadhyay, J.N., 2008, Non-linear transient response of laminated composite shells, *Journal of Engineering Mechanics*, 134(11), pp. 983-990.

Narita Y. and Leissa A.W., 1984, Vibrations of corner point supported shallow shells of rectangular planform, *Earthquake Engineering and Structural Dynamics*, 12, pp.651-661.

Narita, Y. and Nitta, T., 1998, Optimal design by using various solutions for vibration of laminated shallow shells on shear diaphragms. *Journal of Sound and Vibration*, 214, pp. 227-244.

Narita, Y. and Robinson, P., 2006, Maximizing the fundamental frequency of laminated cylindrical panels using layerwise optimization. *International Journal of Mechanical Sciences*, 48, pp. 1516-1524.

Narita, Y. and Zaho, X., 1998, An optimal design for the maximum fundamental frequency of laminated shallow shells, *International Journal of Solids and Structures*, 35, pp. 2571-2583.

Narita, Y., Itoh, M. and Zhao, X., 1996, Optimal design by genetic algorithm for maximum fundamental frequency of laminated shallow shells, *Advanced Composite Letters*, 5(1), pp. 21-24.

Nayak A.N. and Bandyopadhyay J.N., 2002a, Free vibration analysis and design aids of stiffened conoidal shells, *ASCE Journal of Engineering Mechanics*, 128(4), pp. 419–427.

Nayak A.N. and Bandyopadhyay J.N., 2002b, On the free vibration of stiffened shallow shells, *Journal of Sound and Vibration*, 255(2), pp. 357–382.

Nayak A.N. and Bandyopadhyay J.N., 2005, Free vibration analysis of laminated stiffened shells, *ASCE Journal of Engineering Mechanics*, 131(1), pp. 100–105.

Nayak A.N. and Bandyopadhyay J.N., 2006, Dynamic response analysis of stiffened conoidal shells, *Journal of Sound and Vibration*, 291, pp. 1288-1297.

Neogi, S.D., Karmakar, A and Chakravorty, D. 2017, Finite element analysis of laminated composite skewed hypar shell roofs under oblique impact with friction, *11th International Symposium on plasticity and Impact Mechanics*, 173, pp.314-322.

Nguyen-Thanh, N., Rabczuk, T., Nguyen-Xuan, H. and Bordas, S.P., 2008, A smoothed finite element method for shell analysis, *Computer Methods in Applied Mechanics and Engineering*, 198(2), pp.165-177.

Noor A.K., Starnes J.H. and Peters J.M., 1996, Nonlinear and postbuckling responses of curved composite panels with cutouts, *Composite Structures*, 34, pp. 213-240.

Nwoji, C.U., Ani, D.G., Oguaghamba, O.A. and Ibeabuchi, V.T., 2021, Static bending of isotropic circular cylindrical shells based on the higher order shear deformation theory of Reddy and Liu, *International Journal of Applied Mechanics and Engineering*, 26(3), pp.141-162.

Pradyumna, S. and Bandyopadhyay, J.N., 2008, Static and free vibration analyses of laminated shells using a higher-order theory, *Journal of Reinforced Plastics and Composites*, 27, pp. 167-186.

Prusty, B.G. and Satsangi, S.K., 2001a, Analysis of stiffened shell for ships and ocean structures by finite element method, *Ocean Engineering*, 28, pp.621-638.

Prusty, B.G. and Satsangi, S.K., 2001b, Finite element transient dynamic analysis of laminated stiffened shells, *Journal of Sound and Vibration*, 248(2), pp.215-233.

Qatu M.S. and Leissa A.W., 1991a, Vibration studies for laminated composite twisted cantilever plates, *International Journal of Mechanical Sciences*, 33(11), pp.927-940.

Qatu M.S. and Leissa A.W., 1991b, Free vibrations of completely free doubly curved laminated composite shallow shells, *Journal of Sound and Vibration*, 151(11), pp.9-29.

Qatu M.S. and Leissa A.W., 1991c, Natural frequencies for cantilevered doubly curved laminated composite shallow shells, *Composite Structures*, 17, pp.227-255.

Qatu M.S., Asadi E. and Wang W., 2012, Review of recent literature on static analyses of composite shells: 2000-2010, *Open Journal of Composite Materials*, 2, pp.61-86.

Qatu M.S., Sullivan R. W. and Wang W., 2010, Recent research advances on the dynamic analysis of composite shells:2000-2009, *Composite Structures*, 93, pp.14-31.

Qatu, M.S., 2002a, Recent research advances in the dynamic behavior of shells: 1989-2000, Part 1: Laminated Composite shells, *Applied mechanics Rev. (ASME),* 55(4), pp.325-350.

Qatu, M.S., 2002b, Recent research advances in the dynamic behavior of shells: 1989-2000, Part 2: Homogeneous shells, *Applied Mechanics Rev. (ASME),* 55(5), pp.415-434.

Rao, A.R.M. and Arvind, N., 2005. A scatter search algorithm for stacking sequence optimisation of laminate composites. *Composite Structures*, 70(4), pp. 383–402.

Reddy J.N. and Chandrashekhara K., 1985, Geometrically non-linear transient analysis of laminated doubly curved shells, *International Journal of Non-Linear Mechanics*, 20(2), pp.79-90.

Reddy, B.S., Kumar, J.S., Reddy, A.R. and Reddy, K.V.K, 2012, Bending analysis of laminated composite plates using finite element method, *International Journal of Engineering Science and Technology*, 4(2), pp.177-190.

Rikards R., Chate A. and Ozolinsh O., 2001, Analysis for buckling and vibrations of composite stiffened shells and plates, *Composite Structures*, 51, pp.361–370.

Ross, P.J., 1996, Taguchi techniques for Quality Engineering. 2nd edn., New York: McGraw-Hill.

Rossow, M. P. and Ibrahimkhail, A.K., 1978, Constrained method analysis of stiffened plates, *Computers & Structures*, 8, pp.51-60.

Roy, T. and Chakraborty, D., 2009. Optimal vibration control of smart fiber reinforced composite shell structures using improved genetic algorithm. *Journal of Sound and Vibration*, 319, pp. 15-40.

Ruotolo, R, 2001, A comparison of some thin shell theories used for the dynamic analysis of stiffened cylinders, *Journal of Sound and Vibration*, 243(5), pp. 847-860.

Sahoo, S. and Chakravorty, D., 2005, Finite element vibration characteristics of composite hypar shallow shells with various edge supports, *Journal of Vibration and Control*, 11(10), pp.1291-1309.

Sahoo, S. and Chakravorty, D., 2006, Deflections, forces and moments of composite stiffened hypar shell roofs under concentrated load, *Journal of Strain Analysis for Engineering Design*, 41(1), pp.81-97.

Sahoo, S. and Chakravorty, D., 2006a, Stiffened composite hypar shell roofs under free vibration, behavior and optimization aids, *Journal of Sound and Vibration*, 295, pp.362-377.

Sahoo, S., 2011, Free vibration of laminated composite hypar shell roofs with cut-out, *Advances in Acoustics and Vibration*, 2011, pp.1-13.

Sahoo, S., 2012, Behavior and optimization aids of composite stiffened hypar shell roofs with cutout under free vibration, *ISRN Civil Engineering*, ID 989785, pp.1-14.

Sahoo, S., 2013, Dynamic characters of stiffened composite conoidal shell roofs with cut-outs: Design aids and selection guidelines, *Journal of Engineering*, ID 230120, pp.1-18.

Sahoo, S., 2014a, Free vibration of laminated composite stiffened saddle shell roofs with cut-outs, *IOSR Journal of Mechanical and Civil Engineering*, ICAET-2014, pp.30-34.

Sahoo, S., 2014b, Laminated composite stiffened shallow spherical panels with cut-outs under free vibration – a finite element approach, *Engineering Science and Technology, An International Journal*, 17(4), pp. 247-259.

Sahoo, S., 2015a, Free vibration behavior of laminated composite stiffened elliptic paraboloidal shell panel with cut-out, *Curved and Layered Structures*, 2(1), pp.162-182.

Sahoo, S., 2015b, Laminated composite stiffened cylindrical shell panels with cut-outs under free vibration, *International Journal of Manufacturing, Materials, and Mechanical Engineering*, 5(3), pp.37-63.

Sahoo, S., 2016, Performance evaluation of free vibration of laminated composite stiffened hyperbolic paraboloid shell panel with cut-out, *International Journal of Engineering and Technologies*, 7, pp.1-24.

Sai Ram K.S. and Babu T.S., 2001a, Study of bending of laminated composite shells, Part I: shells without a Cutout, *Composite Structures*, 51(1), pp.103-116.

Sai Ram K.S. and Babu T.S., 2001b, Study of bending of laminated composite shells, Part II: shells with a Cutout, *Composite Structures*, 51(1), pp.117-126.

Sanders Jr. JL., 1970, Cutouts in Shallow shells, *J. Appl. Mech.*, 37, pp.374-383.

Schwarte J., 1994, Vibrations of corner point supported rhombic hypar-shells, *Journal of Sound and Vibration*, 175(1), pp.105-114.

Sebaey, T.A., Lopes, C.S., Blanco, N., Mayugo, J.A. and Costa, J., 2013, Two-pheromone ant colony optimization to design dispersed laminates for aeronautical structural applications, *Advances in Engineering Software*, 66(4), pp. 10–18.

Shadmehri, F, Hoa, S. and Hojjati, M, 2014, The effect of displacement field on bending, buckling and vibration of cross-ply circular cylindrical shells, *Mechanics of Advanced Materials and Structures*, 21, pp.14-22.

Shahgholian-Ghahfarokhi, D. and Rahimi, G., 2020, A sensitivity study of the free vibration of composite sandwich cylindrical shells with grid cores, *Iranian Journal of Science and Technology, Transactions of Mechanical Engineering*, 44, pp. 149–162.

Sinha, G., Sheikh, A H. and Mukhopadhyay, M., 1992, A new finite element model for the analysis of arbitrary stiffened shells, *Finite Elements in Analysis and Design*, 12, pp.241-271.

Sivasubramonian B., Kulkarni A.M. and Rao G.V., 1997, Free vibration of curved panels with cutouts, *Journal of Sound and Vibration*, 200(2), pp.227-234.

Srinivasa C.V., Suresh Y.J. and Prema Kumar W.P., 2014, Experimental and finite element studies on free vibration of cylindrical skew panels, *International Journal of Advanced Structural Engineering*, 6(1), pp.1-11.

Stegmann, J. and Lund, E., 2005. Discrete material optimization of general composite shell structures. *International Journal of Numerical Methods in Engineering*, 62, pp. 2009-2027.

Taguchi, G., 1990, Introduction to Quality Engineering. Tokyo: Asian Productivity Organization.

Tamboli, N. and Kulkarni, A.B., 2014, Bending analysis of paraboloid revolution shell, *International Journal of Civil Engineering Research*, 5(4), pp.307-314.

Topal U., 2006, Mode-frequency analysis of laminated spherical shell, In: Proceedings of the 2006 IJME. INTERTECH International Conference-Session ENG P501-001, Kean University, NJ; 19-21 October.

Topal, U., 2009, Multi-objective optimization of laminated composite cylindrical shells for maximum frequency and buckling load. *Materials & Design*, 30, pp. 2584-2594.

Topal, U., 2012, Frequency optimization of laminated composite spherical shells. *Science and Engineering of Composite Materials*, 19(4), pp. 381-386.

Tornabene F., Fantuzzi N., Bacciocchi M. and Dimitri R., 2015, Dynamic analysis of thick and thin elliptic shell structures made of laminated composite materials, *Composite Structures*, 133, pp.278-299.

Tornabene F., Fantuzzi N., Bacciocchi M., 2014a, The local GDQ method applied to general higher-order theories of doubly-curved laminated composite shells and panels: the free vibration analysis, *Composite Structures*, 116, pp.637-660.

Tornabene F., Fantuzzi N., Viola E. and Reddy J.N., 2014b, Winkler-Pasternak foundation effect on the static and dynamic analyses of laminated doubly-curved and degenerate shells and panels, *Composites Part B Engineering*, 57(1), pp.269-296.

Tornabene F., Viola E. and Fantuzzi N., 2013, General higher-order equivalent single layer theory for free vibrations of doubly-curved laminated composite shells and panels, *Composite Structures*, 104(1), pp.94-117.

Vo-Duy, T., Duong-Gia, D., Ho-Huu, V., Vu-Do, H.C. and Nguyen-Thoi, T., 2017, Multi-objective optimization of laminated composite beam structures using NSGA-II algorithm, *Composite Structures*, 168, pp. 498–509.

Xuebin, Li., 2008, Study on free vibration analysis of circular cylindrical shells using wave propagation, *Journal of Sound and Vibration*, 311, pp.667-682.

Ye T., Jin G., Chen Y. and Shi S., 2014a, A unified formulation for vibration analysis of open shells with arbitrary boundary conditions, *International Journal of Mechanical Sciences*, 81, pp.42–59.

Ye T., Jin G., Chen Y., Ma X. and Su Z., 2013, Free vibration analysis of laminated composite shallow shells with general elastic boundaries, *Composite Structures*, 106, pp.470–490.

Ye T., Jin G., Su Z. and Jia X., 2014b, A unified Chebyshev–Ritz formulation for vibration analysis of composite laminated deep open shells with arbitrary boundary conditions, *Arch. Appl. Mech.*, 84, pp.441–471.

Zhang C., Jin G., Ma X. and Ye T., 2016, Vibration analysis of circular cylindrical double-shell structures under general coupling and end boundary conditions, *Applied Acoustics*, 110, pp.176-193.

Research Article Open Access

Puja B. Chowdhury, Anirban Mitra, and Sarmila Sahoo*

Relative performance of antisymmetric angle-ply laminated stiffened hypar shell roofs with cutout in terms of static behavior

DOI 10.1515/cls-2016-0003
Received Nov 16, 2015; accepted Dec 02, 2015

Abstract: A review of literature reveals that bending analysis of laminated composite stiffened hypar shells with cutout have not received due attention. Being a doubly ruled surface, a skewed hypar shell fulfils aesthetic as well as ease of casting requirements. Further, this shell allows entry of north light making it suitable as civil engineering roofing units. Hypar shell with cutout subjected to uniformly distributed load exhibits improved performances with stiffeners. Hence relative performances of antisymmetric angle-ply laminated composite stiffened hypar shells in terms of displacements and stress resultants are studied in this paper under static loading. A curved quadratic isoparametric eight noded element and three noded beam elements are used to model the shell surface and the stiffeners respectively. Results obtained from the present study are compared with established ones to check the correctness of the present approach. A number of additional problems of antisymmetric angle-ply laminated composite stiffened hypar shells are solved for various fibre orientations, number of layers and boundary conditions. Results are interpreted from practical application standpoints and findings important for a designer to decide on the shell combination among a number of possible options are highlighted.

Keywords: stiffened hypar shell; cutout; antisymmetric angle ply composite; finite element method

1 Introduction

Hypar shells are used in civil engineering industry to cover large column free areas such as in stadiums, airports and shopping malls. Being a doubly curved and doubly ruled surface, it satisfies aesthetic as well as ease of casting requirements of the industry. Moreover, hypar shell allows entry of daylight and natural air which is preferred in food processing and medicine units. Cutout is sometimes necessary in roof structure to allow entry of light, to provide accessibility of other parts of the structure, for venting and at times to alter the resonant frequency. Shell structure that are normally thin walled, when provided with cutout, exhibits improved performances with stiffeners. To use these doubly curved, doubly ruled surfaces efficiently, the behavior of these forms under bending are required to be understood comprehensively. The use of laminated composites to fabricate shells is preferred to civil engineers from second half of the last century. The reasons are high strength/stiffness to weight ratio, low cost of fabrication and better durability. Moreover, the stiffness of laminated composites can be altered by varying the fiber orientations and lamina thicknesses which gives designer flexibility. As a result, laminated shells are found more cost effective compared to the isotropic ones as application of laminated composites to fabricate shells reduces their mass induced seismic forces and foundation costs.

A thorough scrutiny of available literature on the bending behavior of laminated composite hypar shells with a cutout reveals that no study has been reported so far on this aspect. Sanders Jr. [1] and Ghosh and Bandyopadhyay [2] have considered the bending of isotropic shells with a cutout. The static behavior of a cylindrical composite panel in presence of cutouts has been reported using a geometrically non-linear theory [3] while the free vibration of cylindrical panel with square cutout has been studied based on finite element method [4]. The axisymmetric free vibration of isotropic shallow spherical shell with circular cutout has also been analyzed [5]. Madenci and Barut [6] studied buckling of composite panels in presence of cutouts. Non-linear post-buckling analysis of composite cylindrical panels with central circular cutouts but having no stiffeners was studied by Noor et al. [7] to consider the effect of edge shortening as well as uniform temperature change. Later Sai Ram and Babu [8, 9] investigated the bending behavior of axisymmetric composite spherical shell both punctured and un-punctured using the finite element method based on a higher order theory. Qatu

Puja B. Chowdhury: Department of Civil Engineering, Heritage Institute of Technology, Kolkata 700107, India
Anirban Mitra: Department of Mechanical Engineering, Jadavpur University, Kolkata 700032, India
***Corresponding Author: Sarmila Sahoo:** Department of Civil Engineering, Heritage Institute of Technology, Kolkata 700107, India, E-mail: sarmila.sahoo@gmail.com

Available online at www.sciencedirect.com

ScienceDirect

Materials Today: Proceedings 4 (2017) 575–583

materialstoday: PROCEEDINGS

www.materialstoday.com/proceedings

5th International Conference of Materials Processing and Characterization (ICMPC 2016)

Bending analysis of laminated stiffened hypar shell roofs with cutout

Puja Basu Chaudhuri[a], Anirban Mitra[b], Sarmila Sahoo[a,*]

[a]*Department of Civil Engineering, Heritage Institute of Technology,Kolkata 700107, India*

[b]*Department of Mechanical Engineering, Jadavpur University, Kolkata 700032, India*

Abstract

A review of existing literature reveals that bending analysis of laminated composite stiffened hypar shells with cutout is scanty.Skewed hypar shell is aesthetically appealing and being doubly ruled provides ease in casting. Further, this type of shell allows entry of north light making it suitable as civil engineering roofing units. Hence an extensive study of antisymmetric angle-ply laminated composite stiffened hypar shells with cutout for different type of practical boundary conditions isconsidered under same intensity of loading. However, results having maximum practical implications are analyzed herefor the sake of brevity.The shell combinations among a number of possible options arechosen. The shell characteristics along some typical lines of dominating values of the respective shell characteristics are studied for different lamination angles.

Selection and peer-review under responsibility of Conference Committee Members of 5th International Conference of Materials Processing and Characterization (ICMPC 2016).

Keywords: stiffened hypar shell; cutout; antisymmetric angle ply composite; finite element method.

1. Introduction

Hypar shells are doubly curved and doubly ruled surface, Hypar shells are used in civil engineering industry to cover large column free areas like stadiums, airports and shopping malls. Cutout is used in roof structure to allow entry of light, venting and to provide accessibility of parts of the structure, and also to alter the resonant frequency.Thin walled structures with cutout exhibits improved performances with stiffeners. The behavior of these forms under bending is required to be understood comprehensively to use it efficiently. Moreover, laminated compositeis preferred to civil engineers to fabricate plates and shells [1, 2].Because laminated composite has high strength/stiffness to weight ratio, low cost of fabrication and better durability.

*Corresponding author. Tel.: +919831591923;
*E-mail address:*sarmila.sahoo@gmail.com

Selection and peer-review under responsibility of Conference Committee Members of 5th International Conference of Materials Processing and Characterization (ICMPC 2016).

Available online at www.sciencedirect.com

ScienceDirect

Materials Today: Proceedings 4 (2017) 9718–9722

materialstoday: PROCEEDINGS

www.materialstoday.com/proceedings

ICEMS 2016

Deflection, forces and moments of composite stiffened hypar shells with cutout

Puja Basu Chaudhuri[a], Anirban Mitra[b], Sarmila Sahoo[a]*

[a]*Department of Civil Engineering, Heritage Institute of Technology, Kolkata 700107, India*
[b]*Department of Mechanical Engineering, Jadavpur University, Kolkata 700032, India*

Abstract

Among the various forms of doubly curved shells, hypar shell is aesthetically appealing and used as roofing units in large column free areas. Cutout is in general provided in roof structures to allow entry of light, venting and to enhance accessibility of parts of the structure, and sometimes to alter the resonant frequency. Though some studies are available for other forms of shells, very few literatures appear to have been published on the effects of cutouts on bending behavior of hypar shell. Finite element method using an eight noded shell element and a three noded beam element both curved and isoparametric is applied to analyze the bending behavior of stiffened hypar shell with cutout. Hypar shell stiffened along the margin of cutouts under the same intensity of loading and different boundary conditions for antisymmetric angle ply lamination is studied for five types of cutouts. The displacements, force and moment resultants are computed at the nodal points of different boundary elements around the openings. The comparative performance of shell characteristics around the opening for different cutouts including longitudinal and transverse of equivalent size reveals that size of the opening is a governing criterion to determine the shell characteristics. Also boundary constraints have large impact on deflection and static stress resultants.

Selection and Peer-review under responsibility of International Conference on Recent Trends in Engineering and Material Sciences (ICEMS-2016).

Keywords: Hypar shell; cutout; laminated composite; bending.

* Corresponding author. Tel. +91 9831591923.
E-mail address: sarmila.sahoo@gmail.com; sarmila.sahoo@heritageit.edu

Selection and Peer-review under responsibility of International Conference on Recent Trends in Engineering and Material Sciences (ICEMS-2016).

Available online at www.sciencedirect.com

ScienceDirect

Materials Today: Proceedings 5 (2018) 5563–5572

materialstoday: PROCEEDINGS

www.materialstoday.com/proceedings

ICMPC 2017

Free vibration analysis of antisymmetric angle ply laminated composite stiffened hypar shell with cut out

Puja Basu Chaudhuri[a,*], Anirban Mitra[b], Sarmila Sahoo[a]

[a]*Department of Civil Engineering, Heritage Institute of Technology,Kolkata 700107, India*
[b]*Department of Mechanical Engineering, Jadavpur University, Kolkata 700032, India*

Abstract

Laminated composite shells are frequently used in various fields of engineering like aerospace, mechanical, marine and automotive engineering. Among different types, hyperbolic paraboloid shell bounded by straight edges (hypar) is aesthetically appealing, provides ease of casting and used as roofing units in large column free areas. Cutout is generally provided in roof structures to allow entry of light, for ventilation purpose, to enhance accessibility of other parts of the structures and sometimes to alter the resonant frequency. An attempt has been made using finite element method for the analysis of stiffened hypar shell with cut out that applies an eight noded is oparametric shell element with five degrees of freedom and a three noded beam element for stiffeners. The study deals with vibration analysis of a hypar shell stiffened along the margin of cut outs with different boundary conditions and antisymmetric angle ply lamination. The formulation is based on first order shear deformation theory. The reduced method of eigen value solution is chosen for the undamped free vibration analysis. The numerical studies are conducted to determine the effects of degree of orthotropy (E_1/E_2), fibre orientation (θ) and width to thickness ratio (b/h) on the non-dimensional fundamental frequency. The results are given in graphical form and obtained results are compared.

Selection and/or Peer-review under responsibility of 7th International Conference of Materials Processing and Characterization.

Keywords: Stiffened hypar shell; Cutout; Free vibration; Finite element method

* Corresponding author. Tel.: +919674747066;
E-mail address: pujabasu.chaudhury@heritageit.edu

Selection and/or Peer-review under responsibility of 7th International Conference of Materials Processing and Characterization.

Mechanics and Mechanical Engineering 2019; 23:162–171

Research Article

Puja Basu Chaudhuri, Anirban Mitra, and Sarmila Sahoo*

Mode frequency analysis of antisymmetric angle-ply laminated composite stiffened hypar shell with cutout

https://doi.org/10.2478/mme-2019-0022
Received Nov 02, 2017; revised May 10, 2018; accepted Nov 20, 2018

Abstract: This article deals with finite element method for the analysis of antisymmetric angle-ply laminated composite hypar shells (hyperbolic paraboloid bounded by straight edges) that applies an eight-noded isoparametric shell element and a three-noded beam element to study the mode-frequency analysis of stiffened shell with cutout. Two-, 4-, and 10-layered antisymmetric angle-ply laminations with different lamination angles are considered. Among these, 10-layer antisymmetric angle-ply shells are considered for elaborate study. The shells have different boundary conditions along its four edges. The formulation is based on the first-order shear deformation theory. The reduced method of eigen value solution is chosen for the undamped free vibration analysis. The first five modes of natural frequency are presented. The numerical studies are conducted to determine the effects of width-to-thickness ratio (b/h), degree of orthotropy (E_{11}/E_{22}), and fiber orientation angle (θ) on the nondimensional natural frequency. The results reveal that free vibration behavior mainly depends on the number of boundary constraints rather than other parametric variations such as change in fiber orientation angle and increase in degree of orthotropy and width-to-thickness ratio.

Keywords: stiffened hypar shell, cutout, anti-symmetric angle-ply composite, finite element method, mode-frequency analysis

1 Introduction

Laminated composite shells now constitute a large percentage of structures including aerospace, marine, and automotive structural components. Structural engineers have already picked up laminated composite hypar shells (hyperbolic paraboloid bounded by straight edges) as roofing units because these can cover large column-free areas with reduced dead weight. This class of shells has only the radius of cross curvature that is unique to this shell form. Roof structures are sometimes provided with cutout to allow the entry of light, venting and to provide the accessibility of parts of the structures, and also to alter the resonant frequency. Shells with cutout stiffened along the margin are an efficient way to enhance the stiffness of the structure without adding much mass. These stiffeners slightly increase the overall weight of the structure but have positive effect on the structural strength and stability. So to apprehend the laminated composite stiffened hypar shells with cutout and to use this shell form efficiently, its characteristics under vibration need to be explored comprehensively.

The subject of laminated shells has attracted several researchers during the past decade. Considerable attention has been paid to dynamic analyses, including free vibration, impact, transient, shock, etc. From the review of literature, it is observed that shell research has been conducted with emphasis on complicating effects in material such as damping and piezoelectric behavior and complicated structures such as stiffened shells with cutout with various boundary conditions. Applications of various shell theories such as classical, shear deformation, 3D, and nonlinear for various shell geometries have received extensive attention from scholars round the globe [1–8]. Some studies used higher order shell theories [9–16], whereas others [17–23] considered finite element approach based on the first-order shear deformation theory to study the free vibration aspects of stiffened shell panels of different forms, that is, cylindrical, elliptic paraboloid, hyperbolic paraboloid, hypar, conoid, and spherical shells in the pres-

*Corresponding Author: Sarmila Sahoo: Department of Civil Engineering, Heritage Institute of Technology, Kolkata 700107, India; Email: sarmila.sahoo@gmail.com
Puja Basu Chaudhuri: Department of Civil Engineering, Heritage Institute of Technology, Kolkata 700107, India
Anirban Mitra: Department of Mechanical Engineering, Jadavpur University, Kolkata 700032, India

HIGHER MODE VIBRATION OF COMPOSITE STIFFENED HYPAR SHELL WITH CUT-OUT FOR VARYING BOUNDARY CONDITIONS AND PLY ORIENTATION

By

PUJA BASU CHAUDHURI * ANIRBAN MITRA ** SARMILA SAHOO ***

*,*** Department of Civil Engineering, Heritage Institute of Technology, Kolkata, India.
** Department of Mechanical Engineering, Jadavpur University, Kolkata, India.

Date Received: 17/07/2018 Date Revised: 13/06/2019 Date Accepted: 12/08/2019

ABSTRACT

Laminated composite shells are used as roofing units in Civil Engineering applications and hypar shells are most popular because of their ease of construction and aesthetic elegance. The aim of the present study is to analyse higher mode free vibration of composite hypar shells. The purpose is to obtain some design guidelines for the practising engineers dealing with such structures. The methodology adopted here is the finite element method based on first order shear deformation theory. Effect of cross curvature is included in the formulation. The isoparametric finite element consists of eight nodes with five degrees of freedom per node is considered. Three noded beam elements with four degrees of freedom per node are used for stiffeners. The generalised Eigen value solution is chosen for the un-damped free vibration analysis. The formulation is validated first by solving standard problems from literature and then new results are obtained for varying boundary conditions, ply orientation and curvature of the shell. The first five modes of natural frequency are presented. In general, it is observed that fundamental frequency increases with the increase in the number of support constraints. There are, however, few departures from this general tendency when two shells of different laminations are compared. Sometimes lamination order may influence the frequency of stiffened composite shell with cut-out more significantly than its boundary conditions. Symmetric lamination exhibits reasonably good performance and may be adopted for all practical purposes.

Keywords: Free Vibration, Laminated Composite, Stiffened Hypar Shell, Cut-out, Higher Mode.

INTRODUCTION

Laminated composite shell structures characterized by high strength/weight value and reduced dead weight are used in different structures of many engineering fields like civil, mechanical, aerospace and others. In civil engineering application laminated composite shells are used as roofs as these can cover large column free areas. Among the different shell configurations, hypar shell (hyperbolic paraboloid shell bounded by straight edges) is very popular as roofs due to their aesthetic elegance (Figure 1). The shell surface being doubly ruled, it is very easy to construct and construction becomes faster. Roofs are often provided with cutout for entry of light, venting and at times to provide accessibility of parts of the

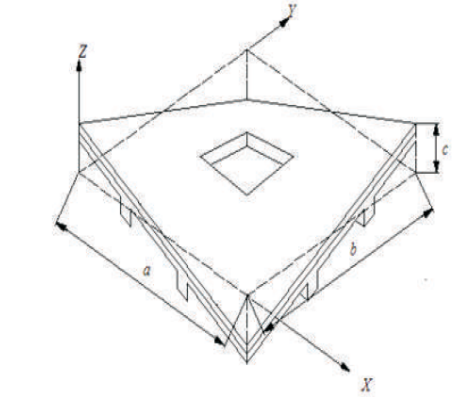

Figure 1. Surface of a Skewed Hypar Shell with Cut-out

Materials Today: Proceedings 66 (2022) 2332–2337

Contents lists available at ScienceDirect

Materials Today: Proceedings

journal homepage: www.elsevier.com/locate/matpr

Design of experiments analysis of fundamental frequency of laminated composite hypar shells with cut-out

Puja Basu Chaudhuri [a], Anirban Mitra [b], Sarmila Sahoo [a,*]

[a] Department of Civil Engineering, Heritage Institute of Technology, Kolkata 700107, India
[b] Department of Mechanical Engineering, Jadavpur University, Kolkata 700032, India

ARTICLE INFO

Article history:
Available online 30 June 2022

Keywords:
Hypar shell
Cut-out
Laminated composite
Natural frequency
Optimization

ABSTRACT

The effect of lamination angle (A), width-to-thickness ratio (B), cut-out location along x-direction (C) and cut-out location along y direction (D) on fundamental frequency of hypar shells made of laminated composites is considered using Taguchi robust design concept. Finite element analysis is done to obtain fundamental frequency of the structure for different parametric variation. Three levels of each parameter are considered to form L_{27} orthogonal array in order to maximize fundamental frequency. Main effect plot identifies the significant parameters. Optimal condition for maximum fundamental frequency is obtained as 45° lamination angle, width-to-thickness ratio of 20, cut-out location along x-direction 0.4 and along y-direction 0.3 (A2B1C3D2). Interaction plots locate the interaction effects between selected parameters. Analysis of Variance study evaluates the significant parameters and their contribution on output, i.e., fundamental frequency. Current investigation reveals, width-to-thickness ratio of shell is the most significant factor while lamination angle and cut-out location have little significance. Among the interacting parameters, interaction between lamination angle & cut-out location (A × C) and interaction between width-to-thickness ratio & cut-out location (B × C) have some significance. Width-to-thickness ratio (B) has 96.76% contribution while lamination angle (A) and cutout locations (C & D) and interactions have low contribution. Residual plots for fundamental frequency are considered and confirmation test validates the present analysis. S/N ratio is found to improve by 12.43% compared to the initial condition.

Selection and peer-review under responsibility of the scientific committee of 2022 International Conference on Recent Advances in Engineering Materials.

1. Introduction

Shells made of laminated composite materials have high strength-to-weight ratio and reduced dead weight. Thus these are hugely used in civil structures particularly as roofs since these can extend over large areas without columns. Hypar shell (hyperbolic paraboloid geometry with straight edges) is popularly used as roofing units due to their aesthetics, doubly ruled surface and ease of construction. Roof structures often require cut-out for entry of light, vents and access to other parts of the structures. Shells with cut-out and stiffened along the margins enhance the stiffness of the structure without appreciable increase in mass. The stiffeners increase the strength and stability significantly. In practical applications, shell roofs involve different combinations of parametric variations and a complete study of dynamic behavior of such structures is essential for effective use. In this respect, fundamental frequency of structures is the minimum frequency at which the structure vibrates when subjected to certain external forces. To avoid any resonance due to ground vibrations and natural disturbances, fundamental frequency of such structures needs to be maximized.

Some earlier studies [1–4] considered bending, vibration and buckling behavior of composite shells. Vibration behavior of hypar shells has also been reported for combinations of boundary conditions [5,6]. Also the role of incorporation of cut-out in the shell structures has been extensively studied for various shell geometries [7–15]. However, optimization of the fundamental frequency for such shell structures has not been considered. No literature is available on optimization of fundamental frequency of composite stiffened hypar shells having cut-out for different parametric variations. Accordingly, a finite element model has been considered for free vibration analysis of composite stiffened hypar shell having cut-out following shallow shell assumptions and incorporating

* Corresponding author.
E-mail address: sarmila.sahoo@heritageit.edu (S. Sahoo).

https://doi.org/10.1016/j.matpr.2022.06.327
2214-7853/
Selection and peer-review under responsibility of the scientific committee of 2022 International Conference on Recent Advances in Engineering Materials.

Mechanics of Advanced Composite Structures Vol (Year) First page – Last page

Semnan University

Mechanics of Advanced Composite Structures

journal homepage: http://MACS.journals.semnan.ac.ir

Maximization of Fundamental Frequency of Composite Stiffened Hypar Shell with Cutout by Taguchi Method

P.B. Chaudhuri [a], A. Mitra [b], S. Sahoo [a]*

[a] *Department of Civil Engineering, Heritage Institute of Technology, Kolkata, 700107, India*
[b] *Department of Mechanical Engineering, Jadavpur University, Kolkata, 700032, India*

KEYWORDS

Laminated hypar shells;
Stiffener;
Cutout;
Fundamental frequency;
Optimization;
Taguchi method.

ABSTRACT

Composite shells find extensive application in modern civil, aerospace and marine structures. In order to avoid resonance, such load-carrying shells need to be optimized from a frequency perspective. Composite shell structures often include cutouts for different functional requirements. Obtaining the best combination of design variables like degree of orthotropy, ply orientation, shallowness of the shell and eccentricity of cutout of laminated shells leads to a problem of combinatorial optimization. This article attempts a numerical study of free vibration response of composite stiffened hypar shells with cutout using finite element procedure and optimization of different parametric combinations based on Taguchi approach. Numerical investigations are carried out following L27 Taguchi design with four design factors, viz., fiber orientation, width/thickness factor of shell, degree of orthotropy and position of the cutout for different edge constraints. For different shell boundaries considered here, width/thickness factor emerges as the most influencing factor followed by degree of orthotropy. The optimum parametric combination for maximum fundamental frequency of cutout borne stiffened hypar shell is obtained from the analysis.

1. Introduction

Competitive demands like light weight, reduced cost, environment-safe, sustainability, dimensional stability etc. have led to the development of laminated composites. Composites find extensive use in different structural applications of mechanical, aerospace and civil engineering. Fibre reinforced composites help in reduction of noise transmission and vibration of structures due to high internal damping. Accordingly, laminated composite is a material of choice to the structural designers. Among various shell forms, aesthetically appealing skewed hypar shells are widely used in roof structures demanding large column free areas. Examples include hangers, auditoriums, exhibition halls, railway stations etc. Shell boundaries are quite often kept free to meet practical requirements. Thin-walled shell structures do perform better when provided with stiffeners, particularly when cutouts are present on the shell surface. Cutouts become a necessity in structural roofs for several requirements like passage of light, accessibility to different parts, venting, and alteration of resonant frequency etc. The vibration frequencies of laminated panels depend on laminations, edge conditions, shell dimensions (thickness, length) and cutout (size and position) [1-3]. Therefore, for cutout borne stiffened hypar shells with various material system and geometric shape, obtaining an appropriate combination of lamination angle, thickness, cutout position and end conditions for maximization of the fundamental frequency becomes an interesting problem. This is more so because fundamental frequency needs to be higher to skip any resonance effect occurring from ground vibrations and other natural disturbances. However, there has not been much of an activity in this respect perhaps due to the complexities involving so many shell parameters and complicated algorithm flow as well.

Design of stacking sequence for optimization of vibration frequency of laminated structures is a common approach [4-6]. Discrete material optimization [7] using finite element approach has also been attempted for optimization of fiber

* Corresponding author. Tel.: +91 3324160358
E-mail address: sarmila.sahoo@gmail.com; sarmila.sahoo@heritageit.edu

Puja Basu Chaudhuri